SUPPLEMENTARY INFORMATION

OF THE MASTER THESIS

PHARMACOKINETICS OF INTRAMUSCULARLY ADMINISTERED THERMORESPONSIVE POLYACRYLAMIDES

BY

ONDŘEJ GROBORZ

Table of Content

S1. NMR spectra

^{1}H, ^{13}C (^{1}H decoupled), ^{19}F and ^{1}H-^{13}C multiplicity-edited ^{1}H-^{13}C HSQC NMR spectra were measured on a Bruker Avance III HD 400 MHz spectrometer (Bruker, Billerica, MA, USA) equipped with a broadband probe. All compounds (5 to 10 mg) were dissolved in MeOH-4d or DMSO-6d (0.70 to 1.00 mL). All 1D spectra were processed in MestReNova 6.0.2 (Mestrelab Research S.L., Santiago de Compostela, Spain), and all 2D spectra were processed in TopSpin 3.6.1 (Bruker, Billerica, MA, USA).

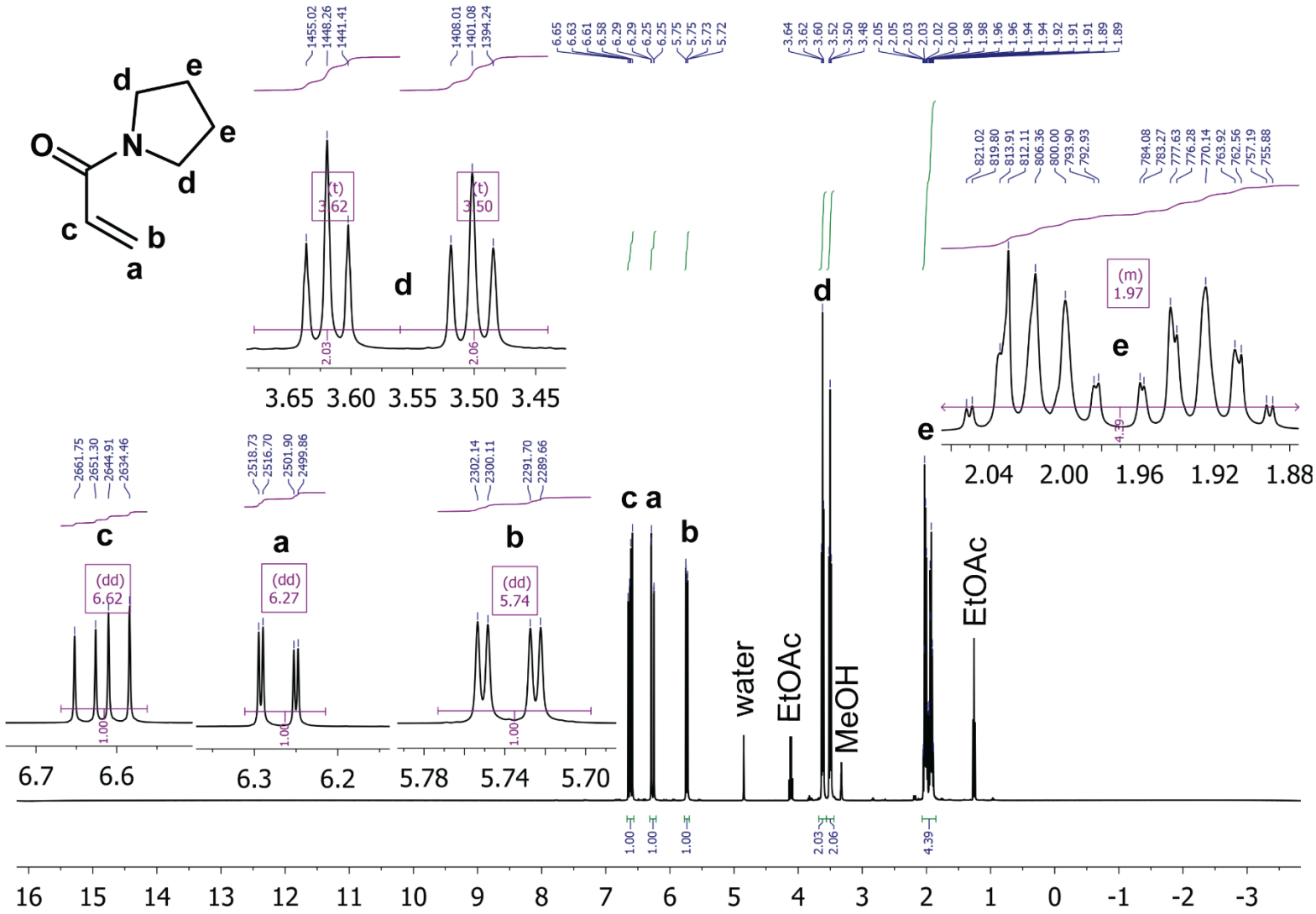

Figure S1. [1]H NMR (400 MHz) spectrum of the ***N*-acryloylpyrrolidine** monomer in MeOH-4d: 6.62 (dd, J = 16.8, 10.4 Hz, 1H), 6.27 (dd, J = 16.8, 2.0 Hz, 1H), 5.74 (dd, J = 10.4, 2.0 Hz, 1H), 3.62 (t, J = 6.8 Hz, 1H), 3.50 (t, J = 6.9 Hz, 1H), and 2.07-1.85 ppm (m, 4H)

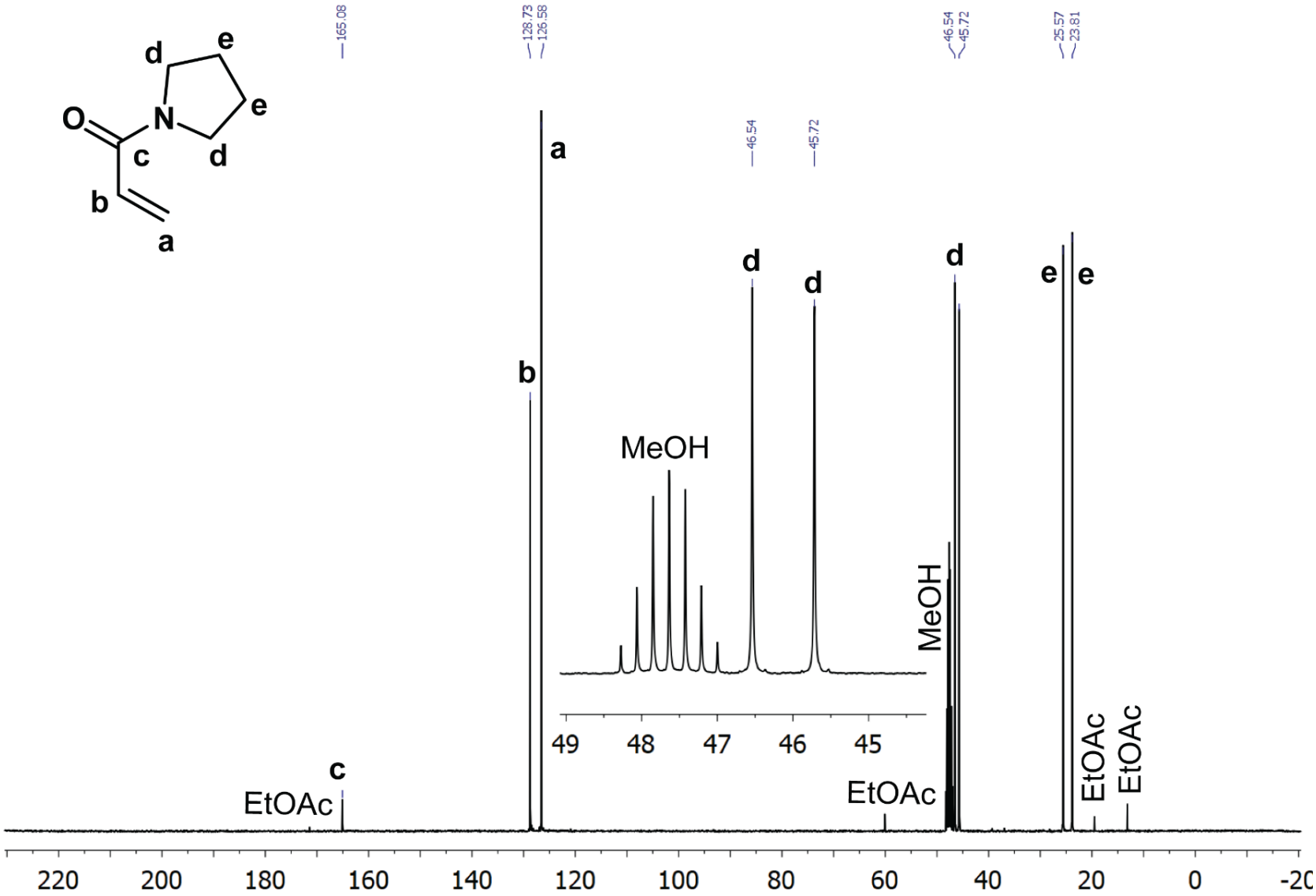

Figure S2. $^{13}C\{^{1}H\}$ NMR (101 MHz) spectrum of the **N-acryloylpyrrolidine** monomer in MeOH-4d: 165.1, 128.7, 126.6, 46.5, 45.7, 25.6, and 23.8 ppm

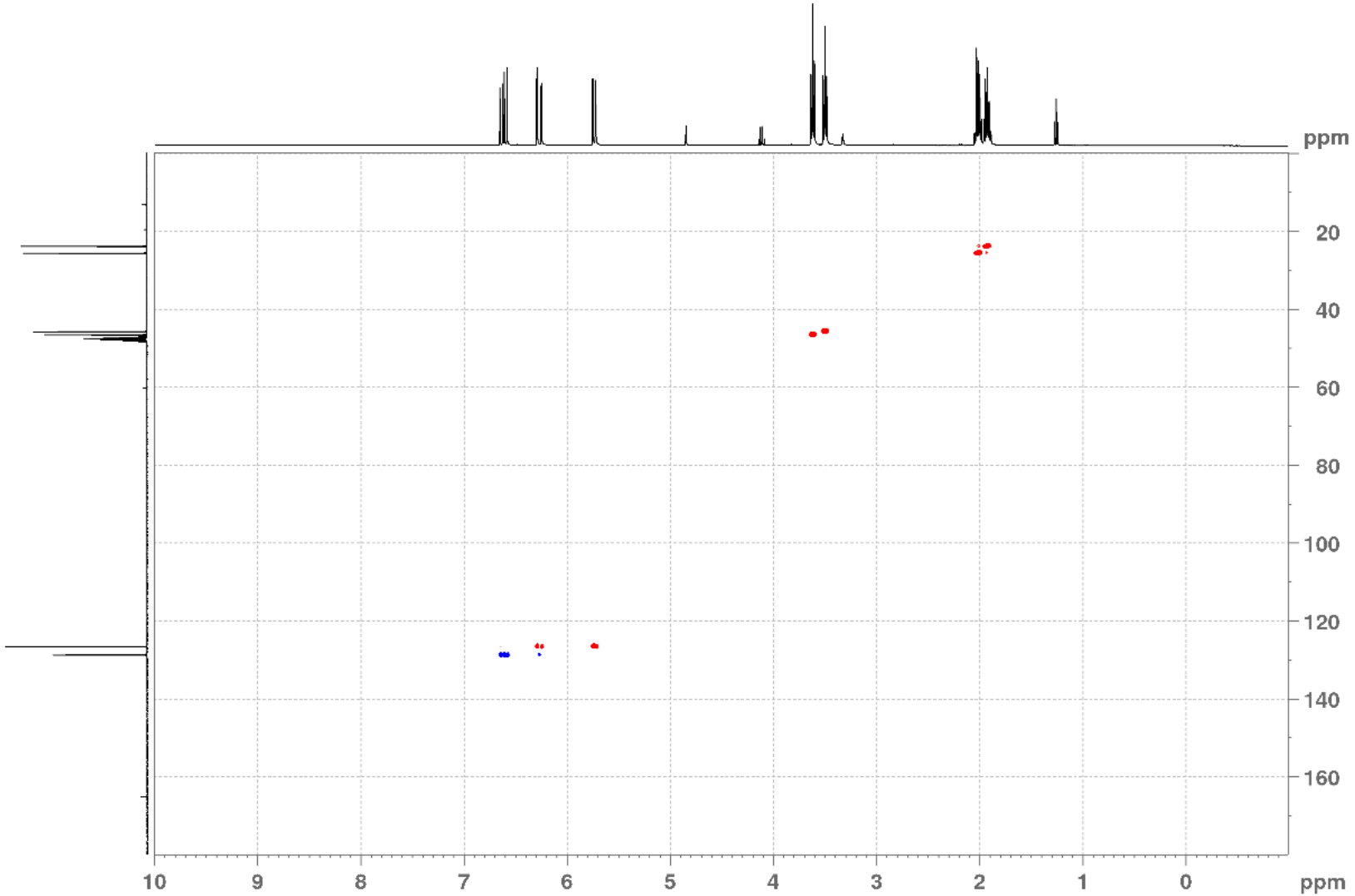

Figure S3. Multiplicity-edited HSQC NMR spectrum (400 MHz) of the **N-acryloylpyrrolidine** monomer in MeOH-4d; negative values (**red**) indicate CH_2 moieties, while positive values (**blue**) indicate CH or CH_3 moieties.

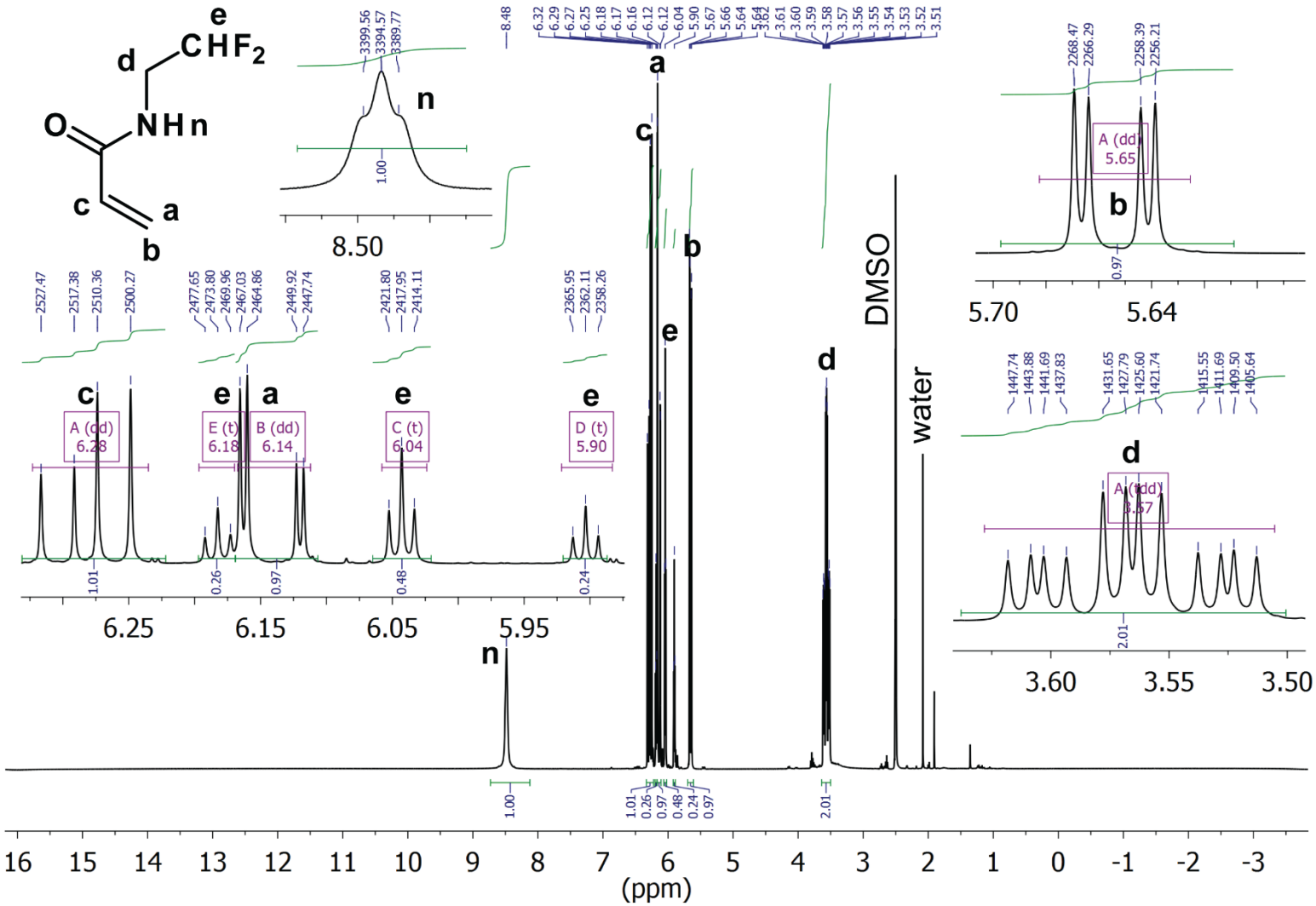

Figure S4. ^{1}H NMR (400 MHz) spectrum of the ***N*-(2,2-difluoroethyl)acrylamide** monomer in DMSO-6d: 8.48 (t, J = 4.9 Hz, 1H), 6.28 (dd, J = 17.1, 10.1 Hz, 1H), 6.14 (dd, J = 17.1, 2.2 Hz, 1H), 6.04 (tt, J = 55.8, 3.8 Hz, 1H), 5.65 (dd, J = 10.1, 2.2 Hz, 1H), and 3.57 ppm (tdd, J = 16.1, 6.0, 3.9 Hz, 2H). The signal **n** in the zoom area was apodized differently from the rest of this spectrum. As shown in the spectrum, the signal **e** is split into three areas, and the total signal integral of all three areas is ≈ 0.97.

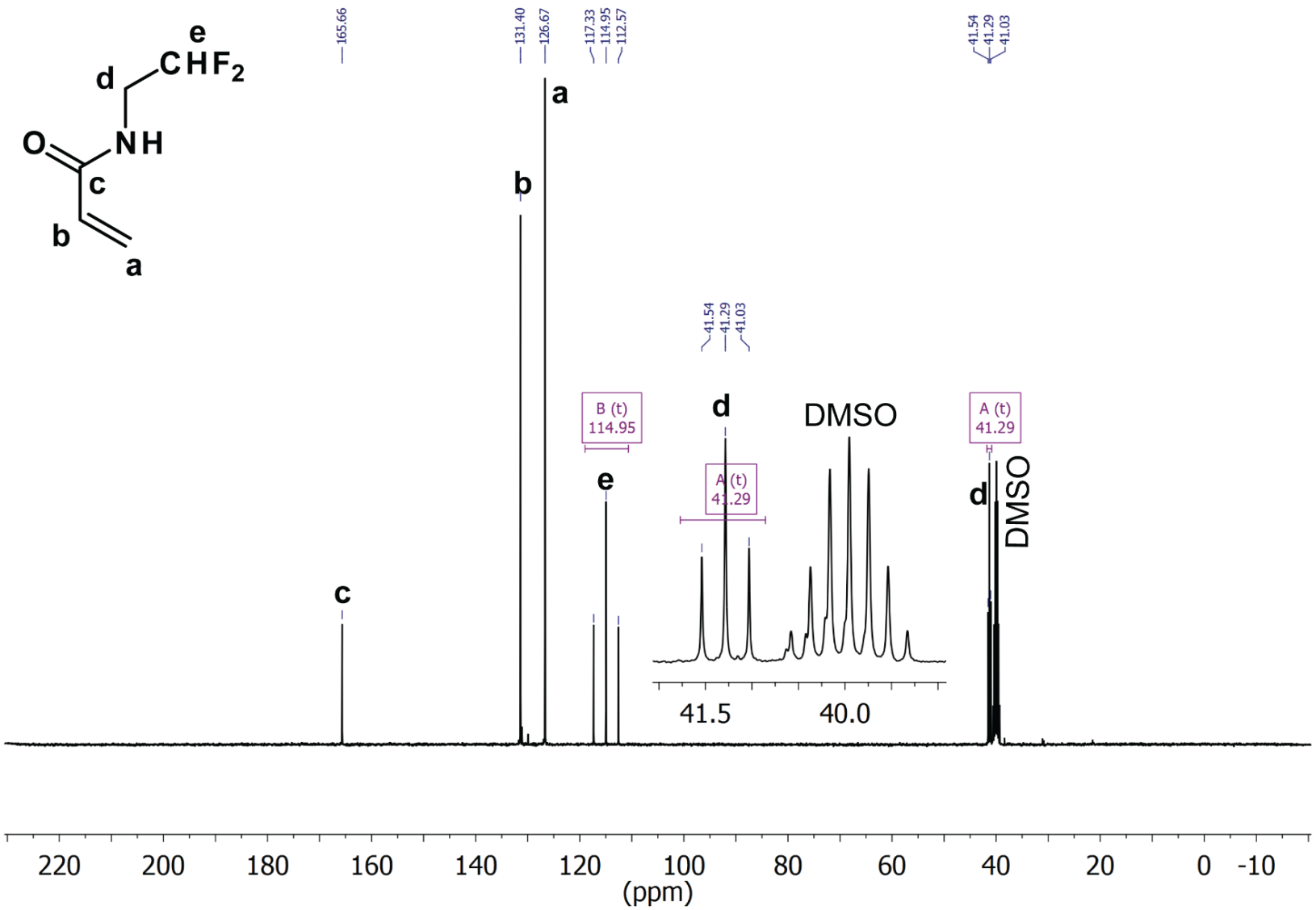

Figure S5. $^{13}C\{^{1}H\}$ NMR (101 MHz) spectrum of the ***N*-(2,2-difluoroethyl)acrylamide** monomer in DMSO-6d: 165.66, 131.40, 126.67, 114.95 (t, $J = 239.7$ Hz), and 41.29 ppm (t, $J = 25.6$ Hz).

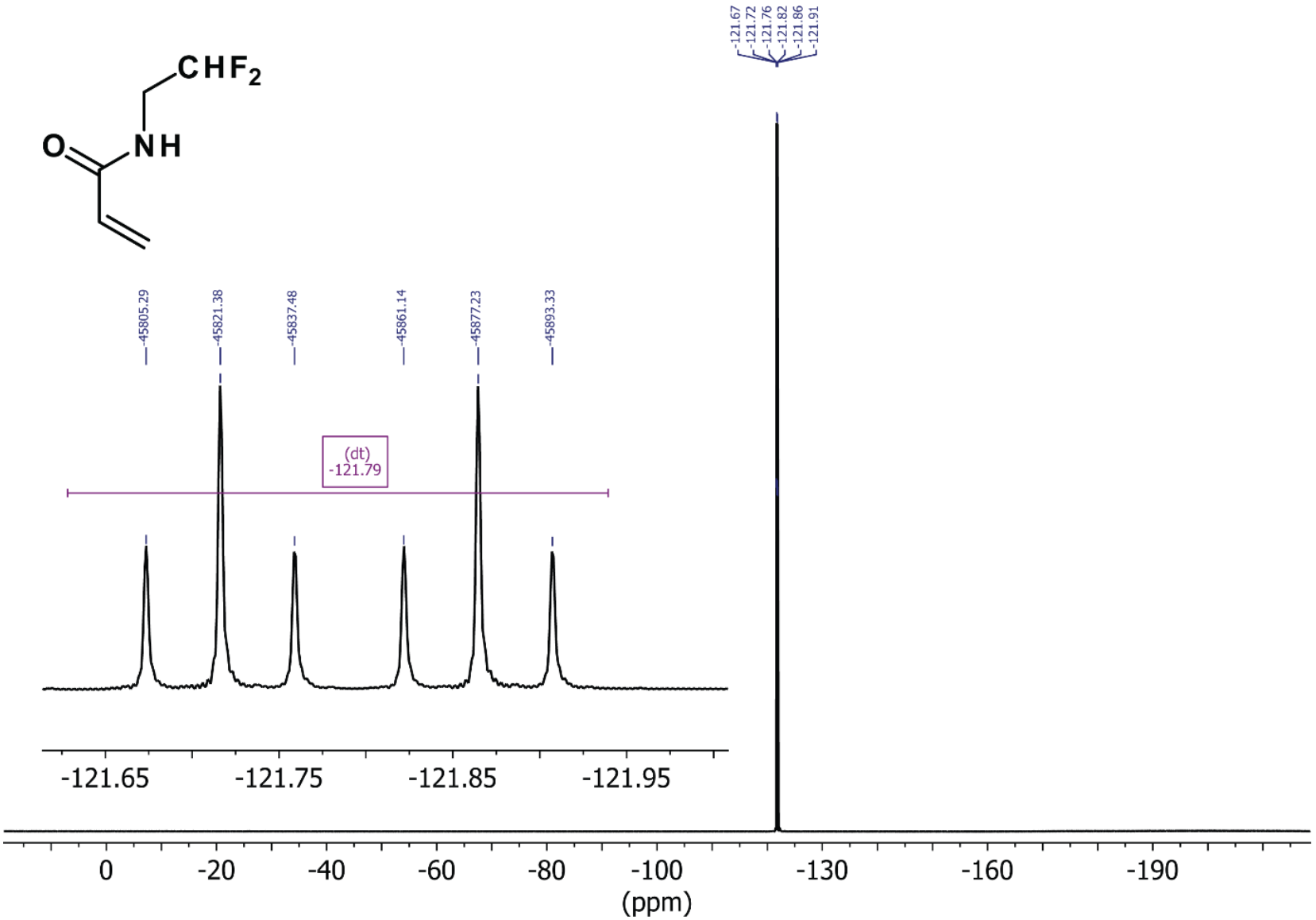

Figure S6. ^{19}F NMR (376 MHz) spectrum of the ***N*-(2,2-difluoroethyl)acrylamide** monomer in DMSO-6d: –121.79 ppm (dt, J = 55.9, 16.1 Hz; 2F)

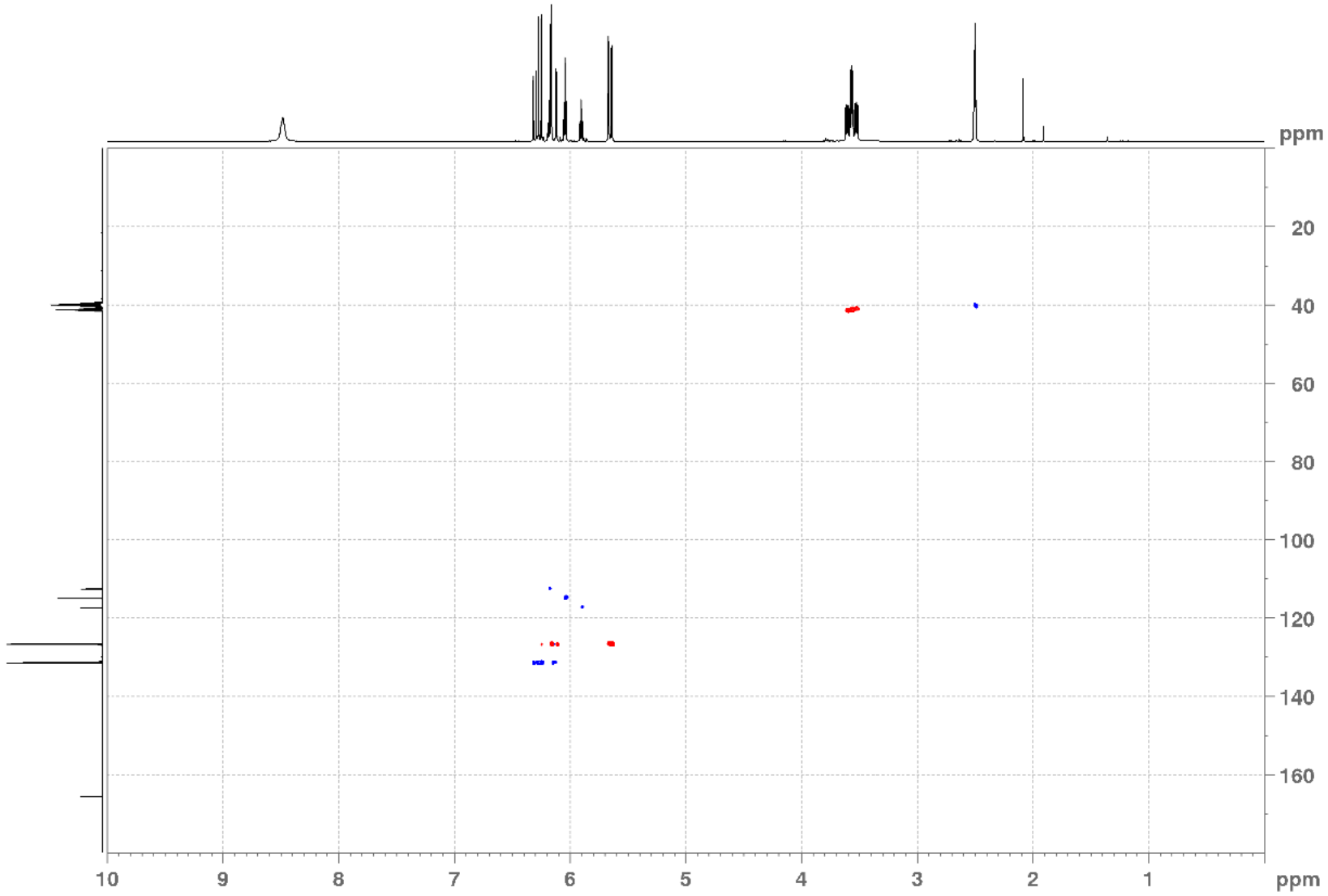

Figure S7. Multiplicity-edited HSQC NMR (400 MHz) spectrum of ***N*-(2,2-difluoroethyl)acrylamide** in DMSO-6d; negative values (**red**) indicate CH_2 moieties, while positive values (**blue**) indicate CH or CH_3 moieties.

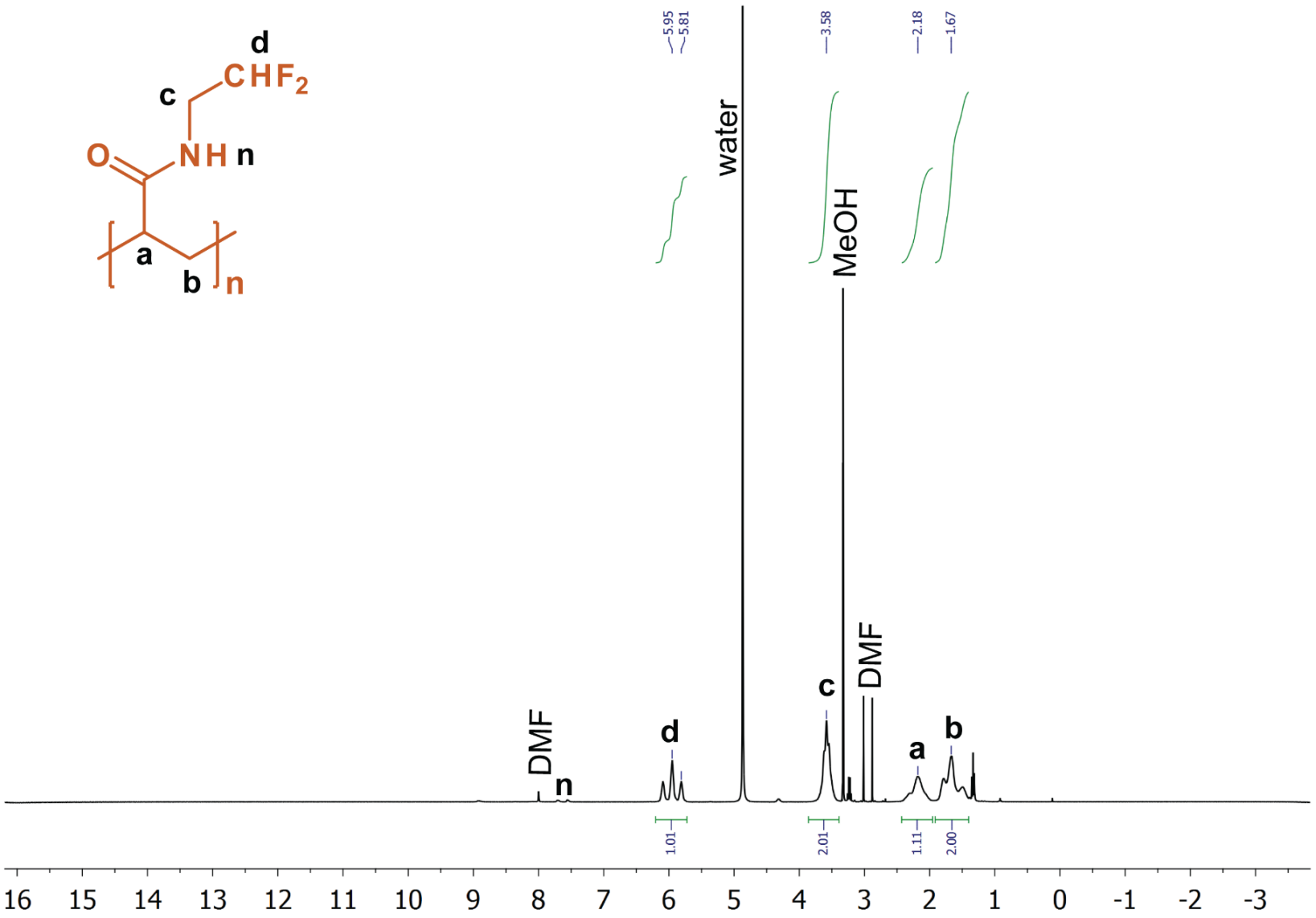

Figure S8. ^{1}H NMR (400 MHz) spectrum of the **pDFEA** polymer in MeOH-4d: 8.00 (1H), 5.95 (t, J = 56.1, 1H), 3.58 (t, J = 14.4 Hz, 2H), 2.18 (1H), and 1.67 ppm (2H).

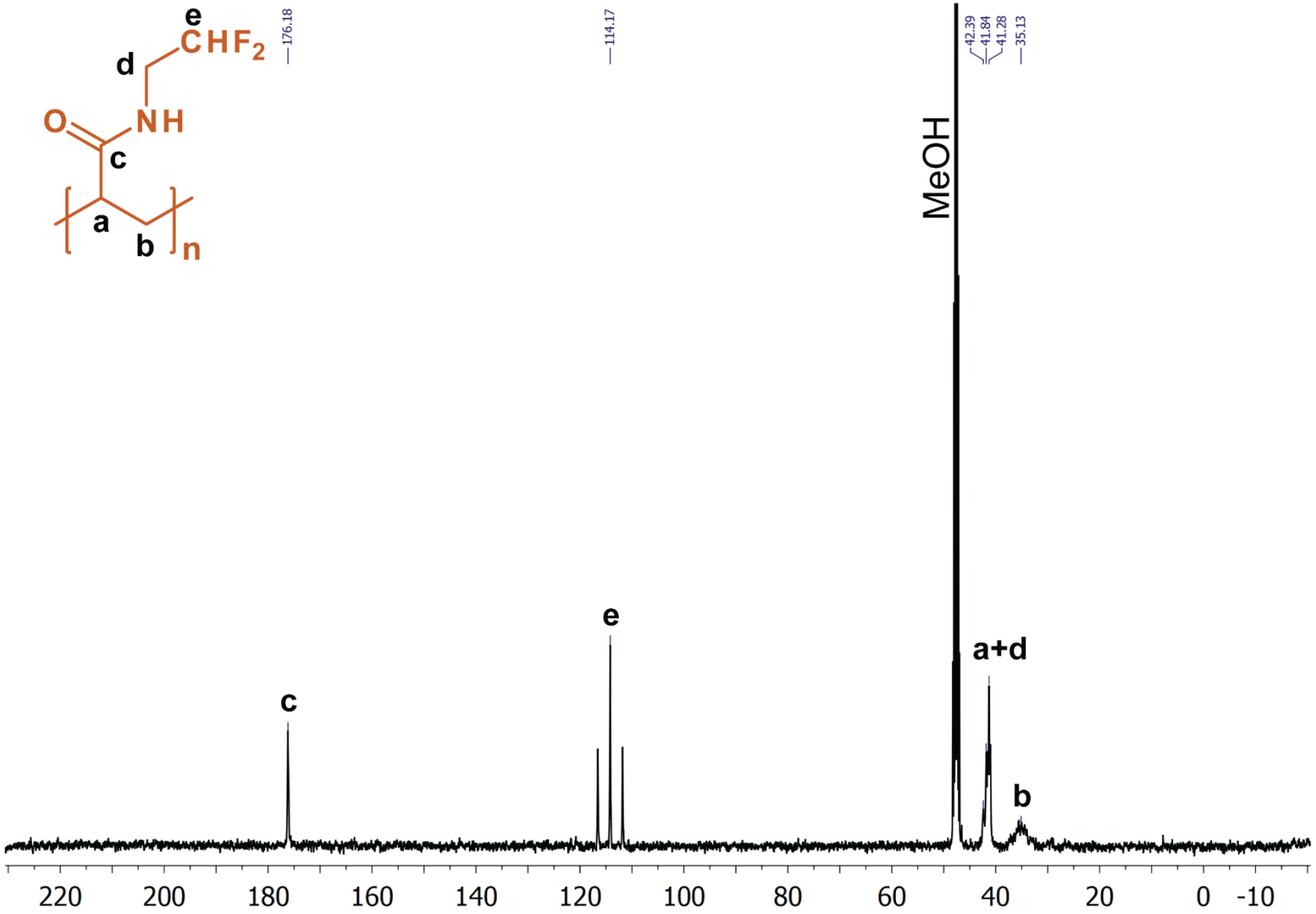

Figure S9. $^{13}C\{^{1}H\}$ NMR (101 MHz) spectrum of the **pDFEA** polymer in MeOH-4d: 176.2, 114.2 (J = 239.5 Hz), 41.8 (t, J = 28.1 Hz), and 35.1 ppm

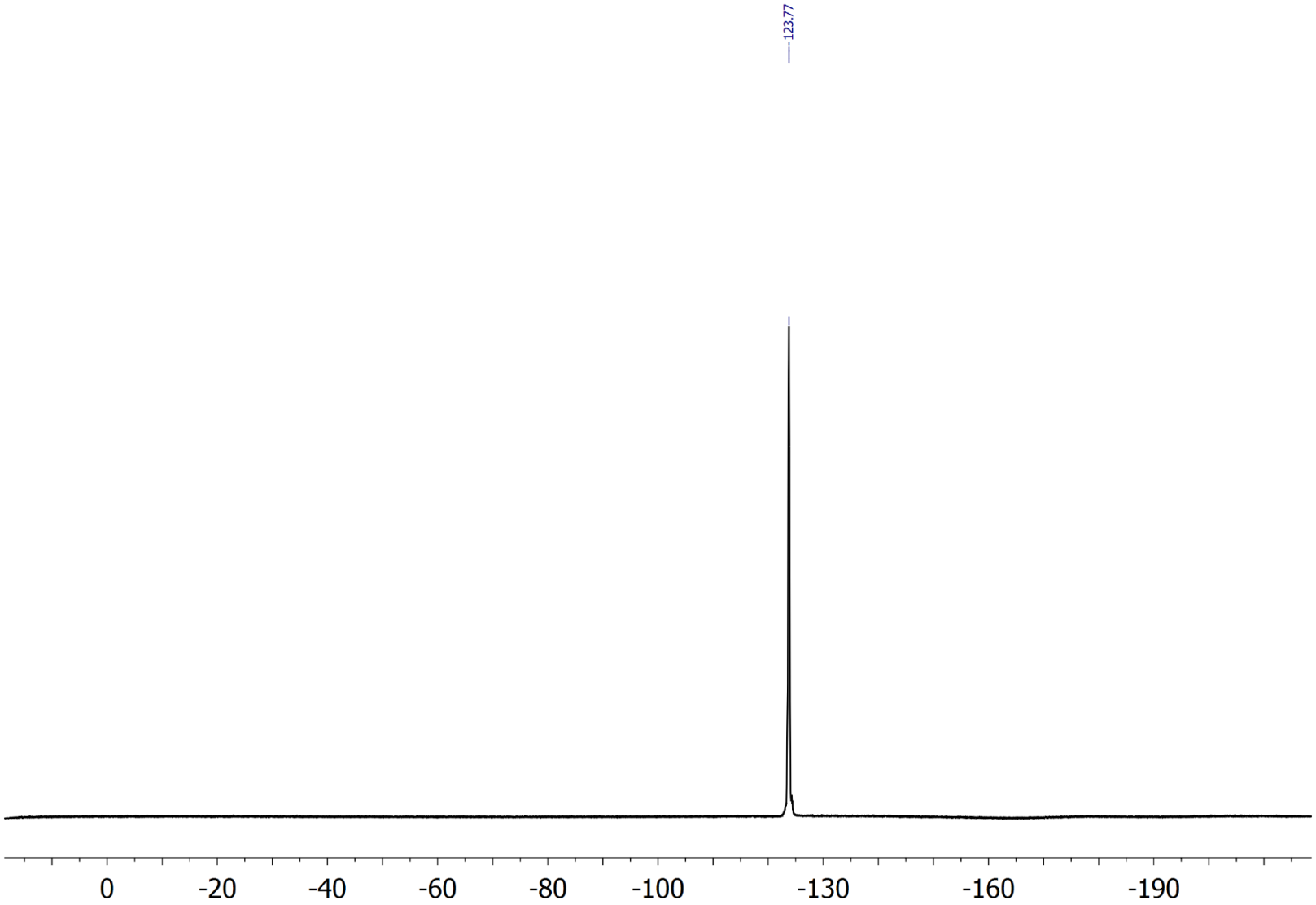

Figure S10. ^{19}F NMR (376 MHz) spectrum of the **pDFEA** polymer in MeOH-4d: –123.8 ppm

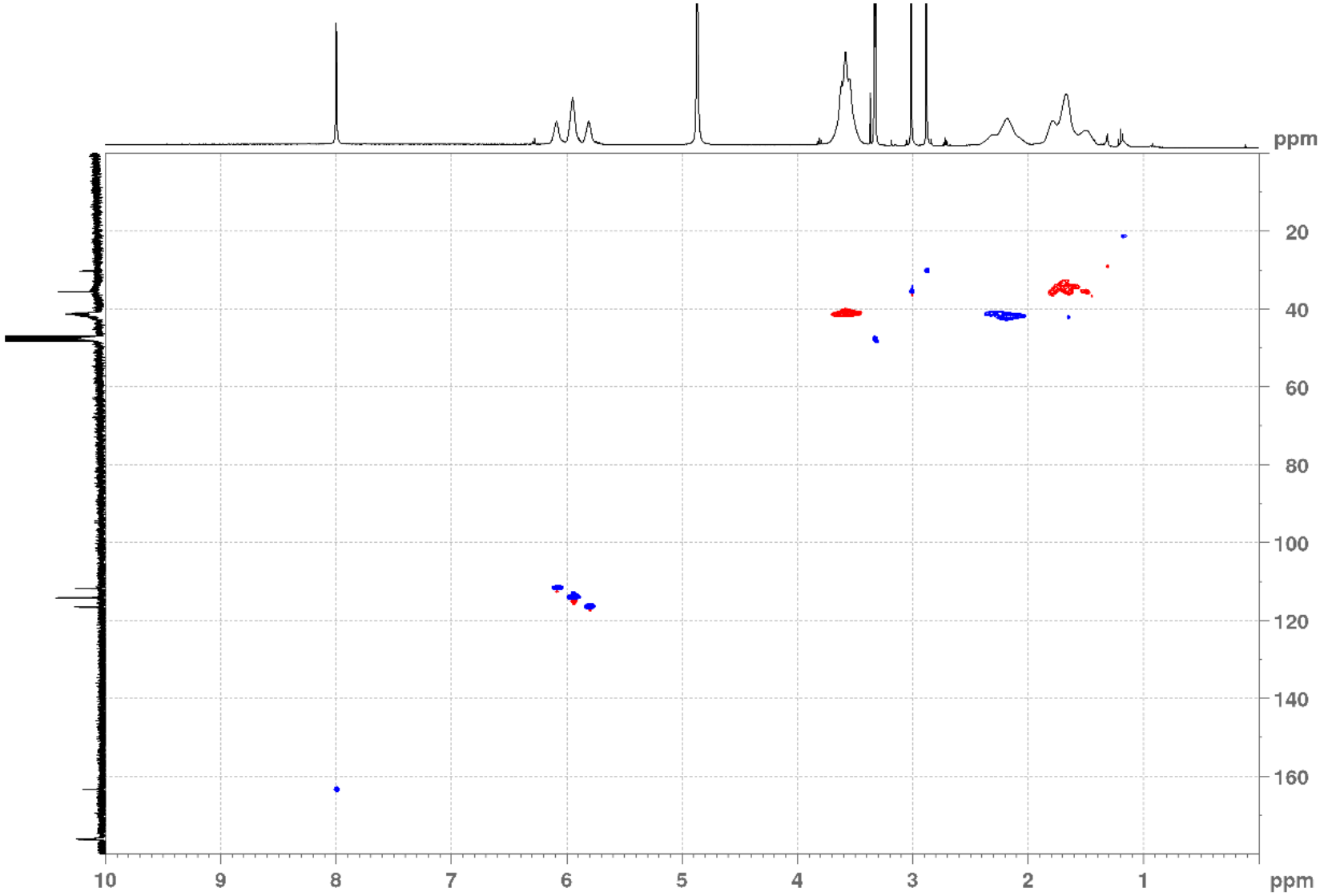

Figure S11. Multiplicity-edited HSQC NMR (400 MHz) spectrum of **pDFEA** polymer in MeOH-4d; negative values (**red**) indicate CH_2 moieties, while positive values (**blue**) indicate CH or CH_3 moieties.

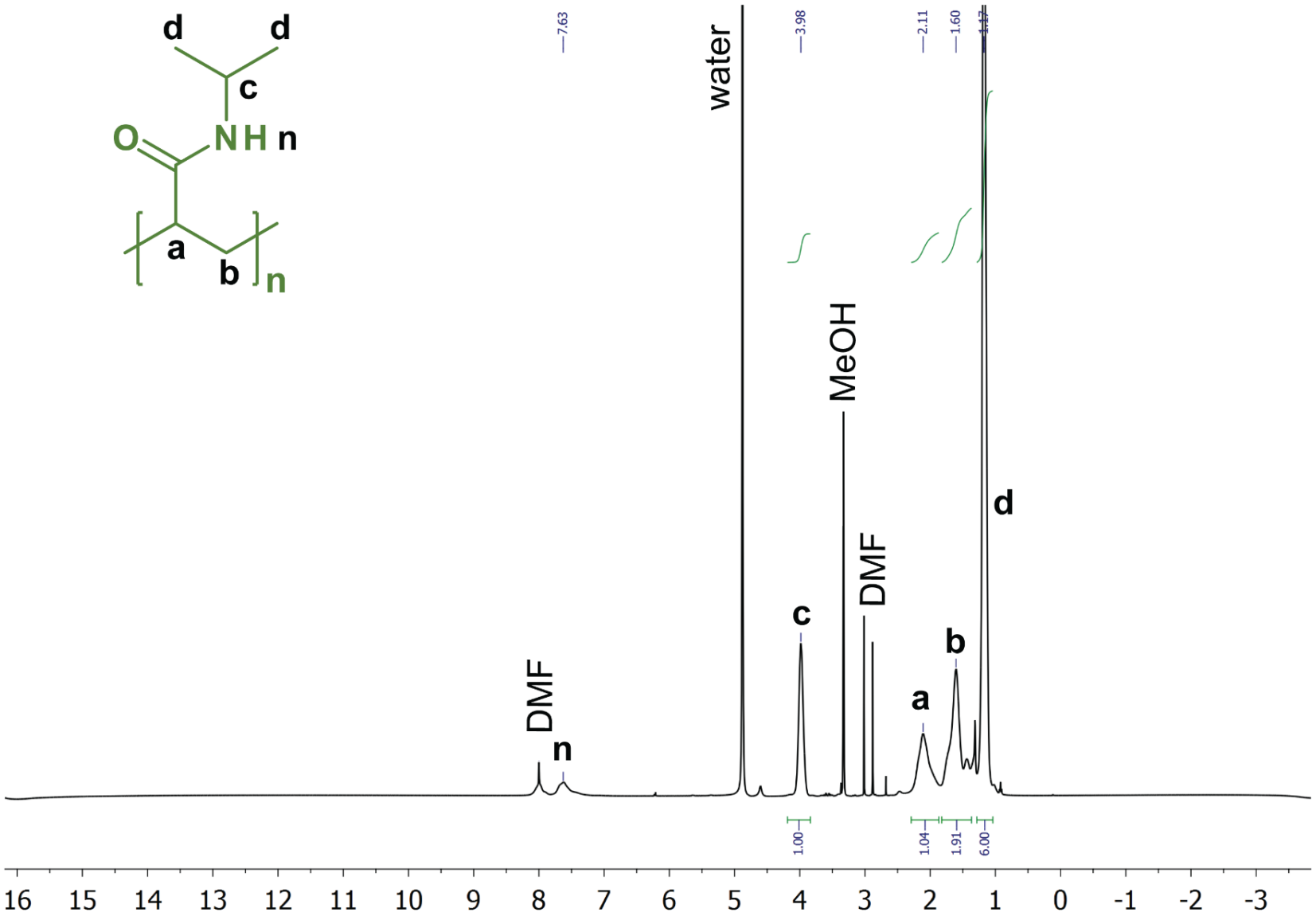

Figure S12. ^{1}H NMR (400 MHz) spectrum of the **pNIPAM** polymer in MeOH-4d: 7.63 (1H), 3.98 (1H), 2.11 (1H), 1.60 (2H), and 1.17 ppm (6H)

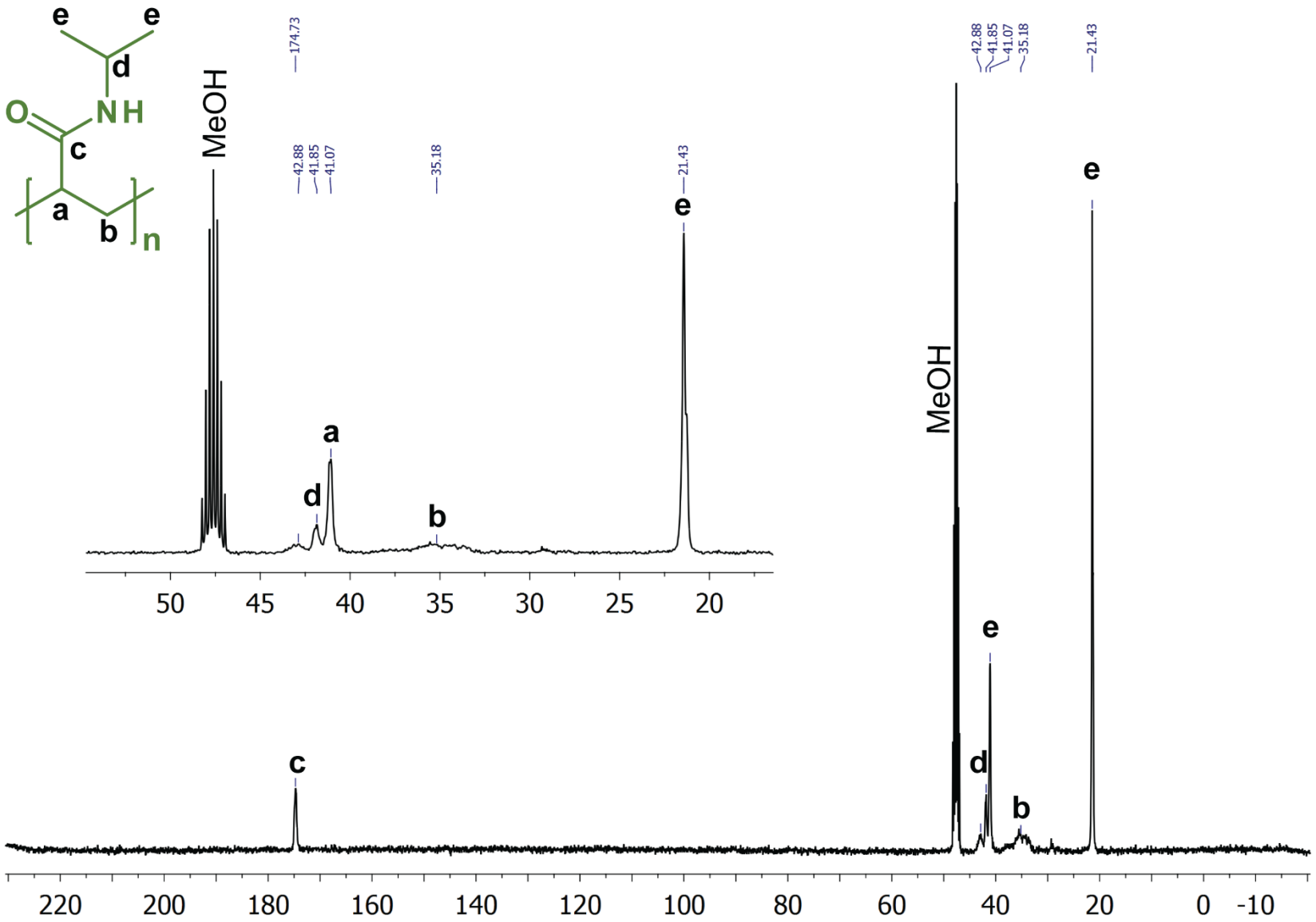

Figure S13. $^{13}C\{^{1}H\}$ NMR (101 MHz) spectrum of the **pNIPAM** polymer in MeOH-4d: 174.8, 42.9, 41.1-41.9, 35.0, and 21.4 ppm

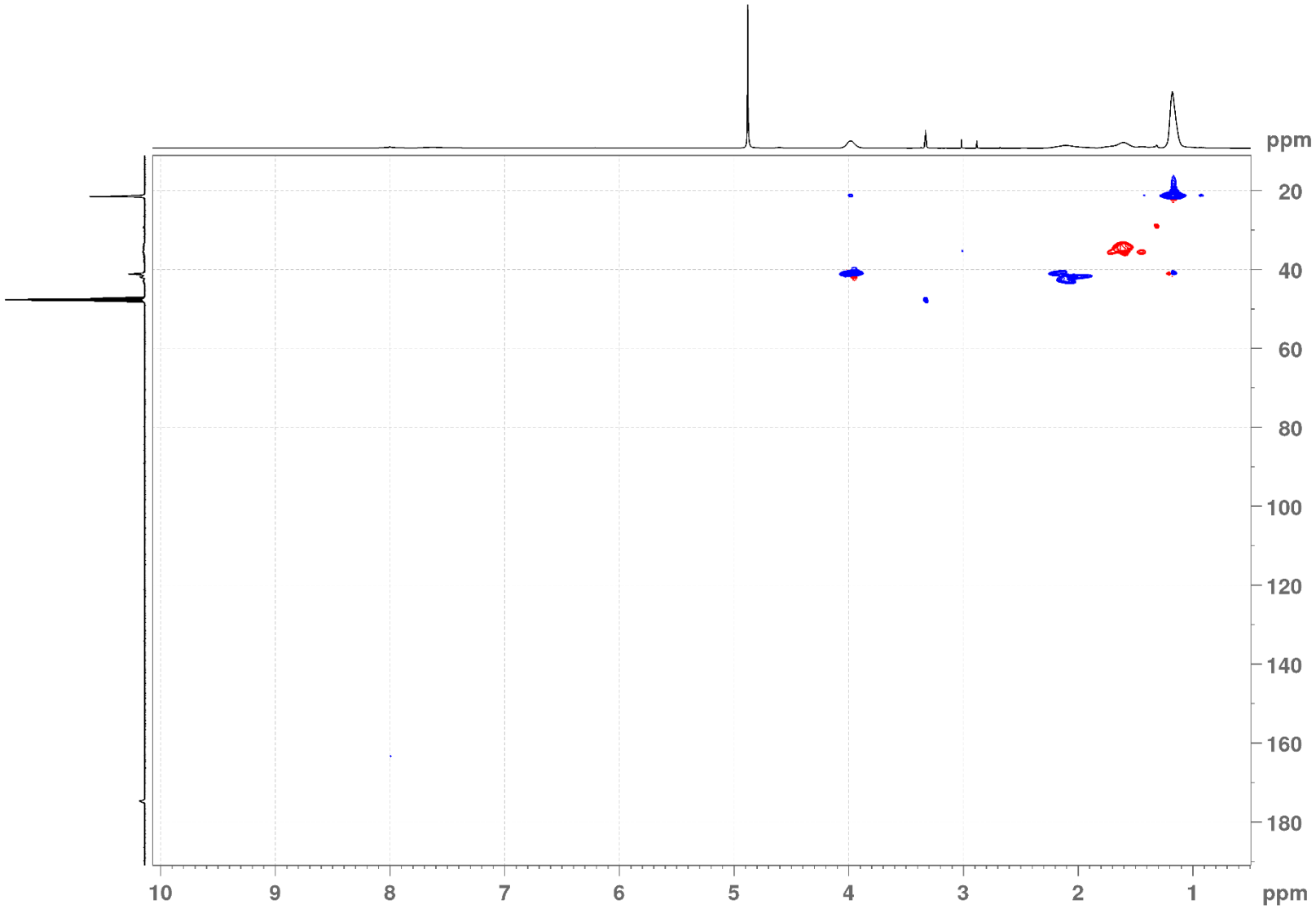

Figure S14. Multiplicity-edited HSQC NMR (400 MHz) spectrum of the **pNIPAM** polymer in MeOH-4d; negative values (**red**) indicate CH_2 moieties, while positive values (**blue**) indicate CH or CH_3 moieties.

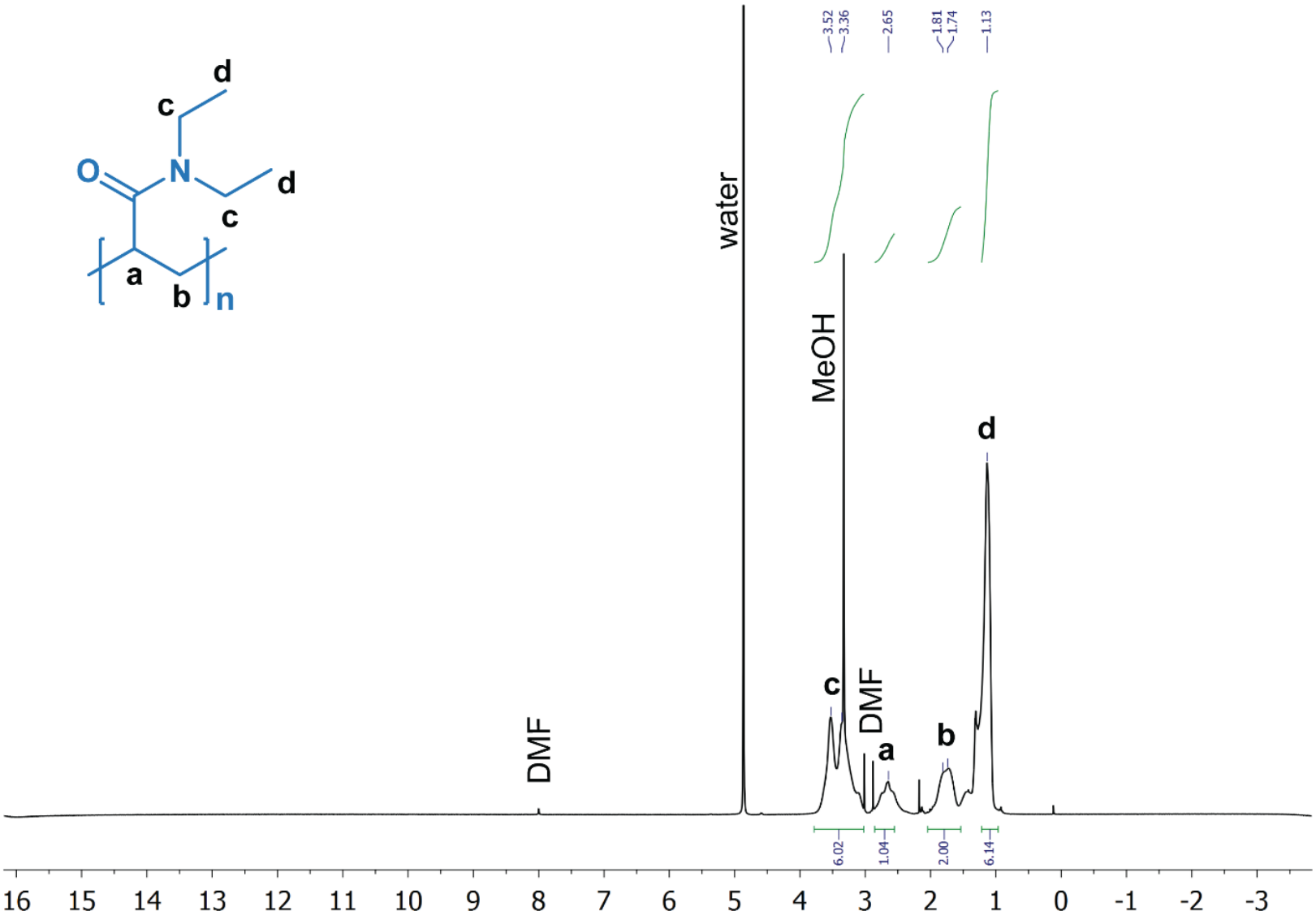

Figure S15. ^{1}H NMR (400 MHz) spectrum of the **pDEA** polymer in MeOH-4d: 3.52-3.36 (4H), 2.65 (1H), 1.74-1.81 (2H), and 1.13 ppm (6H)

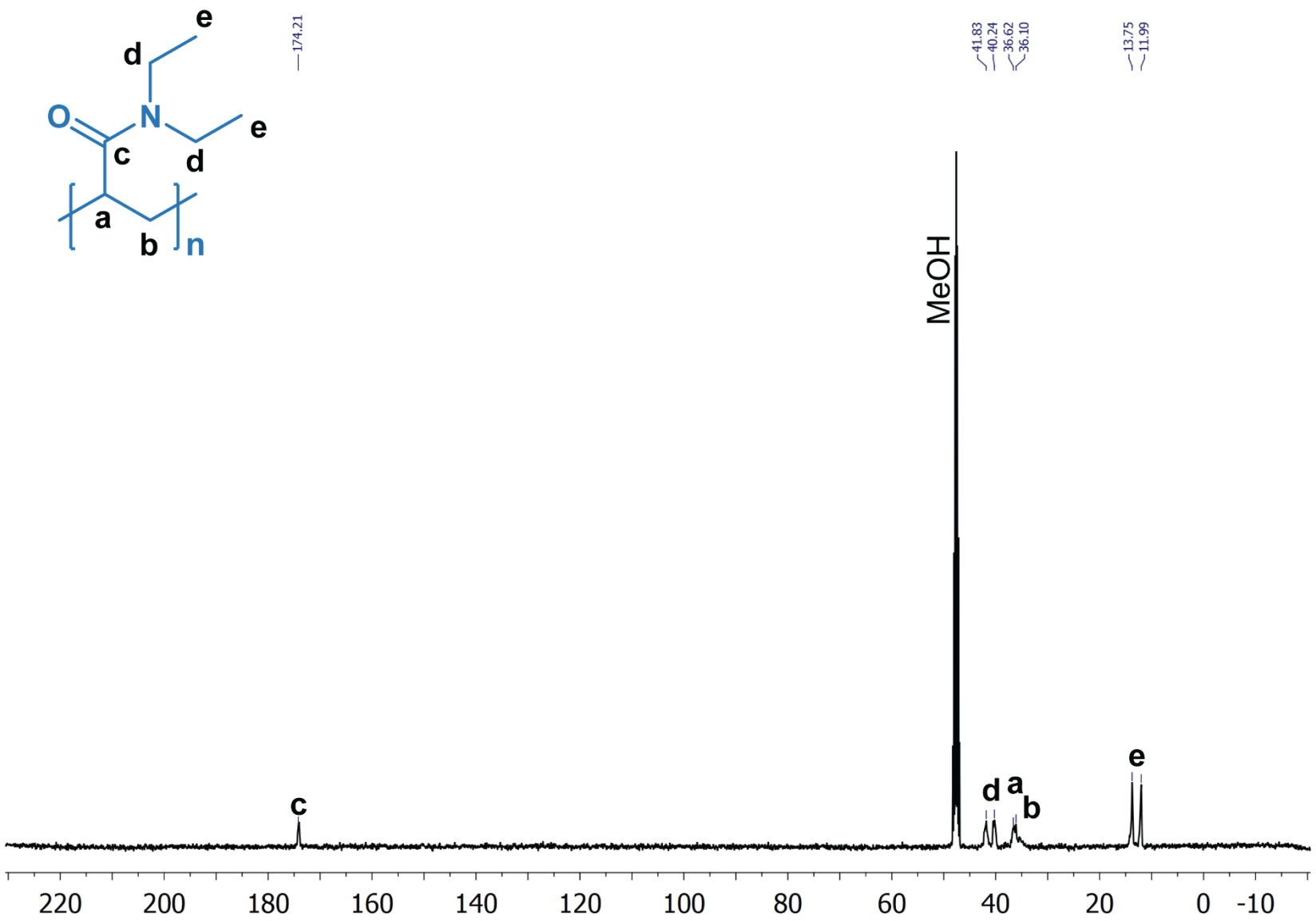

Figure S16. $^{13}C\{^{1}H\}$ NMR (101 MHz) spectrum of the **pDEA** polymer in MeOH-4d: 174.2, 40.2-41.8, 36.6, 36.1, and 12.0-13.8 ppm

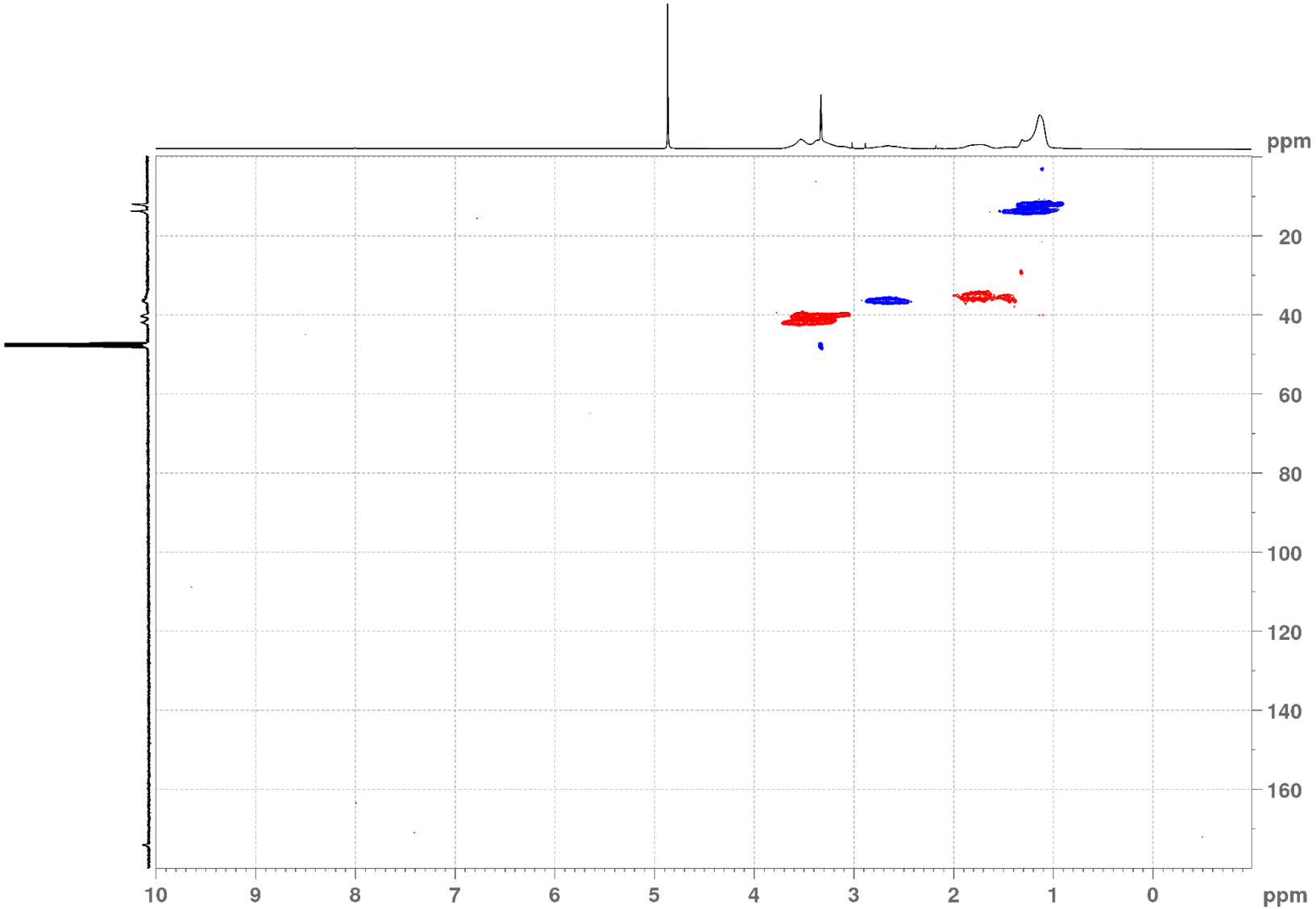

Figure S17. Multiplicity-edited HSQC NMR (400 MHz) spectrum of the **pDEA** polymer in MeOH-4d; negative values (**red**) indicate CH_2 moieties, while positive values (**blue**) indicate CH or CH_3 moieties.

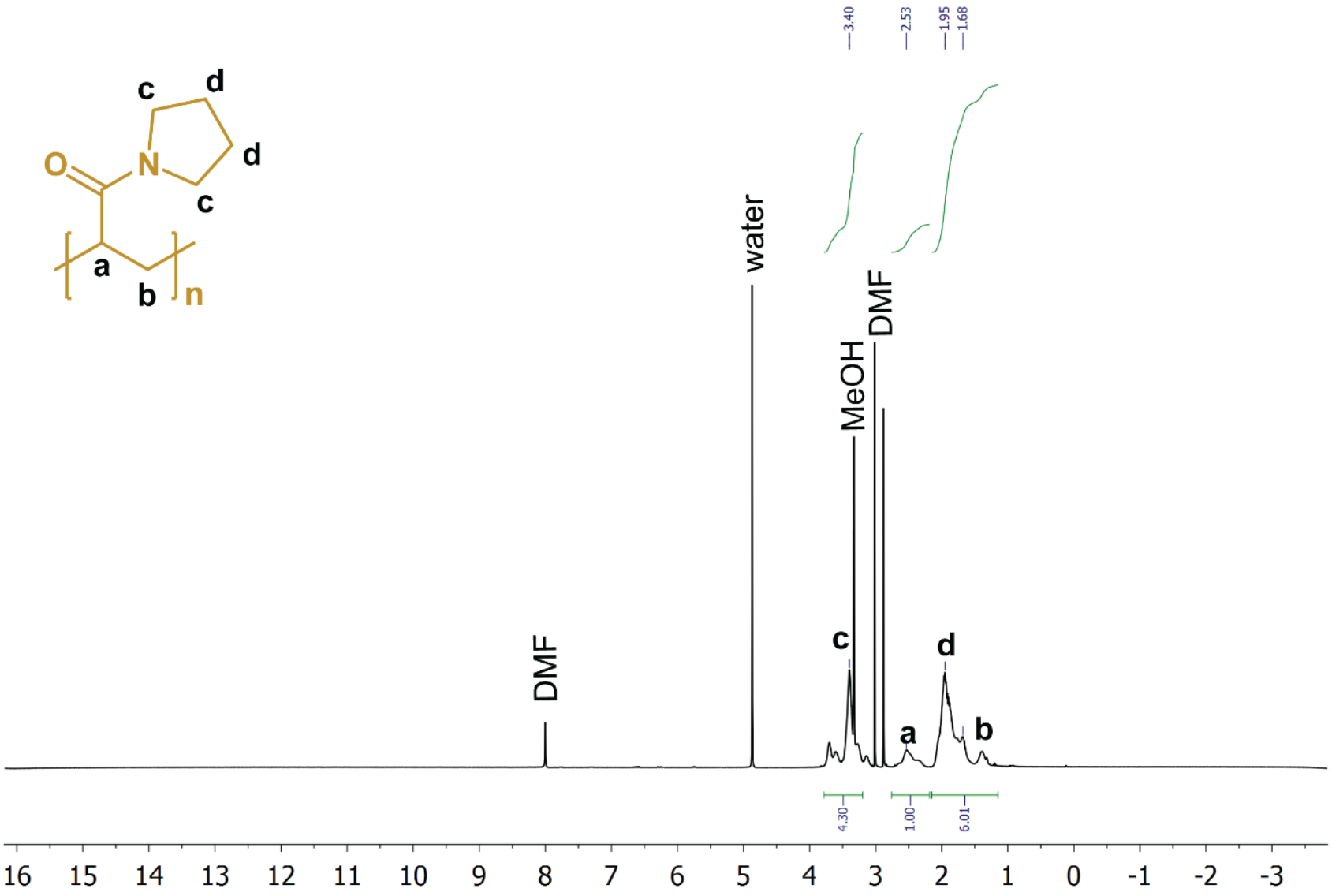

Figure S18. [1]H NMR (400 MHz) spectrum of the **pAP** polymer in MeOH-4d: 3.1-3.8 (4H), 2.3-2.7 (1H), 1.96 (4H), and 1.68 ppm (2H)

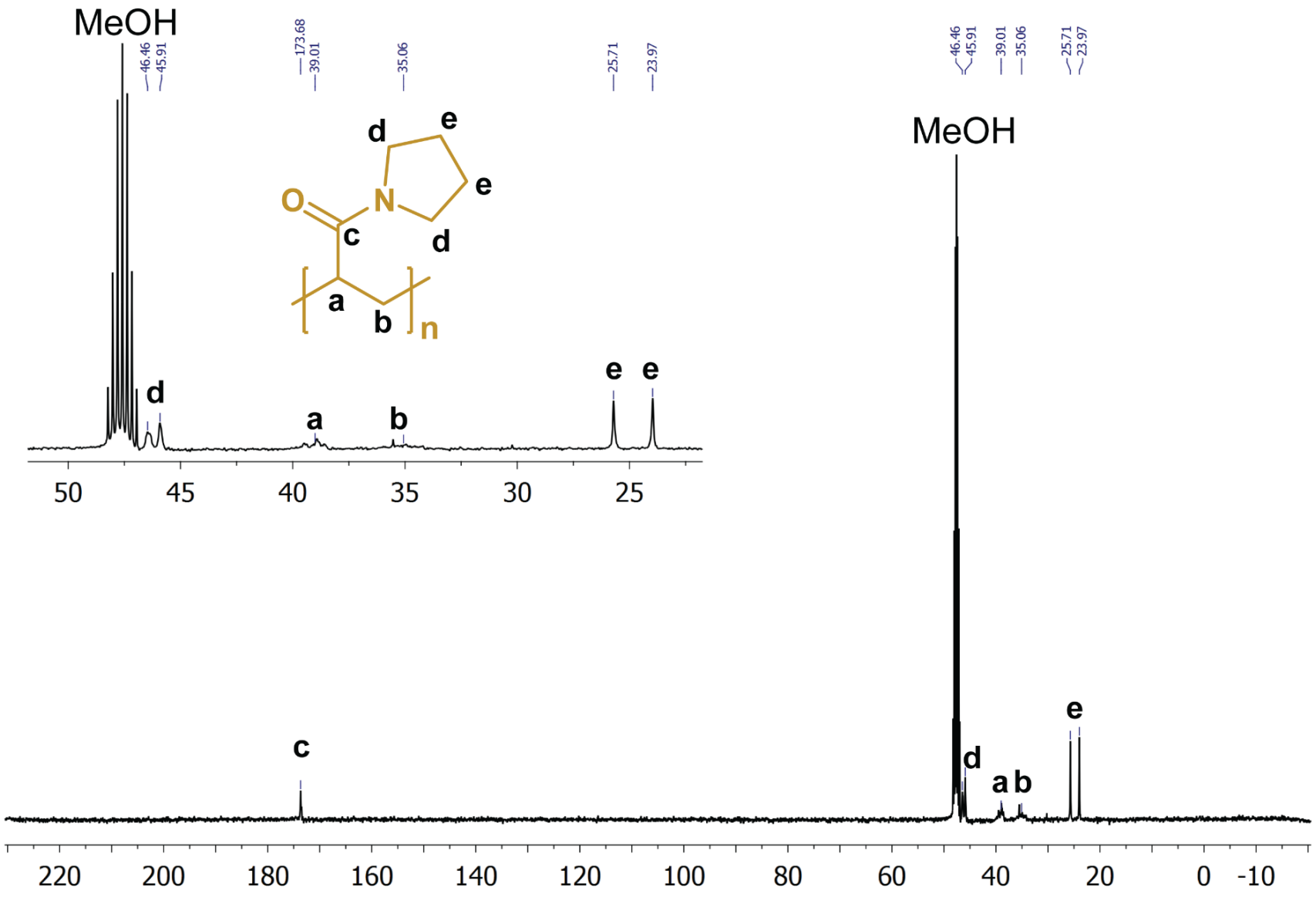

Figure S19. $^{13}C\{^{1}H\}$ NMR (101 MHz) spectrum of the **pAP** polymer in MeOH-4d: 173.7, 45.9-46.5, 39.0, 35.0, 24.0-25.7 ppm

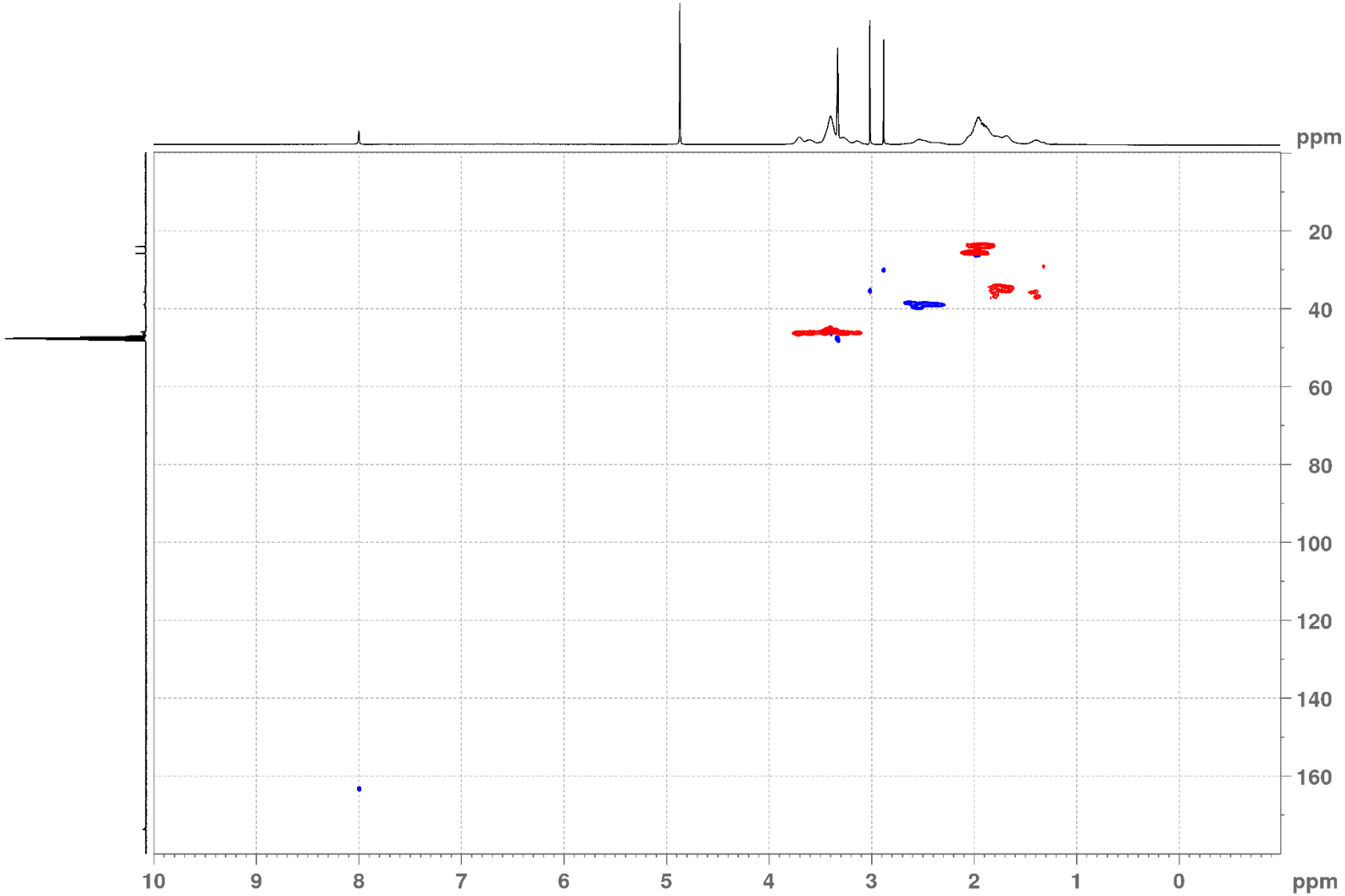

Figure S20. Multiplicity-edited HSQC NMR (400 MHz) spectrum of the **pAP** polymer in MeOH-4d; negative values (**red**) indicate CH_2 moieties, while positive values (**blue**) indicate CH or CH_3 moieties.

S2. Size exclusion chromatograms (SEC traces)

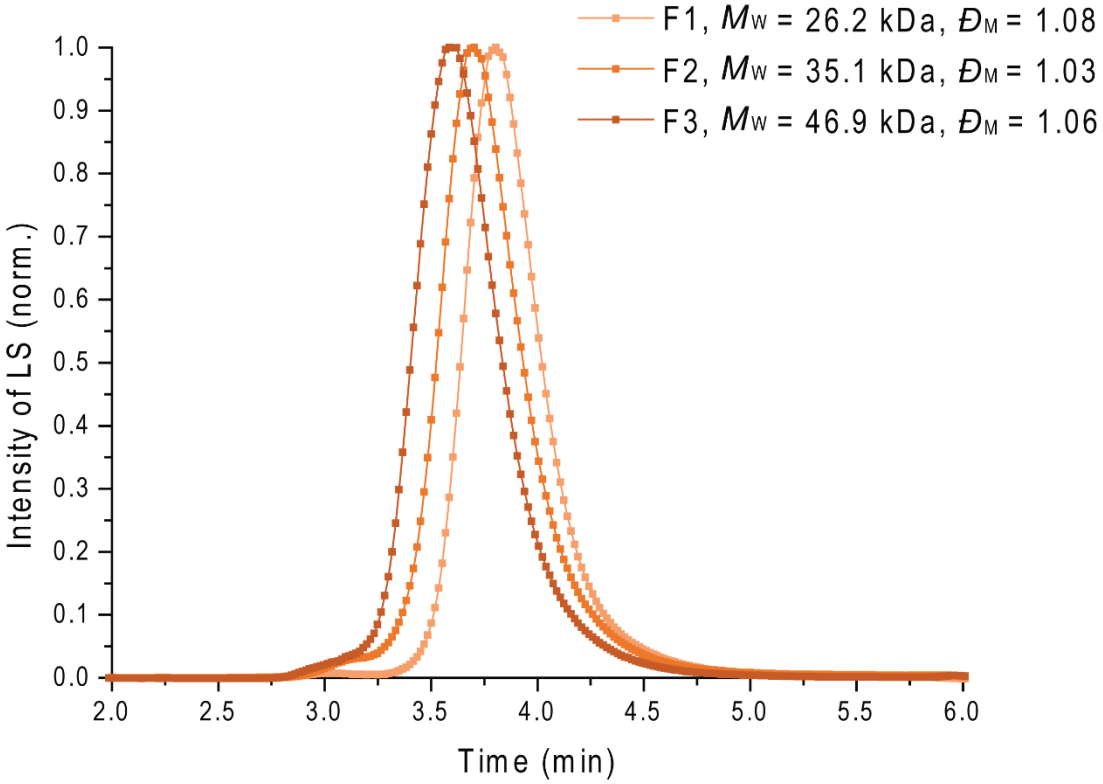

Figure S21. Size exclusion chromatograms of **pDFEA** polymers; mobile phase methanol and sodium acetate buffer (0.3 M, pH 6.5) mixture (80:20 v/v, flow rate of 0.6 mL·min^{-1}). These data were subsequently used to determine the M_w, M_n, and dispersity ($Đ_M$) of the polymers.

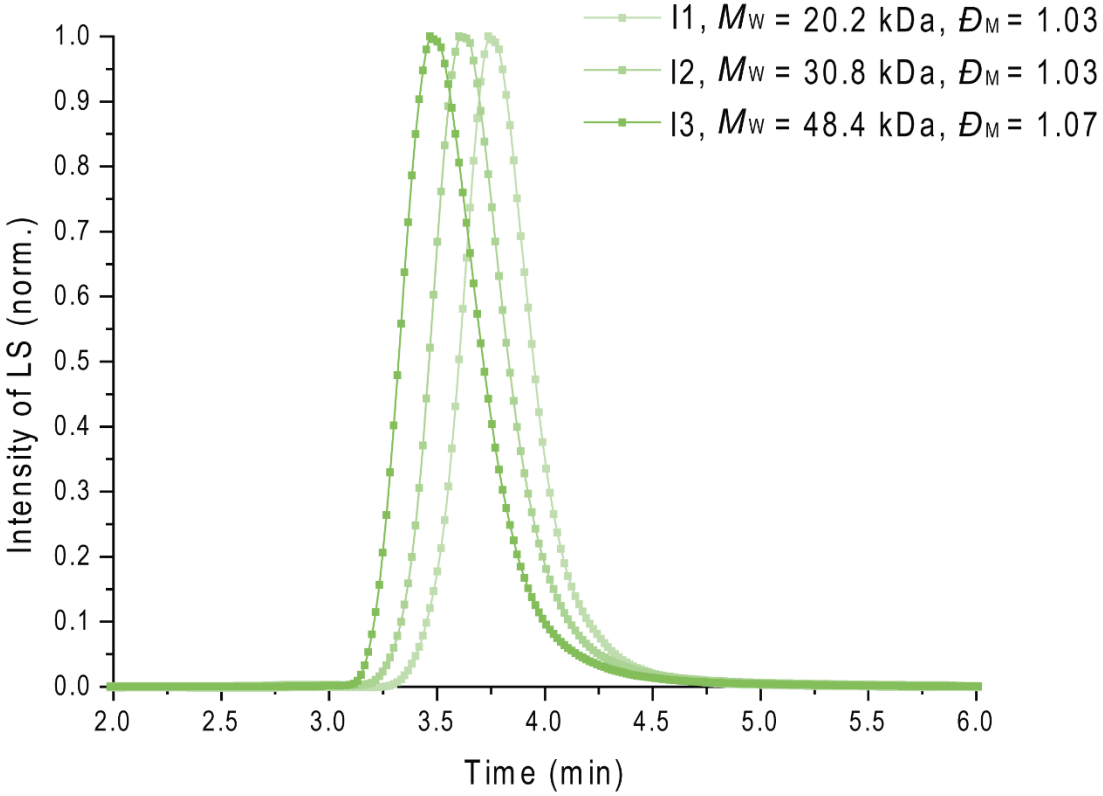

Figure S22. Size exclusion chromatograms of **pNIPAM** polymers; mobile phase methanol and sodium acetate buffer (0.3 M, pH 6.5) mixture (80:20 v/v, flow rate of 0.6 mL·min^{-1}). These data were subsequently used to determine the M_w, M_n, and dispersity ($Đ_M$) of the polymers.

.

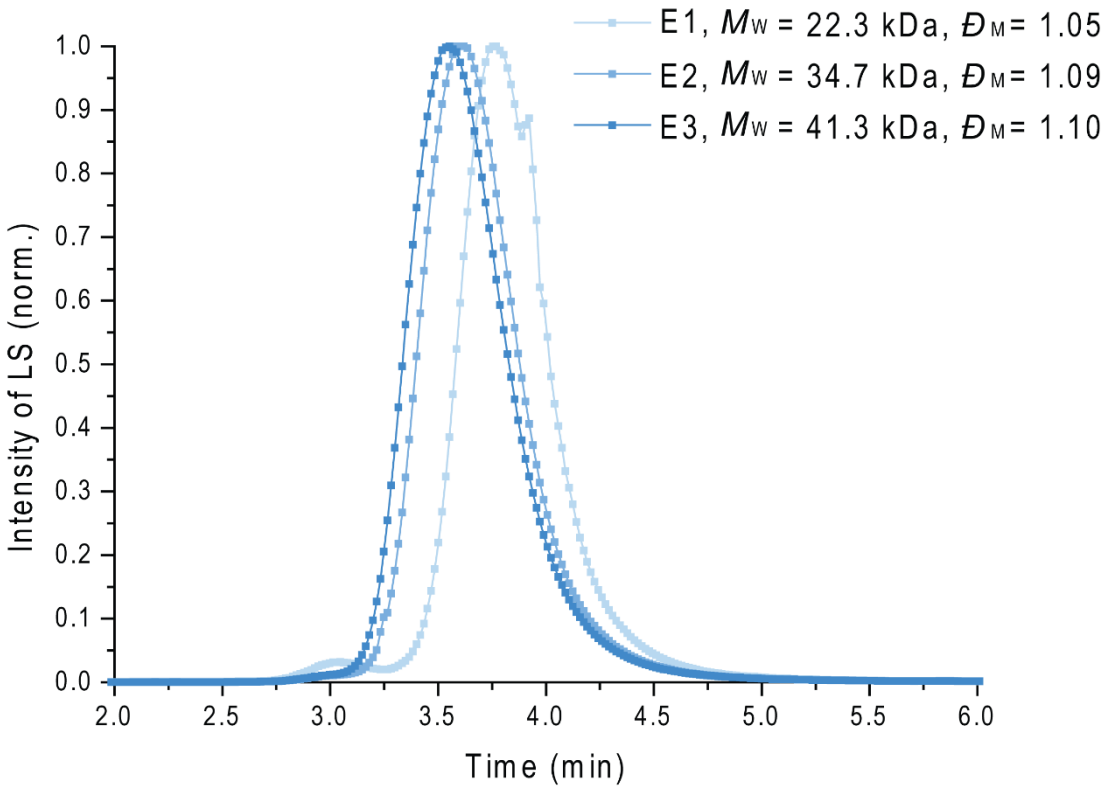

Figure S23. Size exclusion chromatograms of **pDEA** polymers; mobile phase methanol and sodium acetate buffer (0.3 M, pH 6.5) mixture (80:20 v/v, flow rate of 0.6 mL·min^{-1}). These data were subsequently used to determine the M_w, M_n, and dispersity ($Đ_M$) of the polymers.

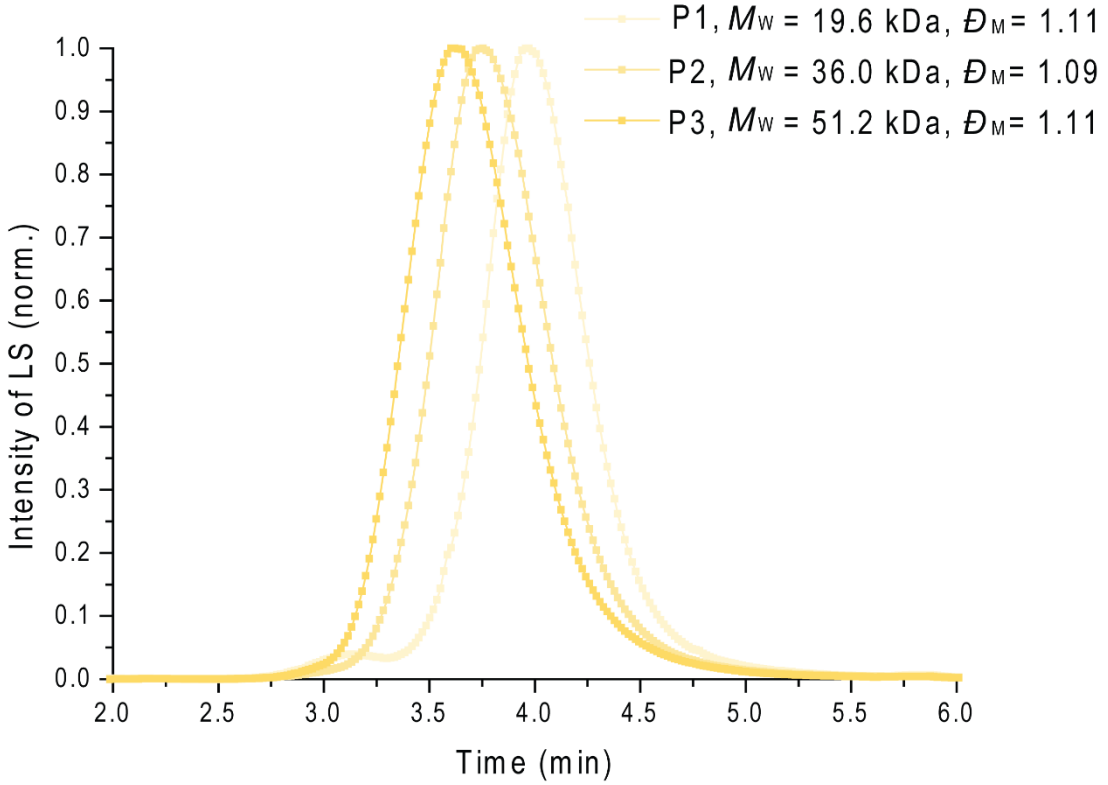

Figure S24. Size exclusion chromatograms of **pAP** polymers; mobile phase methanol and sodium acetate buffer (0.3 M, pH 6.5) mixture (80:20 v/v, flow rate of 0.6 mL·min^{-1}). These data were subsequently used to determine the M_w, M_n, and dispersity ($Đ_M$) of the polymers.

S3. Turbidimetric data – tables

Table S1. T_{CP} values in various solvents (water, PBS and FBS) as a function of the concentration of **pDFEA** polymers (**F1**, **F2**, and **F3**); the data are expressed as mean of 6 experiments and their standard deviation (SD). An asterisk (*) indicates concentration points with multiple outlier points, that were excluded.

Polymer *c* **(mg/ml)**	**F1 (°C)** $T_{CP} \pm SD$	**F2 (°C)** $T_{CP} \pm SD$	**F3 (°C)** $T_{CP} \pm SD$	**F1 (°C)** $T_{CP} \pm SD$	**F2 (°C)** $T_{CP} \pm SD$	**F3 (°C)** $T_{CP} \pm SD$	**F1 (°C)** $T_{CP} \pm SD$	**F2 (°C)** $T_{CP} \pm SD$	**F3 (°C)** $T_{CP} \pm SD$
Medium	**Ultrapure water**			**Phosphate saline buffer**			**Foetal Bovine Serum**		
1.25	-	-	-	64.07 ± 0.05	55.25 ± 0.04	52.22 ± 0.04	33.85 ± 0.10	48.00 ± 0.17	49.97 ± 0.35
2.50	-	-	-	27.07 ± 0.23	30.75 ± 0.12	42.32 ± 0.25	28.25 ± 0.19	37.90 ± 0.23	34.60 ± 0.11
5.0	-	-	-	29.17 ± 0.14	29.95 ± 0.10	42.08 ± 0.24	24.58 ± 0.08	32.52 ± 0.10	29.99 ± 0.08
10.0	27.21 ± 0.62	34.00 ± 0.90	27.33 ± 0.68	27.05 ± 0.25	29.30 ± 0.11	42.48 ± 0.43	22.60 ± 0.06	30.10 ± 0.22	28.67 ± 0.10
20.0	-	-	-	25.57 ± 0.05	31.64 ± 0.20	43.88 ± 0.23	24.63 ± 0.15	28.87 ± 0.12	40.35 ± 0.10*
40.0	-	-	-	24.14 ± 0.10	24.96 ± 0.36	26.73 ± 0.29	24.90 ± 0.35	28.41 ± 0.08	43.80 ± 0.14

Table S2. T_{CP} values in various solvents (water, PBS and FBS) as a function of the concentration of **pNIPAM** polymers (**I1**, **I2**, and **I3**); the data are expressed as mean of 6 experiments and their standard deviation (SD). An asterisk (*) indicates concentration points with multiple outlier points, that were excluded.

Polymer *c* **(mg/ml)**	**I1 (°C)** $T_{CP} \pm SD$	**I2 (°C)** $T_{CP} \pm SD$	**I3 (°C)** $T_{CP} \pm SD$	**I1 (°C)** $T_{CP} \pm SD$	**I2 (°C)** $T_{CP} \pm SD$	**I3 (°C)** $T_{CP} \pm SD$	**I1 (°C)** $T_{CP} \pm SD$	**I2 (°C)** $T_{CP} \pm SD$	**I3 (°C)** $T_{CP} \pm SD$
Medium	**Ultrapure water**			**Phosphate saline buffer**			**Foetal Bovine Serum**		
1.25	-	-	-	33.42 ± 0.04	30.98 ± 0.04	29.65 ± 0.10	33.62 ± 0.08	30.88 ± 0.04	29.72 ± 0.04
2.50	-	-	-	32.25 ± 0.18	30.18 ± 0.11	29.13 ± 0.05	30.90 ± 0.15	28.62 ± 0.10	27.64 ± 0.05
5.0	-	-	-	31.08 ± 0.10	29.48 ± 0.08	28.75 ± 0.05	28.98 ± 0.10	26.30 ± 0.11	25.70 ± 0.06
10.0	29.98 ± 0.27	31.39 ± 0.17	31.59 ± 0.43	29.25 ± 0.10	28.30 ± 0.06	28.05 ± 0.10	25.67 ± 0.10	24.39 ± 0.10	24.60 ± 0.06
20.0	-	-	-	28.95 ± 0.05	26.80 ± 0.00	28.29 ± 0.04	28.90 ± 0.09	29.23 ± 0.15	33.05 ± 0.32
40.0	-	-	-	26.90 ± 0.34	28.37 ± 0.05	28.28 ± 0.04	28.82 ± 0.34	28.43 ± 0.16	31.03 ± 0.13

Table S3. T_{CP} values in various solvents (water, PBS and FBS) as a function of the concentration of **pDEA** polymers (**E1**, **E2**, and **E3**); the data are expressed as mean of 6 experiments and their standard deviation (SD). An asterisk (*) indicates concentration points with multiple outlier points, that were excluded.

Polymer *c* **(mg/ml)**	**E1 (°C)** $T_{CP} \pm SD$	**E2 (°C)** $T_{CP} \pm SD$	**E3 (°C)** $T_{CP} \pm SD$	**E1 (°C)** $T_{CP} \pm SD$	**E2 (°C)** $T_{CP} \pm SD$	**E3 (°C)** $T_{CP} \pm SD$	**E1 (°C)** $T_{CP} \pm SD$	**E2 (°C)** $T_{CP} \pm SD$	**E3 (°C)** $T_{CP} \pm SD$
Medium	**Ultrapure water**			**Phosphate saline buffer**			**Foetal Bovine Serum**		
1.25	-	-	-	31.88 ± 0.04	31.72 ± 0.04	31.17 ± 0.05	35.77 ± 0.25	32.60 ± 0.24	31.53 ± 0.23
2.50	-	-	-	29.58 ± 0.08	30.85 ± 0.08	29.30 ± 0.09	31.90 ± 0.14	30.00 ± 0.20	29.12 ± 0.15
5.0	-	-	-	28.20 ± 0.06	29.98 ± 0.04	28.35 ± 0.08	28.03 ± 0.20	27.97 ± 0.16	27.07 ± 0.15
10.0	29.28 ± 0.04	30.16 ± 0.11	29.92 ± 0.12	27.37 ± 0.08	28.47 ± 0.10	27.60 ± 0.11	23.95 ± 0.12	25.82 ± 0.17	25.27 ± 0.19
20.0	-	-	-	28.92 ± 0.16*	29.17 ± 0.06*	29.18 ± 0.05*	27.93 ± 0.13	29.47 ± 0.09	29.34 ± 0.07
40.0	-	-	-	28.85 ± 1.34*	28.75 ± 0.07*	28.87 ± 0.06*	27.57 ± 0.23	28.33 ± 0.05	27.88 ± 0.08

Table S4. T_{CP} values in various solvents (water, PBS and FBS) as a function of the concentration of **pAP** polymers (**P1**, **P2**, and **P3**); the data are expressed as mean of 6 experiments and their standard deviation (SD). An asterisk (*) indicates concentration points with multiple outlier points, that were excluded.

Polymer *c* **(mg/ml)**	**P1 (°C)** $T_{CP} \pm SD$	**P2 (°C)** $T_{CP} \pm SD$	**P3 (°C)** $T_{CP} \pm SD$	**P1 (°C)** $T_{CP} \pm SD$	**P2 (°C)** $T_{CP} \pm SD$	**P3 (°C)** $T_{CP} \pm SD$	**P1 (°C)** $T_{CP} \pm SD$	**P2 (°C)** $T_{CP} \pm SD$	**P3 (°C)** $T_{CP} \pm SD$
Medium	**Ultrapure water**			**Phosphate saline buffer**			**Foetal Bovine Serum**		
1.25	-	-	-	64.06 ± 0.05	55.28 ± 0.06	52.22 ± 0.04	75.02 ± 0.79	59.18 ± 0.08	55.31 ± 0.08
2.50	-	-	-	58.35 ± 0.16	52.68 ± 0.08	50.23 ± 0.10	70.70 ± 0.57	53.67 ± 0.19	50.55 ± 0.14
5.0	-	-	-	55.15 ± 0.08	49.15 ± 0.10	47.73 ± 0.08	60.85 ± 0.37	51.83 ± 0.08	48.53 ± 0.08
10.0	58.10 ± 0.10	56.78 ± 0.42	56.2 ± 0.58	53.65 ± 0.10	47.30 ± 0.17	46.27 ± 0.10	56.72 ± 0.34	48.63 ± 0.14	45.73 ± 0.08
20.0	-	-	-	54.65 ± 0.04	50.09 ± 0.02	50.13 ± 0.05	54.62 ± 0.40	58.40 ± 0.14*	49.57 ± 0.08
40.0	-	-	-	54.00 ± 0.14	48.38 ± 0.22	48.08 ± 0.12	49.53 ± 0.38	33.65 ± 0.20	48.98 ± 0.12

Note: At high polymer concentrations (20 and 40 mg/mL), the cloud point temperatures were poorly reproducible and unreliable, and the inter-run-differences were up to 20°C (particularly in **pDFEA** in PBS). At low concentrations (1.25 to 10.0 mg/mL), multiple independent experiments provided the same value of T_{CP} (within a margin of 0.5°C). We kept repeating measurements until two independent runs provided *similar* results and reliable turbidimetry-as-a-function-of-temperature graphs (*i.e.*, the turbidity decreased monotonously and relatively quickly with no sudden or inexplicable changes in trends). Therefore, we concluded that turbidimetry is not a reliable method for determining T_{CP}s at high polymer concentrations and these data were accordingly disregarded from further interpretations. Nevertheless, we present the complete set of our results in **Tables S3** to **S6**.

S4. Raw turbidimetric data

Every polymer solution was measured at least 6 times. If the data from all runs were similar, the data was processed: we calculated the mean values and standard deviations of T_{CP}s (**Table S1 to S4**). Only one cycle is shown in **Figures S25** to **S36** for clarity.

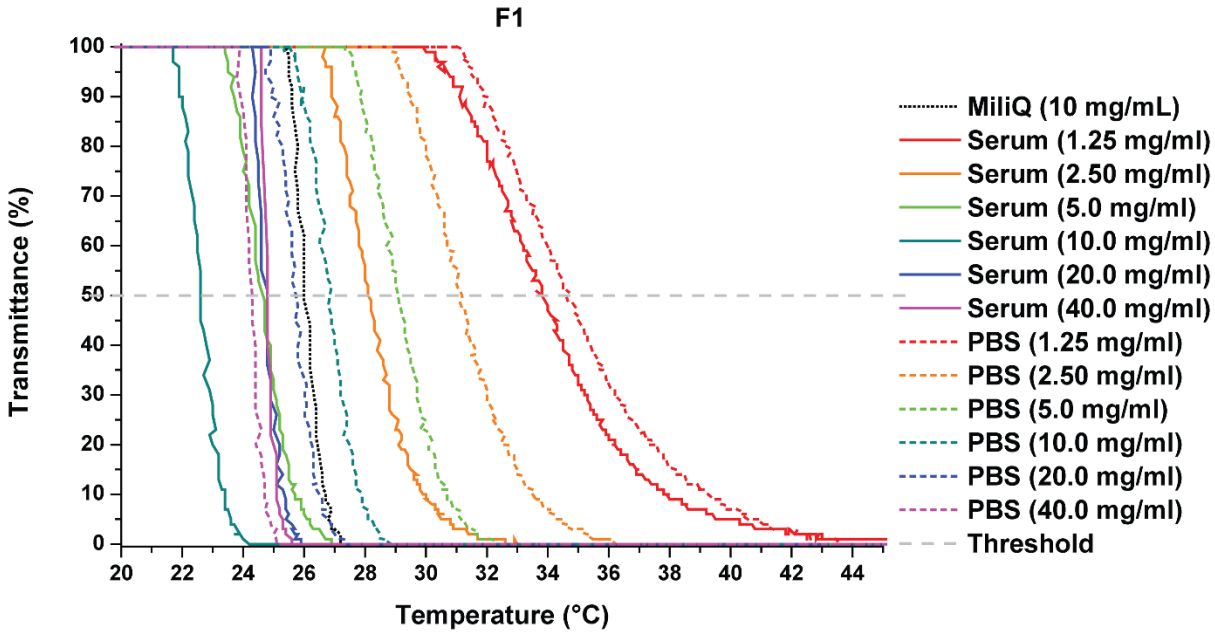

Figure S25. Transmittance of the **F1** (**pDFEA**) solution in ultrapure water (MiliQ), PBS, and FBS (serum), respectively, as a function of temperature

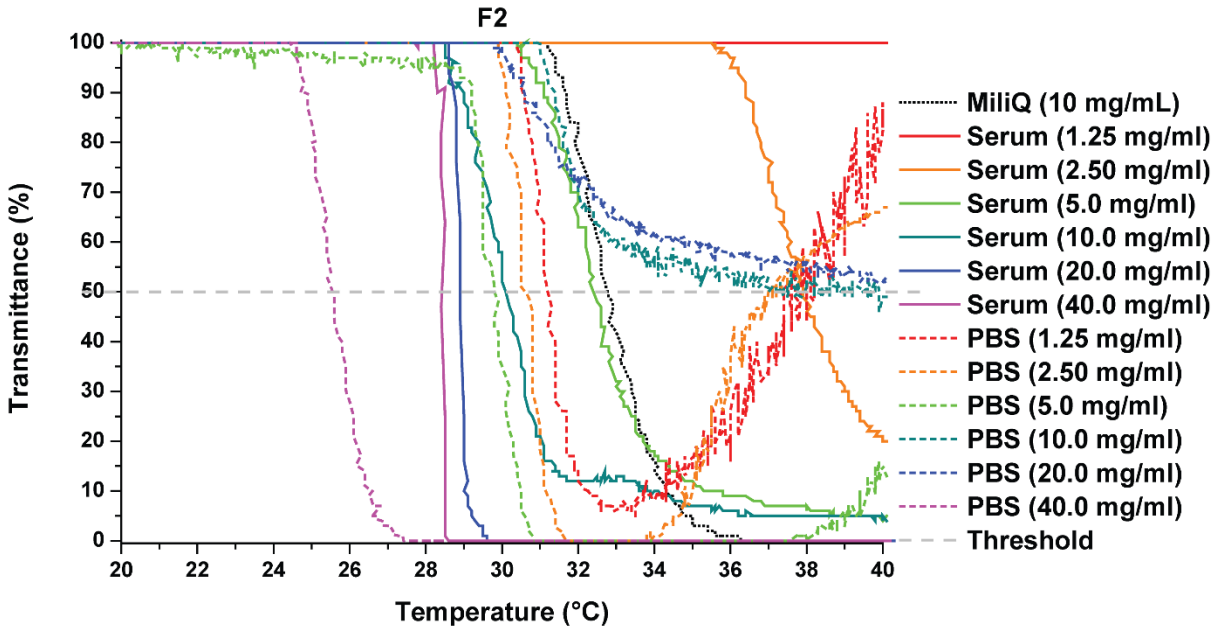

Figure S26. Transmittance of the **F2** (**pDFEA**) solution in ultrapure water (MiliQ), PBS, and FBS (serum), respectively, as a function of temperature

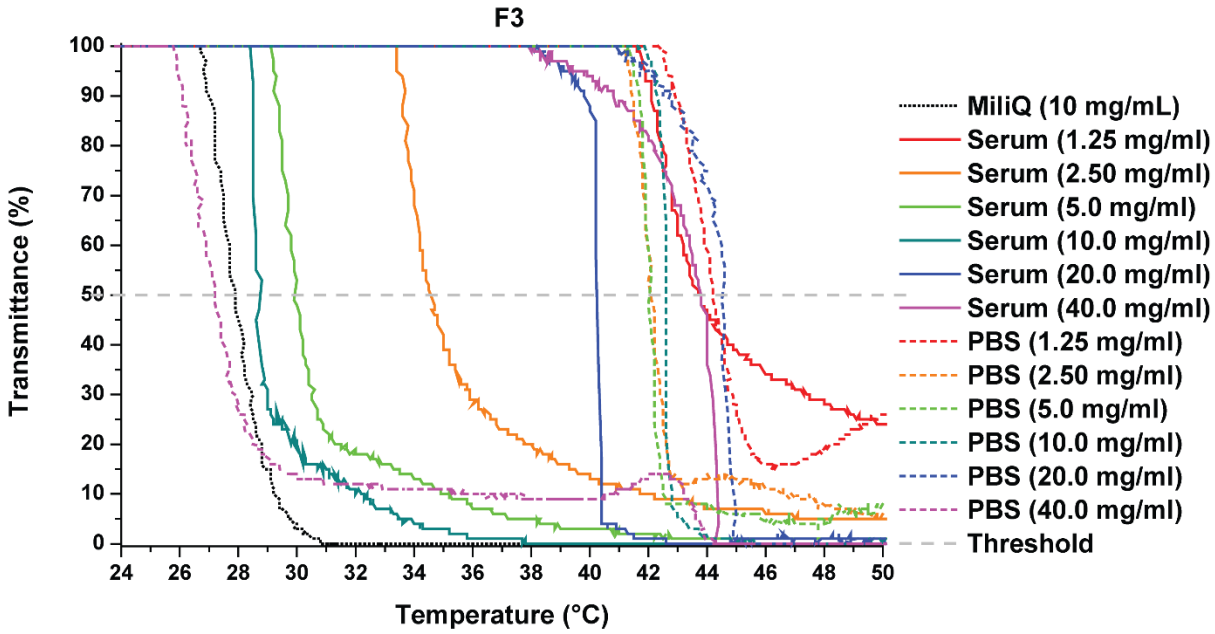

Figure S27. Transmittance of the **F3** (**pDFEA**) solution in ultrapure water (MiliQ), PBS, and FBS (serum), respectively, as a function of temperature

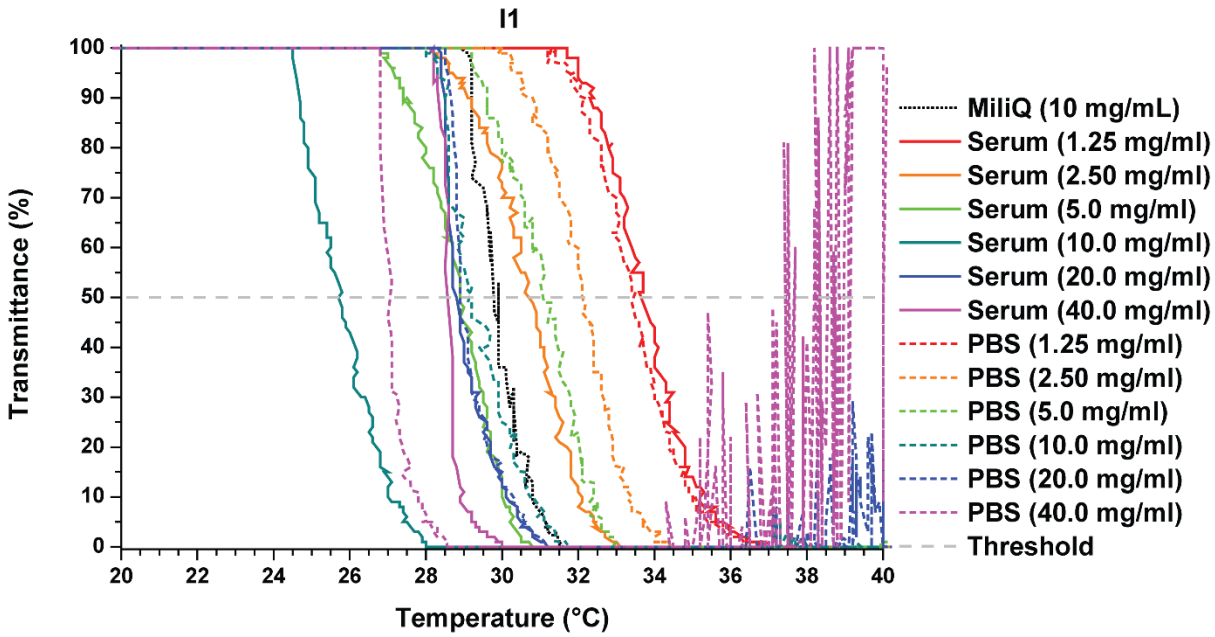

Figure S28. Transmittance of the **I1** (**pNIPAM**) solution in ultrapure water (MiliQ), PBS, and FBS (serum), respectively, as a function of temperature

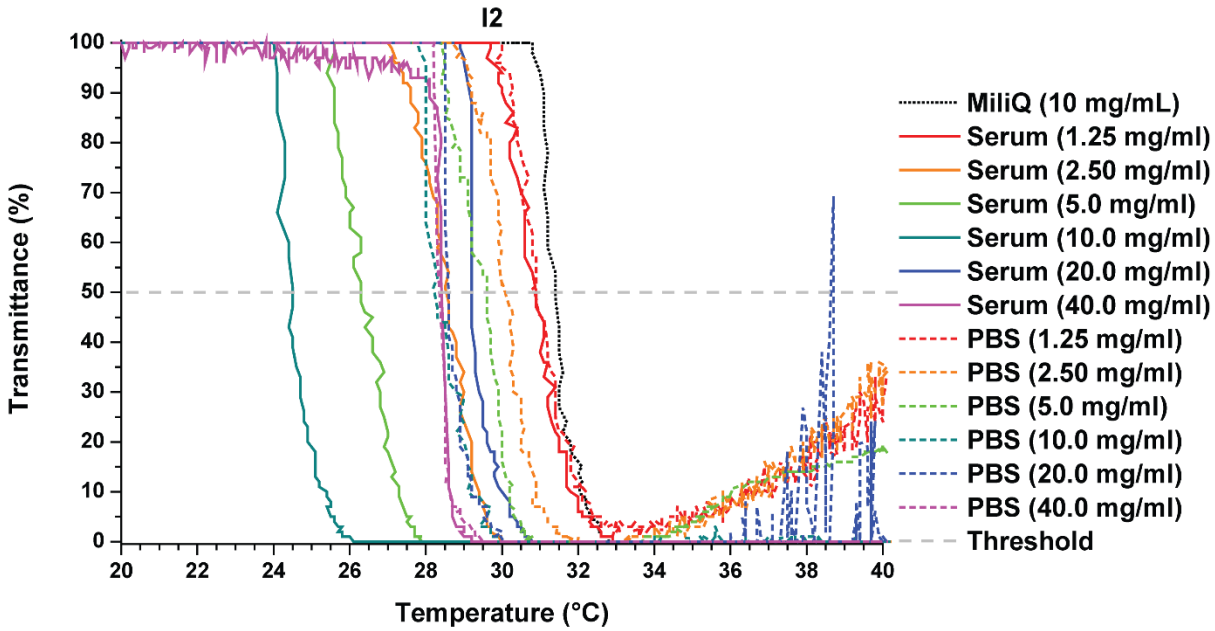

Figure S29. Transmittance of the **I2** (**pNIPAM**) solution in ultrapure water (MiliQ), PBS, and FBS (serum), respectively, as a function of temperature

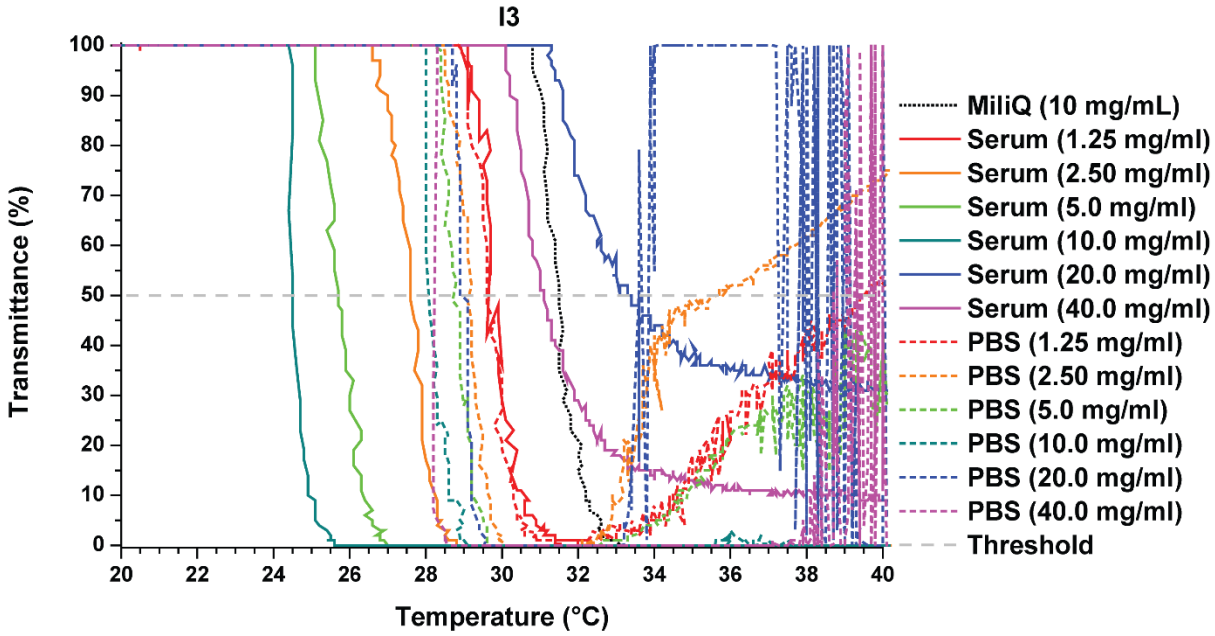

Figure S30. Transmittance of the **I3** (**pNIPAM**) solution in ultrapure water (MiliQ), PBS, and FBS (serum), respectively, as a function of temperature

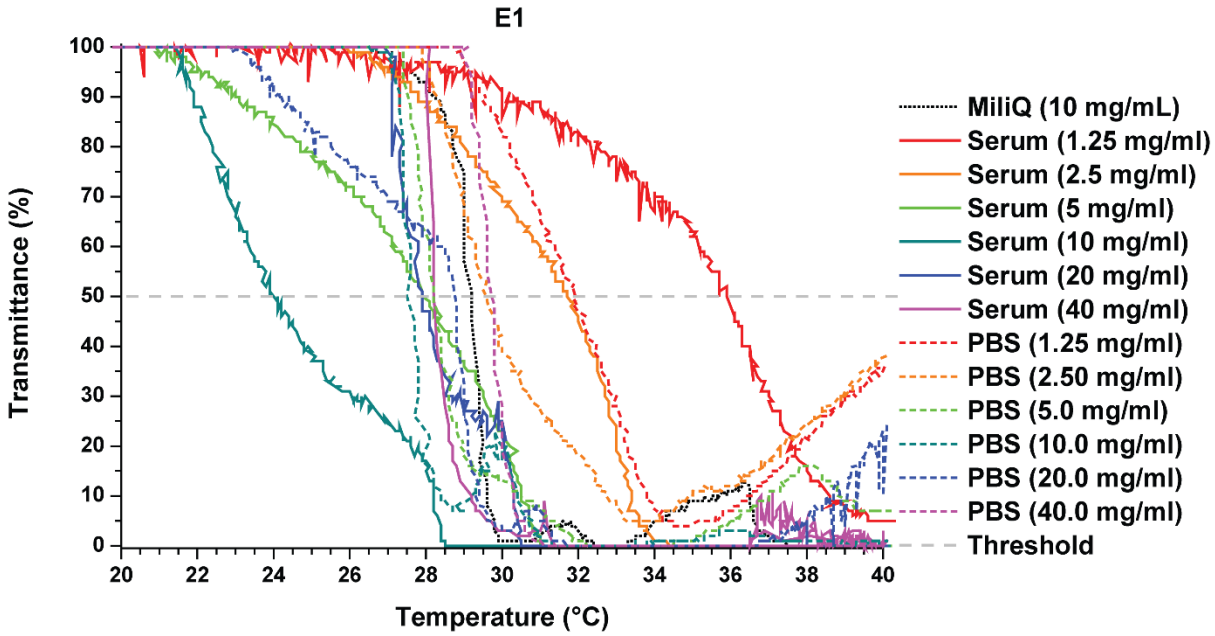

Figure S31. Transmittance of the **E1** (**pDEA**) solution in ultrapure water (MiliQ), PBS, and FBS (serum), respectively, as a function of temperature

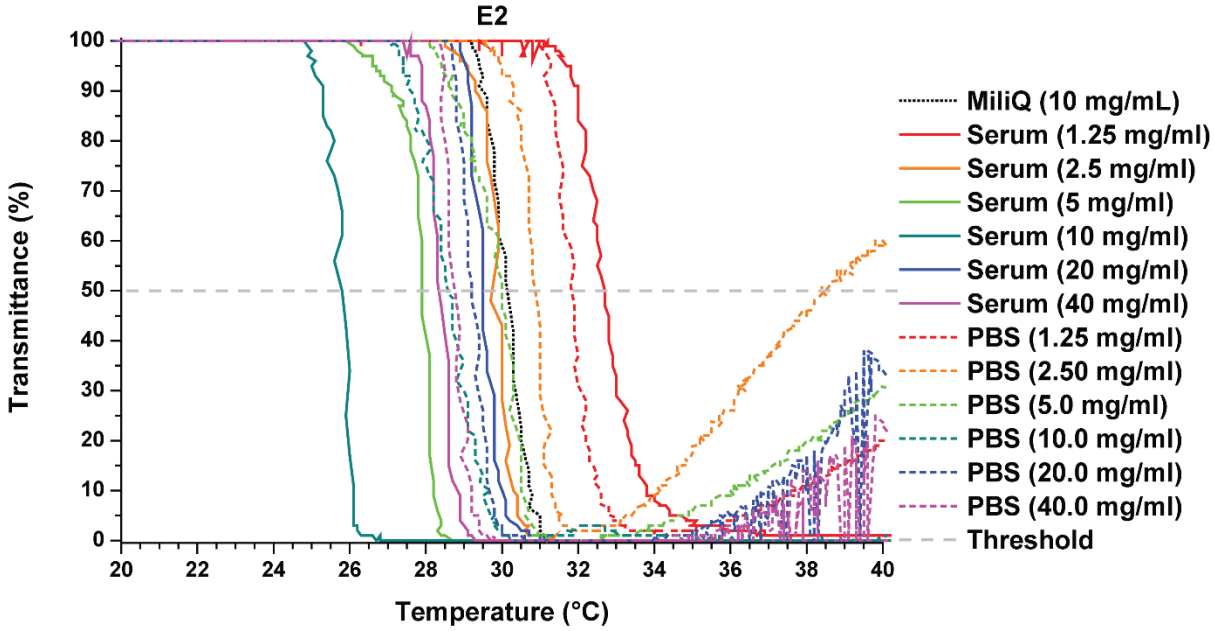

Figure S32. Transmittance of the **E2** (**pDEA**) solution in ultrapure water (MiliQ), PBS, and FBS (serum), respectively, as a function of temperature

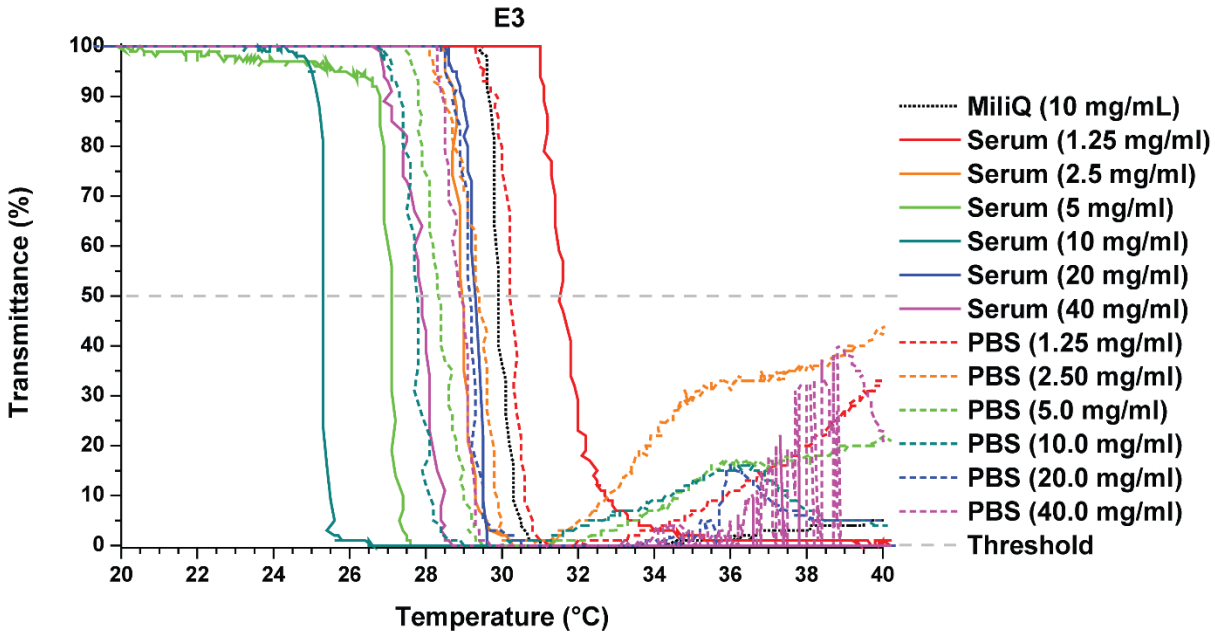

Figure S33. Transmittance of the **E3** (**pDEA**) solution in ultrapure water (MiliQ), PBS, and FBS (serum), respectively, as a function of temperature

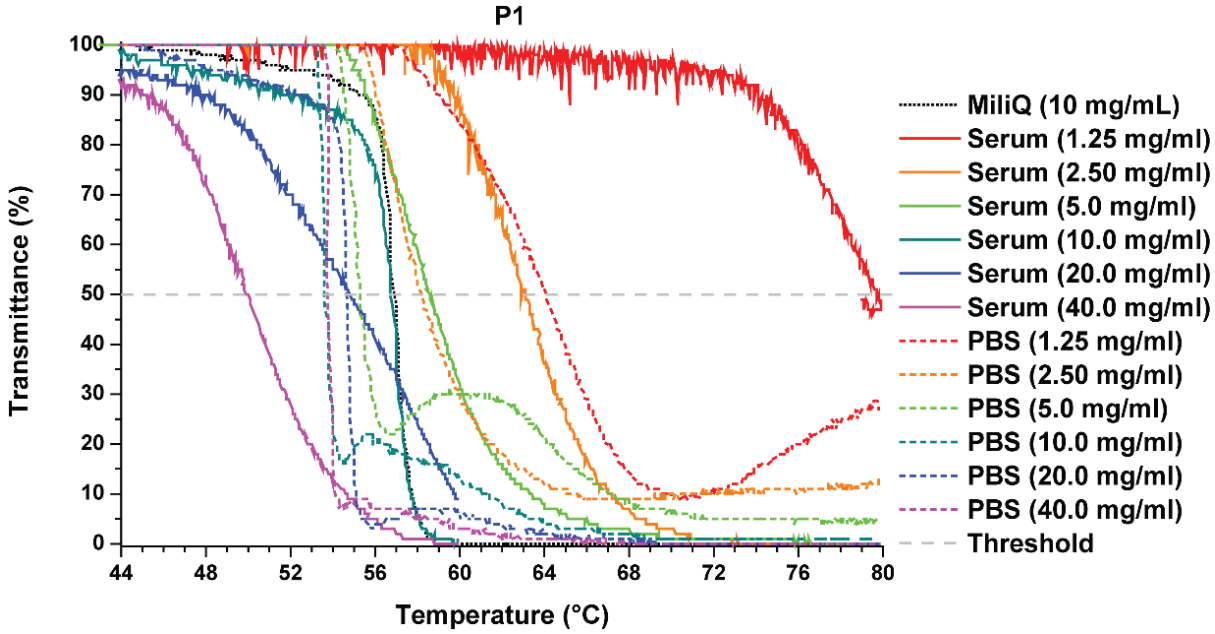

Figure S34. Transmittance of the **P1** (**pAP**) solution in ultrapure water (MiliQ), PBS, and FBS (serum), respectively, as a function of temperature

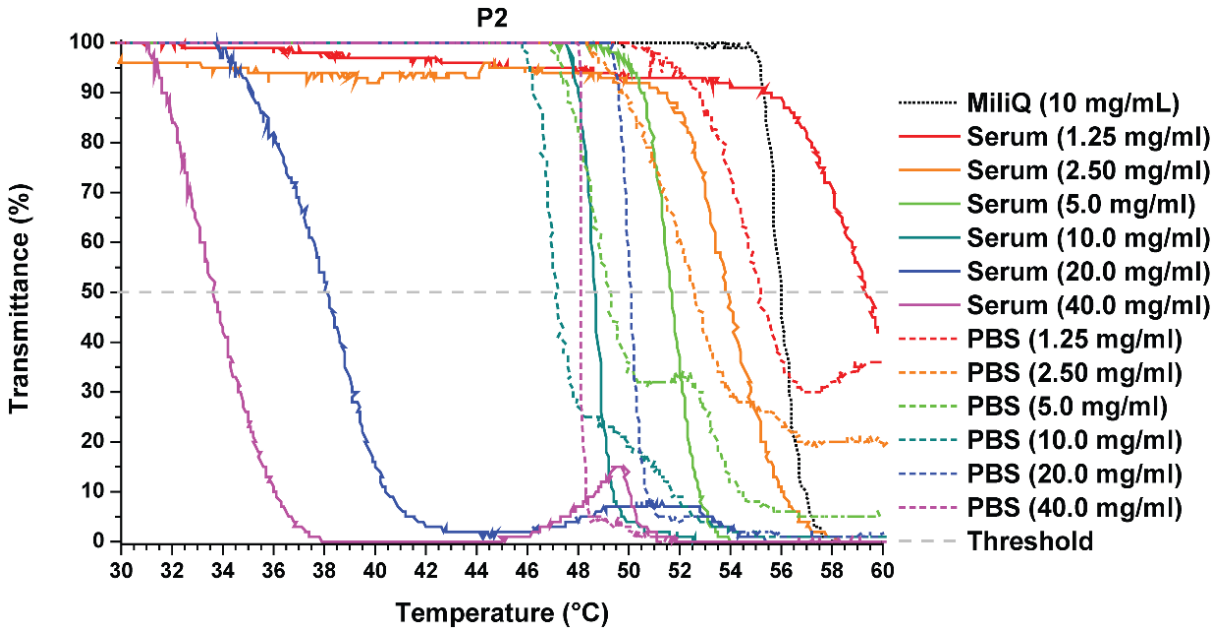

Figure S35. Transmittance of the **P2** (**pAP**) solution in ultrapure water (MiliQ), PBS, and FBS (serum), respectively, as a function of temperature

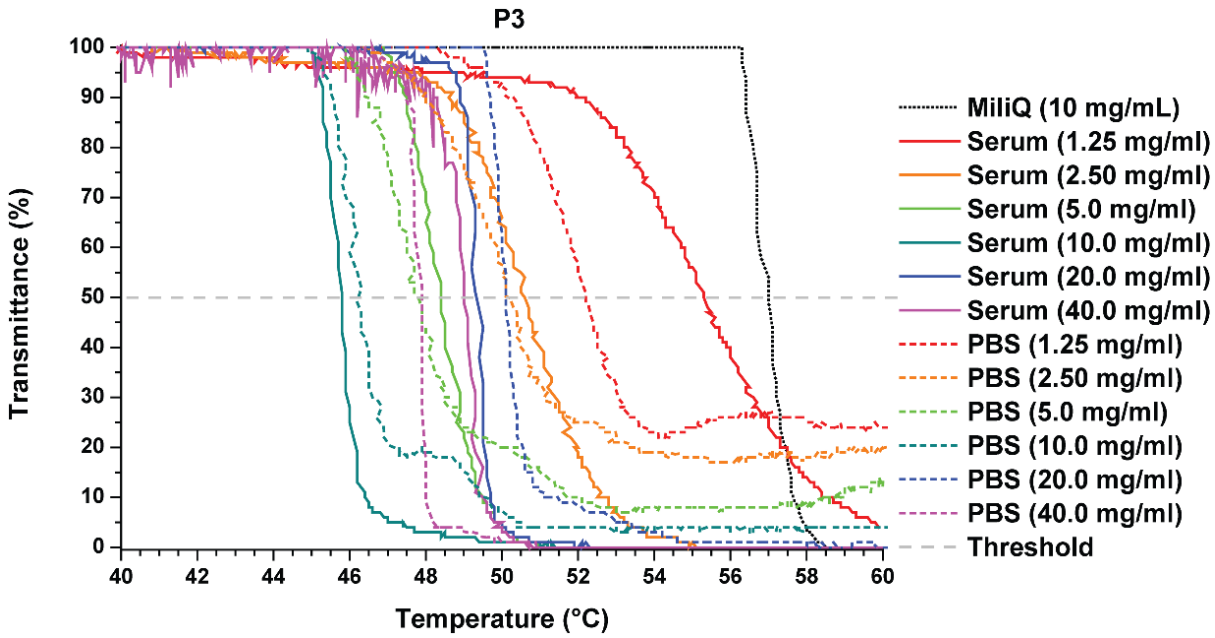

Figure S36. Transmittance of the **P3** (**pAP**) solution in ultrapure water (MiliQ), PBS, and FBS (serum), respectively, as a function of temperature

S5. Isothermal titration calorimetry

S5.1. ITC – titration of polymers F3, I3, E3, and P3

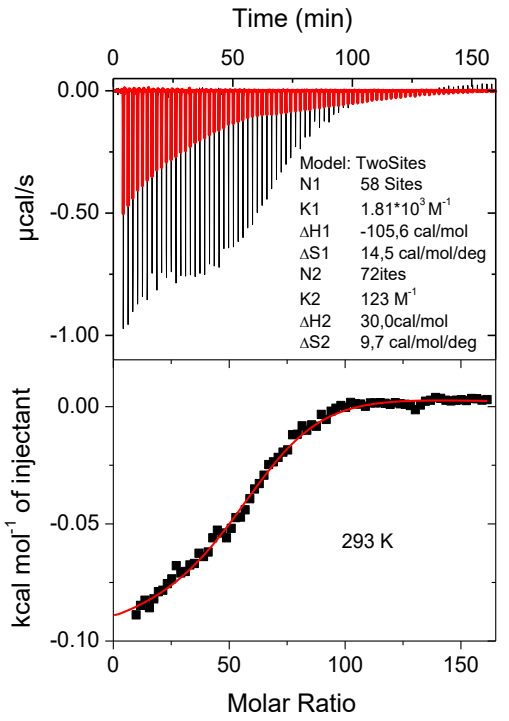

a

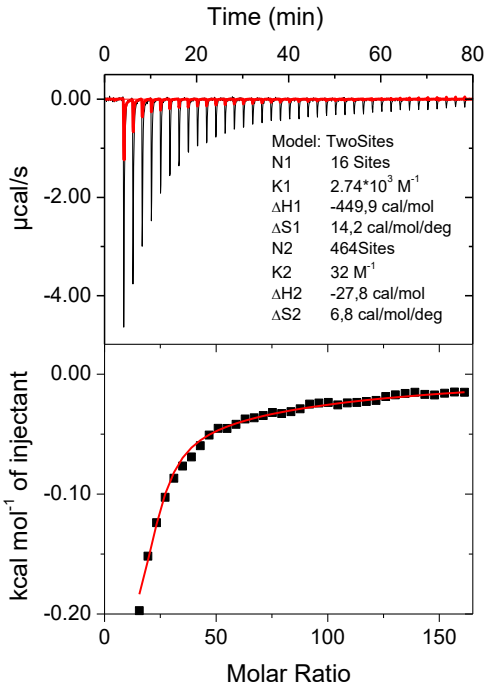

b

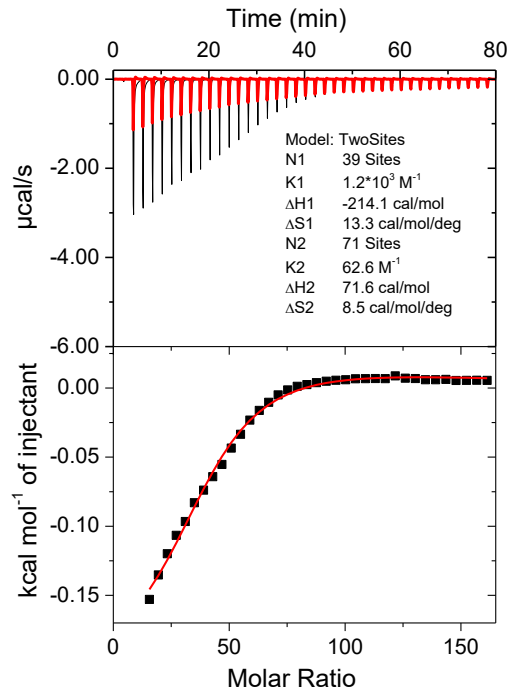

c

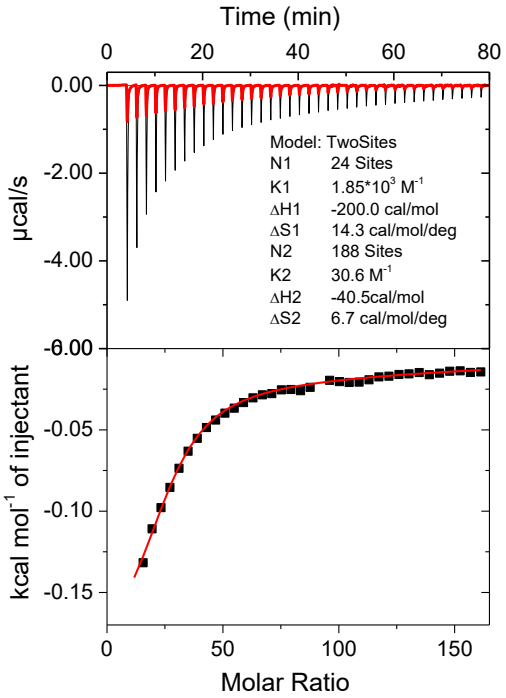

d

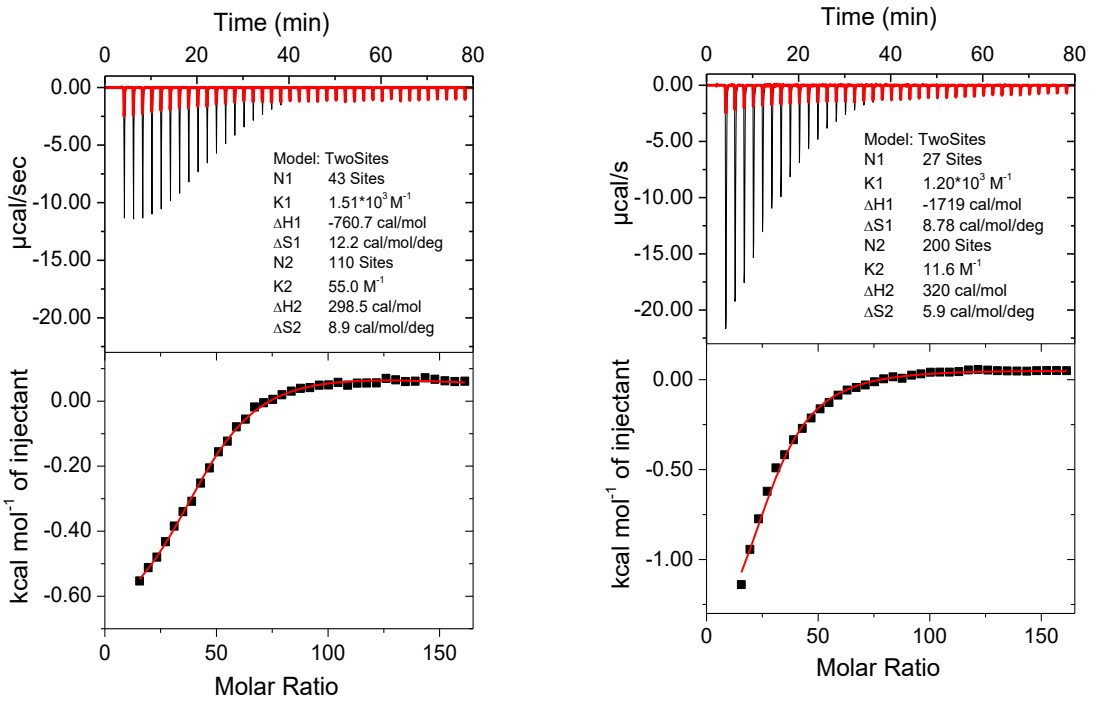

e **f**

Figure S37. Titration of the **F3** (**pDFEA**) solution in ultrapure water with PBS (a,c,e) and FBS (b,d,f) respectively; 293 K (a,b), 301 K (c,d) and 323 K (e,f). Upper graph – heat flux as a function of time; red line – titration of PBS or FBS, respectively, into ultrapure water; black line – titration into polymer solution. Lower graph – integrated heat per 1 mol of titrant (scatter); fit to a two-site model (line).

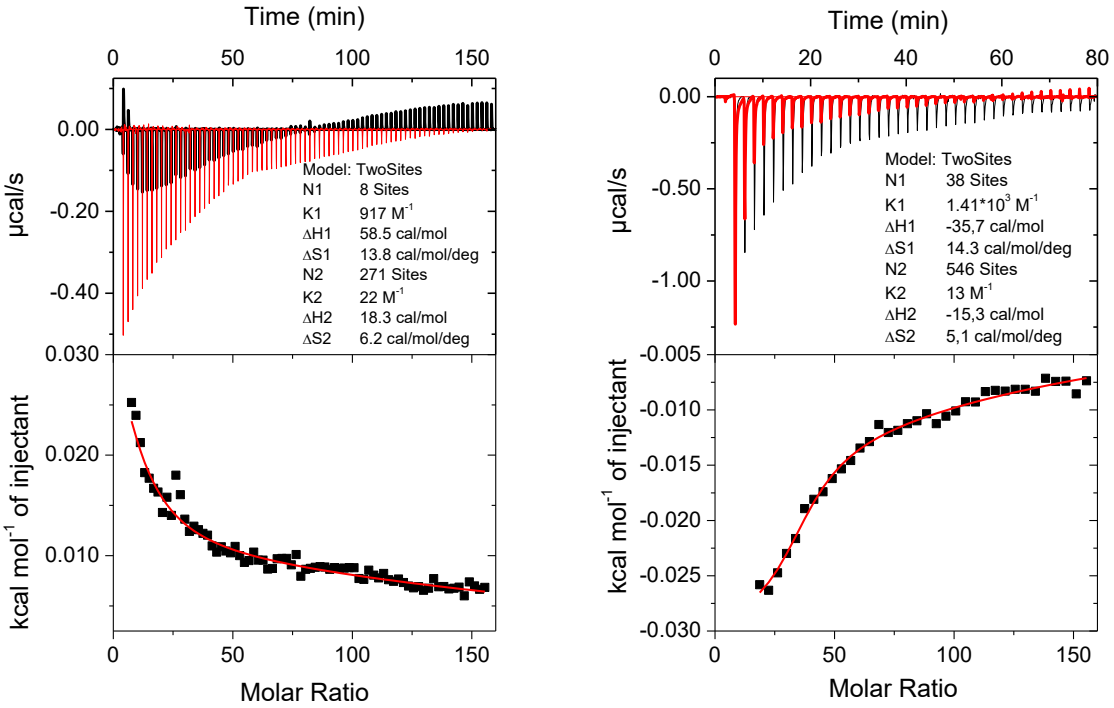

a **b**

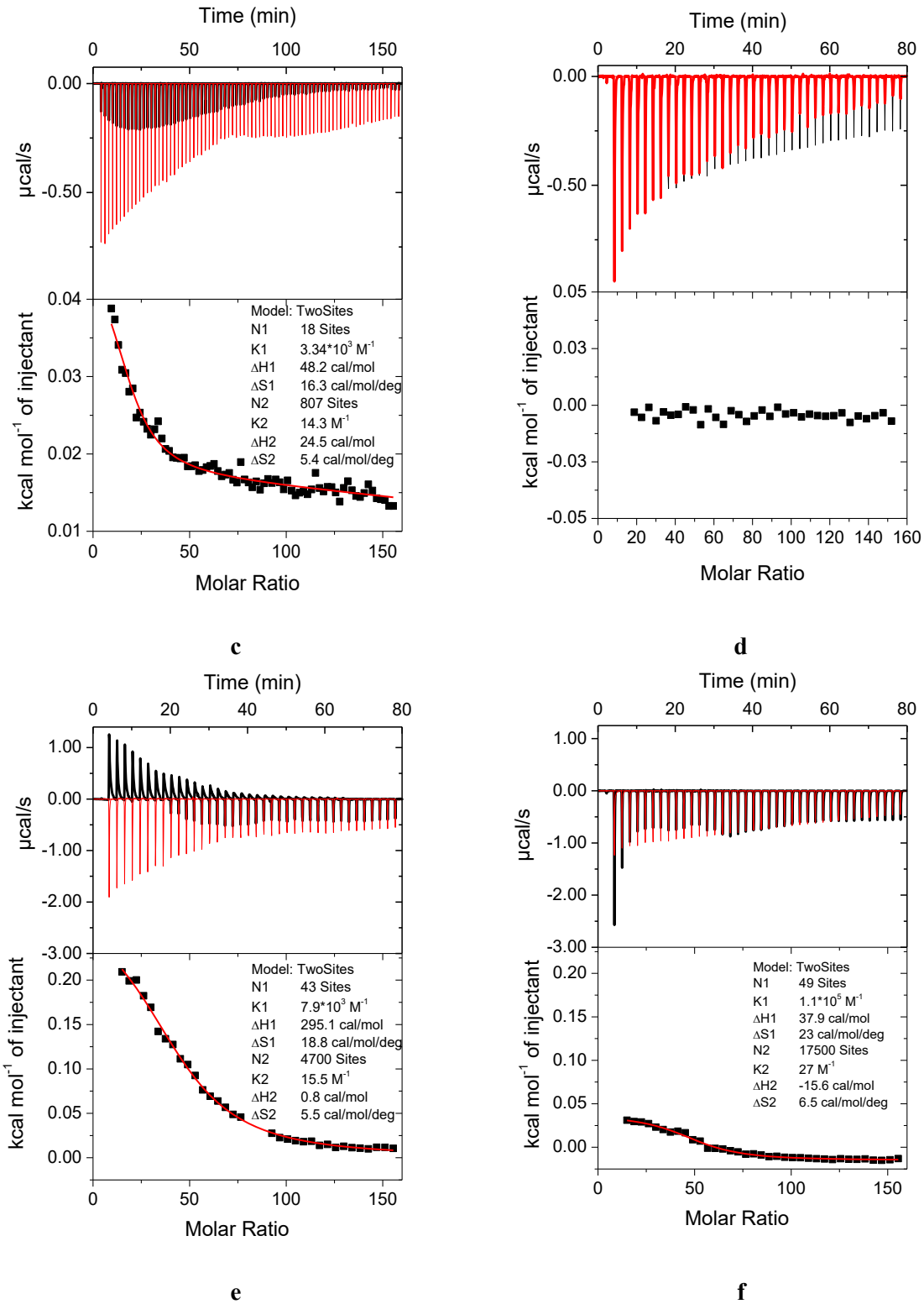

Figure S38. Titration of the **I3** (**pNIPAM**) solution in ultrapure water with PBS (**a**,**c**,**e**) and FBS (**b**,**d**,**f**) respectively; 293 K (**a**,**b**), 303 K (**c**,**d**) and 313 K (**e**,**f**). Upper graph – heat flux as a function of time; red line – titration of PBS or FBS, respectively, into ultrapure water; black line – titration into polymer solution. Lower graph – integrated heat per 1 mol of titrant (scatter); fit to the two-site model (line).

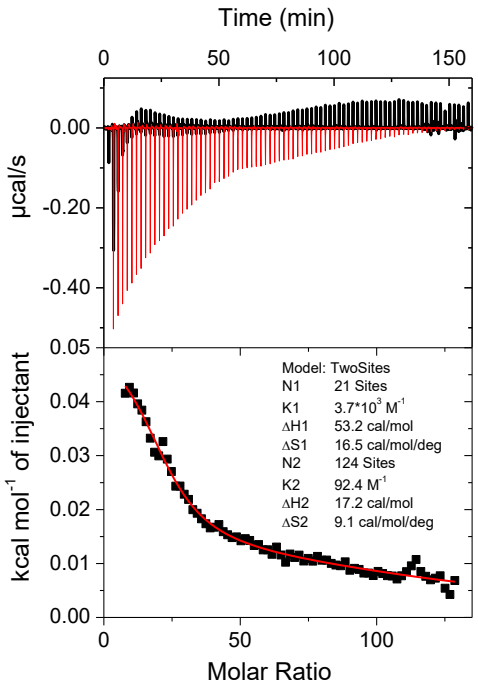
Time (min)
µcal/s
kcal mol-1 of injectant
Molar Ratio
Model: TwoSites
N1 21 Sites
K1 3.7*10^3 M^-1
ΔH1 53.2 cal/mol
ΔS1 16.5 cal/mol/deg
N2 124 Sites
K2 92.4 M^-1
ΔH2 17.2 cal/mol
ΔS2 9.1 cal/mol/deg

a

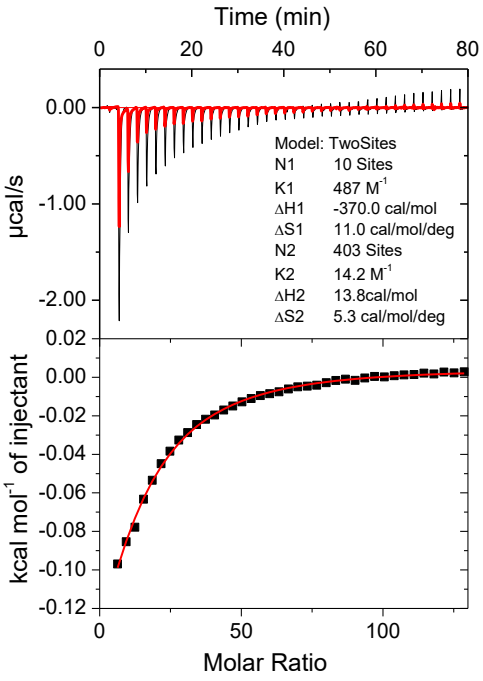
Time (min)
µcal/s
kcal mol-1 of injectant
Molar Ratio
Model: TwoSites
N1 10 Sites
K1 487 M^-1
ΔH1 -370.0 cal/mol
ΔS1 11.0 cal/mol/deg
N2 403 Sites
K2 14.2 M^-1
ΔH2 13.8cal/mol
ΔS2 5.3 cal/mol/deg

b

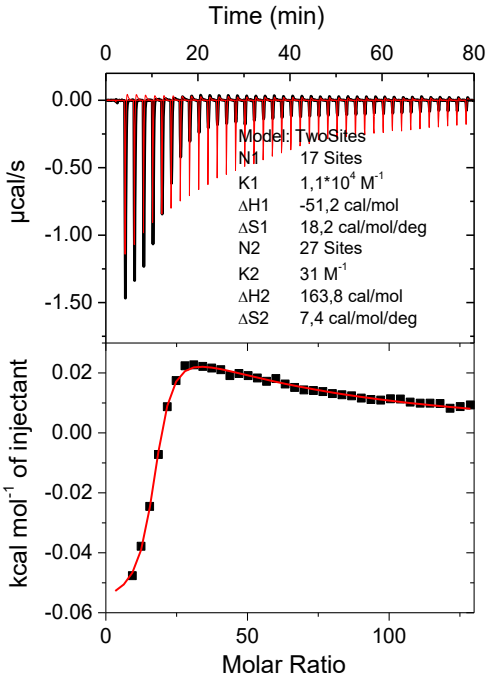
Time (min)
µcal/s
kcal mol-1 of injectant
Molar Ratio
Model: TwoSites
N1 17 Sites
K1 1,1*10^4 M^-1
ΔH1 -51,2 cal/mol
ΔS1 18,2 cal/mol/deg
N2 27 Sites
K2 31 M^-1
ΔH2 163,8 cal/mol
ΔS2 7,4 cal/mol/deg

c

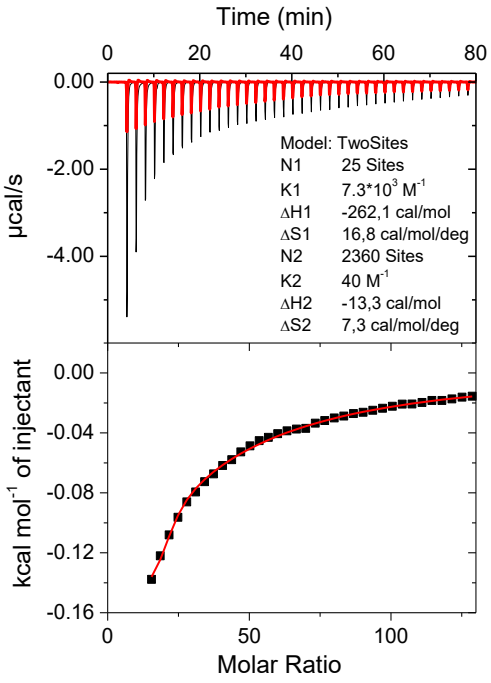
Time (min)
µcal/s
kcal mol-1 of injectant
Molar Ratio
Model: TwoSites
N1 25 Sites
K1 7.3*10^3 M^-1
ΔH1 -262,1 cal/mol
ΔS1 16,8 cal/mol/deg
N2 2360 Sites
K2 40 M^-1
ΔH2 -13,3 cal/mol
ΔS2 7,3 cal/mol/deg

d

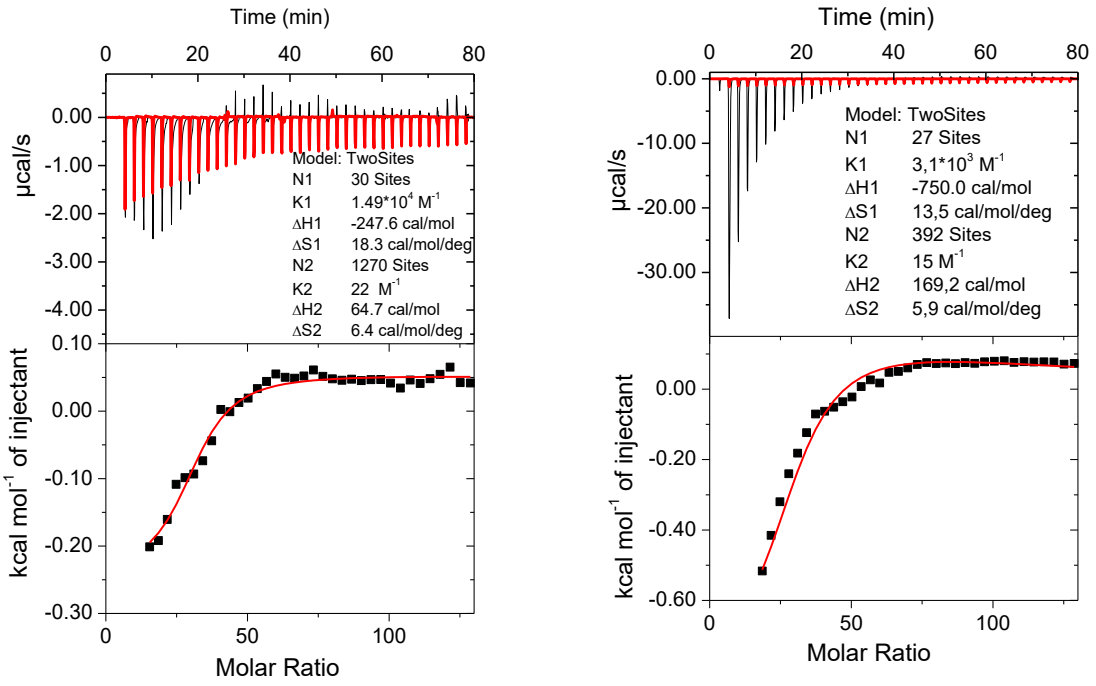

e **f**

Figure S39. Titration of the **E3** (**pDEA**) solution in ultrapure water with PBS (**a**,**c**,**e**) and FBS (**b**,**d**,**f**) respectively; 293 K (**a**,**b**), 301 K (**c**,**d**) and 313 K (**e**,**f**). Upper graph – heat flux as a function of time; red line – titration of PBS or FBS, respectively, into ultrapure water; black line – titration into polymer solution. Lower graph – integrated heat per 1 mol of titrant (scatter); fit to the two independent binding sites model (line).

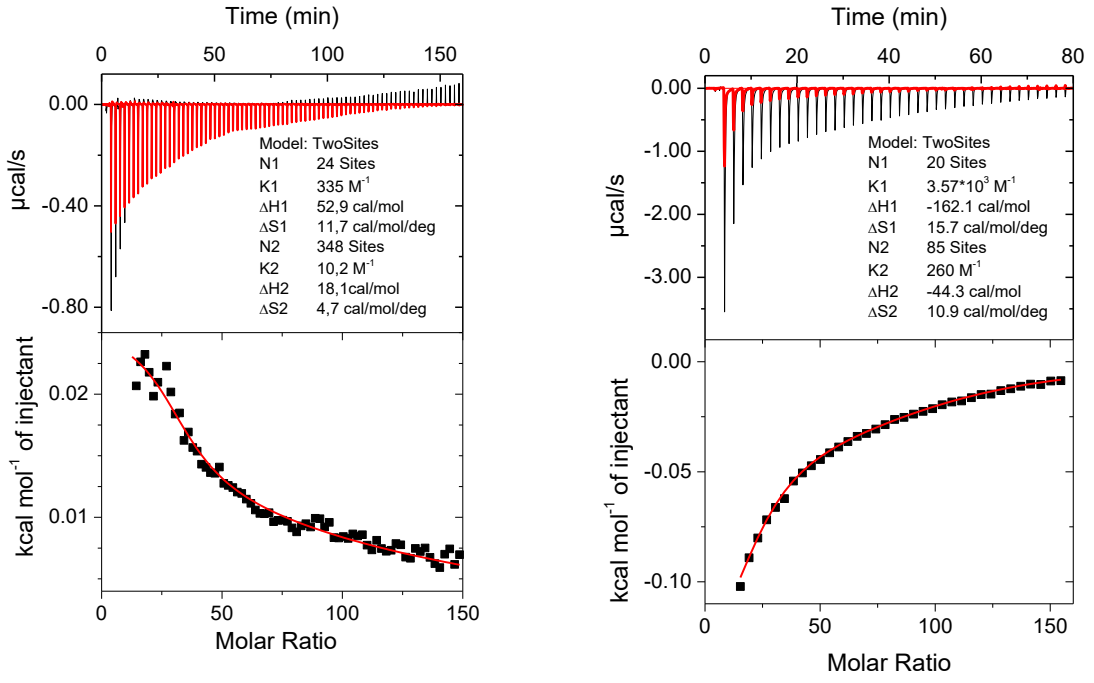

a **b**

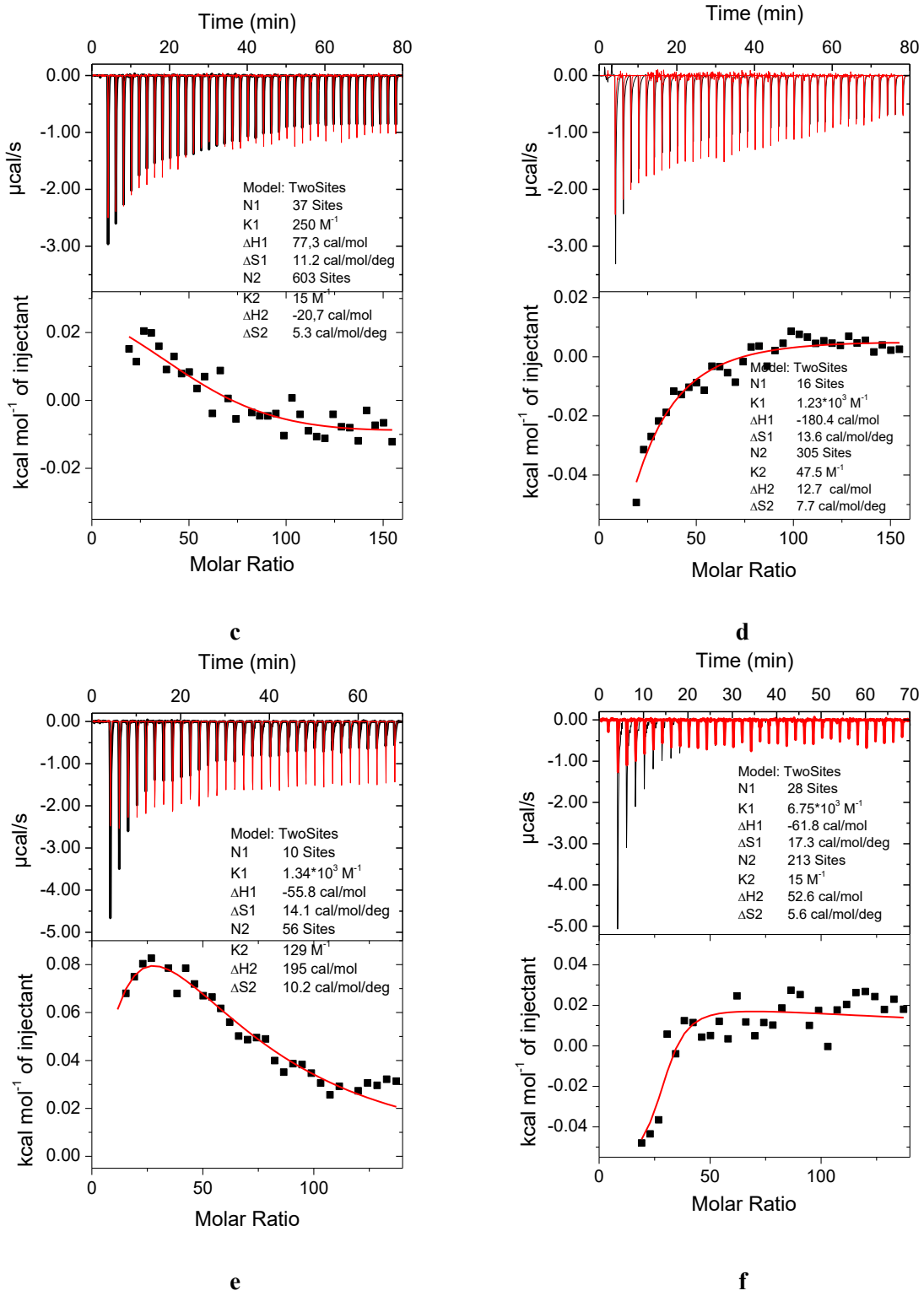

Figure S40. Titration of the **P3** (**pAP**) solution in ultrapure water with PBS (**a**,**c**,**e**) and FBS (**b**,**d**,**f**) respectively; 293 K (**a**,**b**), 323 K (**c**,**d**) and 333 K (**e**,**f**). Upper graph – heat flux as a function of time; red line – titration of PBS or FBS, respectively into ultrapure water; black line – titration into polymer solution. Lower graph – integrated heat per 1 mol of titrant (scatter); fit to the two independent binding sites model (line).

The titration isotherms of complex shape consist of heat effects originating from (**i**) "pseudo-binding" event and (**ii**) non-linear heat of mixing. Therefore, we fitted cumulated reaction heat as a function of titrant-to-analyte molar ratio with **two** independent binding sites model (one Wiseman isoterm[S1] for each effect, both **i** and **ii**). Because the concentration of titrant (PBS or FBS) is unknown (as these mixtures contain many compounds in various concentrations), we chose an arbitrary value 162.7 mM (ionic strength of PBS) for **both** PBS and FBS. Reaction enthalpy as an independent fitting parameter was then normalized to the concentration of analyte (polymer). The remaining fitting parameters (stoichiometry n, binding constant K_a) are influenced by titrant to analyte molar ratio and, therefore, were not used in the results discussion.

The fitting parameters for the second binding site (**ii**) were:
a) $K_{a1} \gg K_{a2}$
b) $\Delta H_1 > \Delta H_2$

S5.2. ITC – enthalpies of F3, I3, E3, and P3

Table S5. Concentrations and pH of polymer solutions; enthalpy Δ*H* (J/mol of monomer) of mixing of polymer solutions with PBS and FBS at various temperatures.

Sample	**F3 (pDFEA)**						**I3 (pNIPAM)**						**E3 (pDEA)**						**P3 (pAP)**					
Conc. (mM)*	0.213						0.221						0.267						0.216					
pH in H_2O**	≈ 4.9						≈ 4.6						≈ 4.0						≈ 5.5					
Titrant	**PBS**			**FBS**			**PBS**			**FBS**			**PBS**			**FBS**			**PBS**			**FBS**		
***T*, K**	**293**	**301**	**323**	**293**	**301**	**323**	**293**	**303**	**313**	**293**	**303**	**313**	**293**	**301**	**313**	**293**	**301**	**313**	**293**	**323**	**333**	**293**	**323**	**333**
Δ*H*, (J/mol)	−73.9	-100.7	−394.4	−86.7	−57.9	−559.6	4.9	9.1	113.1	−14.2	≈ 0.0	19.5	15.8	−12.3	−105.4	−52.5	−92.9	−287.2	14.4	32.3	−6.3	−36.7	−32.6	−19.6
transition conc. (mM)***	17.4	13.4	17.5	9.3	8.8	16.3	11.0	11.0	19.0	21.1	N/A	21.2	9.7	7.0	14.6	8.9	11.6	17.3	12.3	16.3	20.0	12.0	14.6	8.1
transition conc. (mg/mL)******	1.0	0.8	1.0	3.0	2.9	5.3	0.6	0.6	1.1	6.9	N/A	6.9	0.5	0.4	0.8	2.9	3.8	5.6	0.7	0.9	1.1	3.9	4.8	2.6

* polymer concentration in the analyte solution

** pH of aqueous solution of polymer, 10 mg/mL

*** concentration of titrant (PBS or FBS) in units of ionic strength of PBS solution, determined from the coordinate on the *x*-axis (molar ratio) on **Figures S37** to **40**.

**** concentration of titrant in mg/mL

S5.3. ITC - titration of benzoic acid

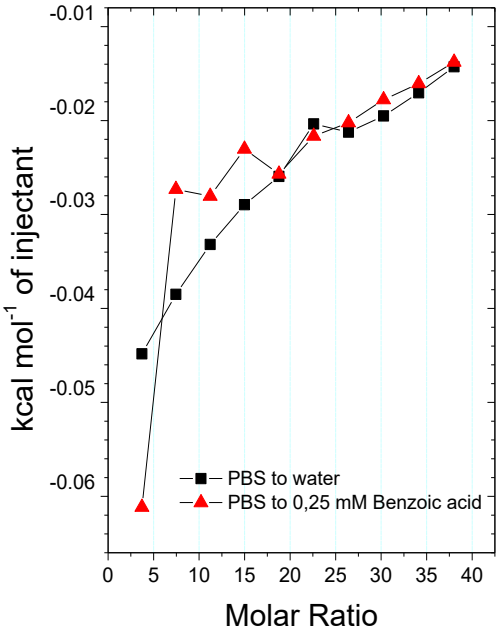

a

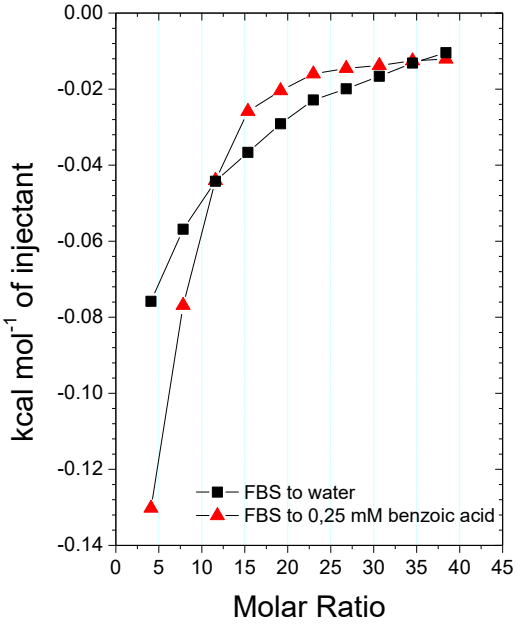

b

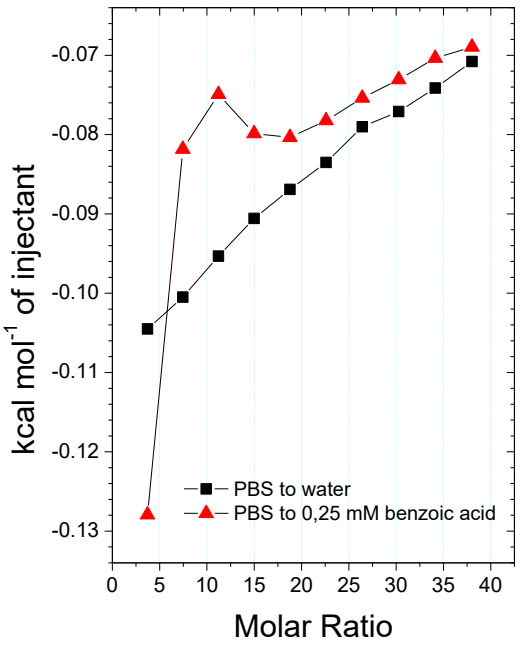

c

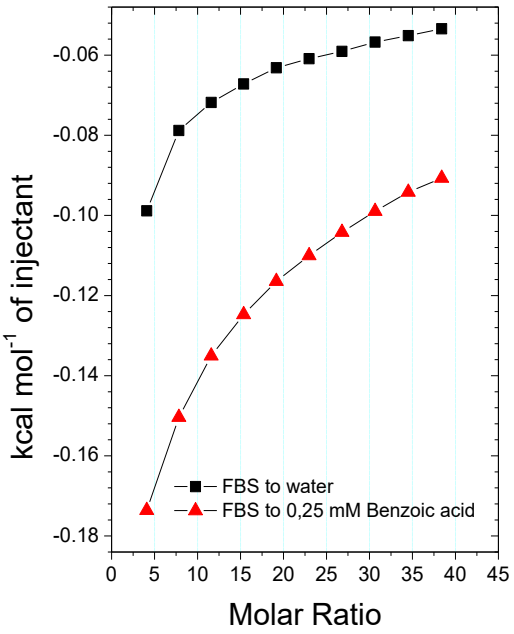

d

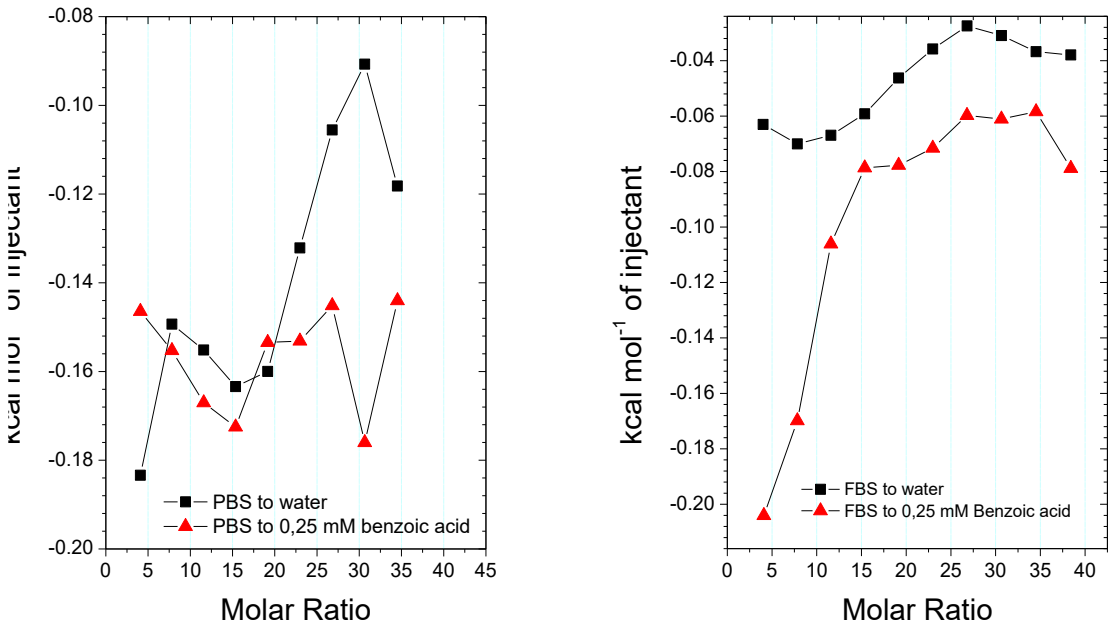

e **f**

Figure S41. ITC isotherms of the titration of the solution of benzoic acid (0.25 mM) with PBS (**a**, **c**, **e**) and FBS (**b**, **d**, **f**) at 293 K (**a**, **b**), 313 K(**c**, **d**) and 333 K (**e**, **f**).

S6. Dynamic light scattering data

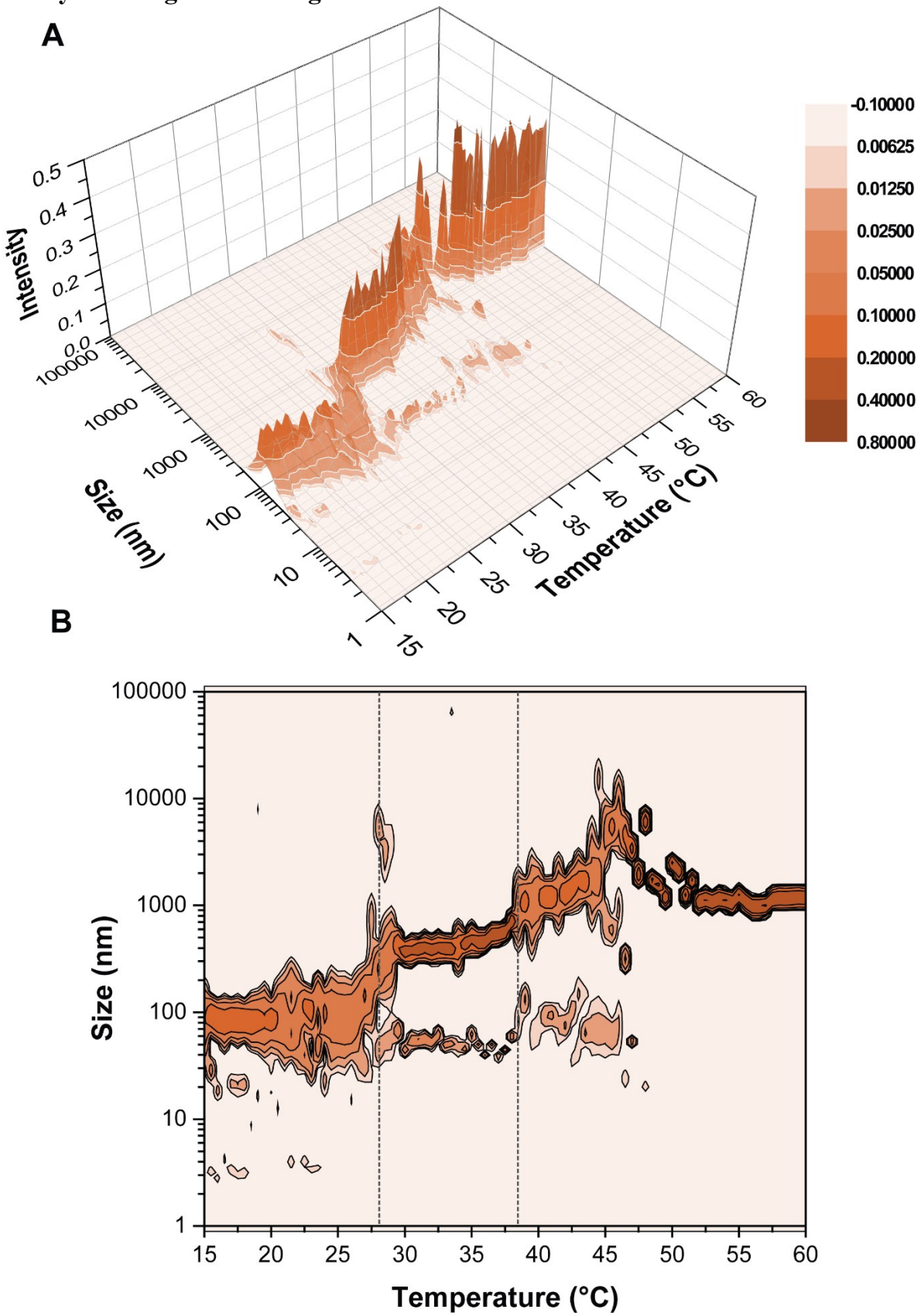

Figure S42. Size distributions of molecular assemblies of polymer **F1** (10 mg/mL in PBS) as a function of temperature; depicted as 3D plot (**A**) and contour graph (**B**). T_{CP1} (dashed lines) was assigned to 28 °C, T_{CP2} was assigned to 38 °C.

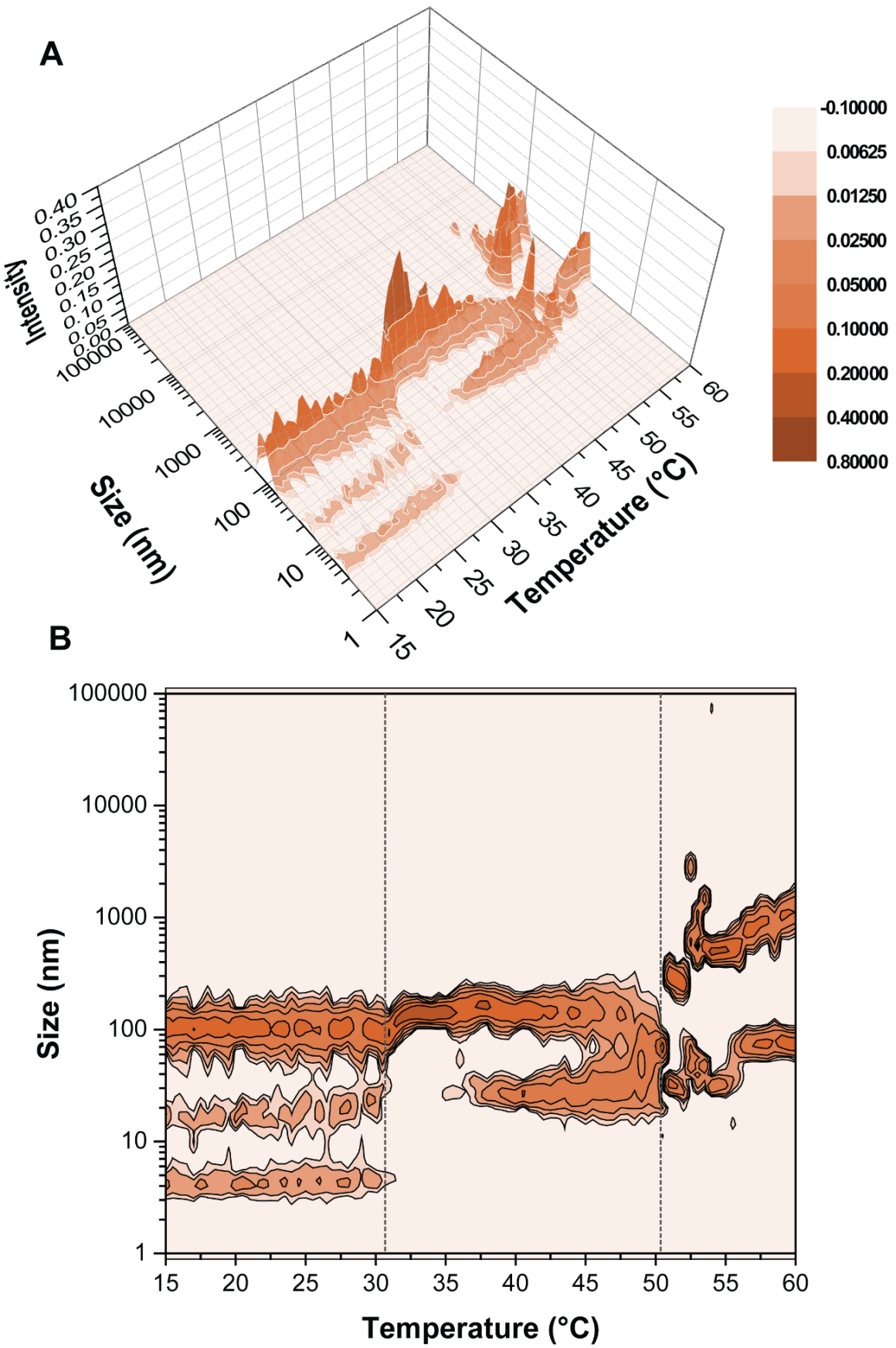

Figure S43. Size distributions of molecular assemblies of polymer **F2** (10 mg/mL in PBS) as a function of temperature; depicted as 3D plot (**A**) and contour graph (**B**). T_{CP1} (dashed lines) was assigned to 31 °C, T_{CP2} was assigned to 50 °C.

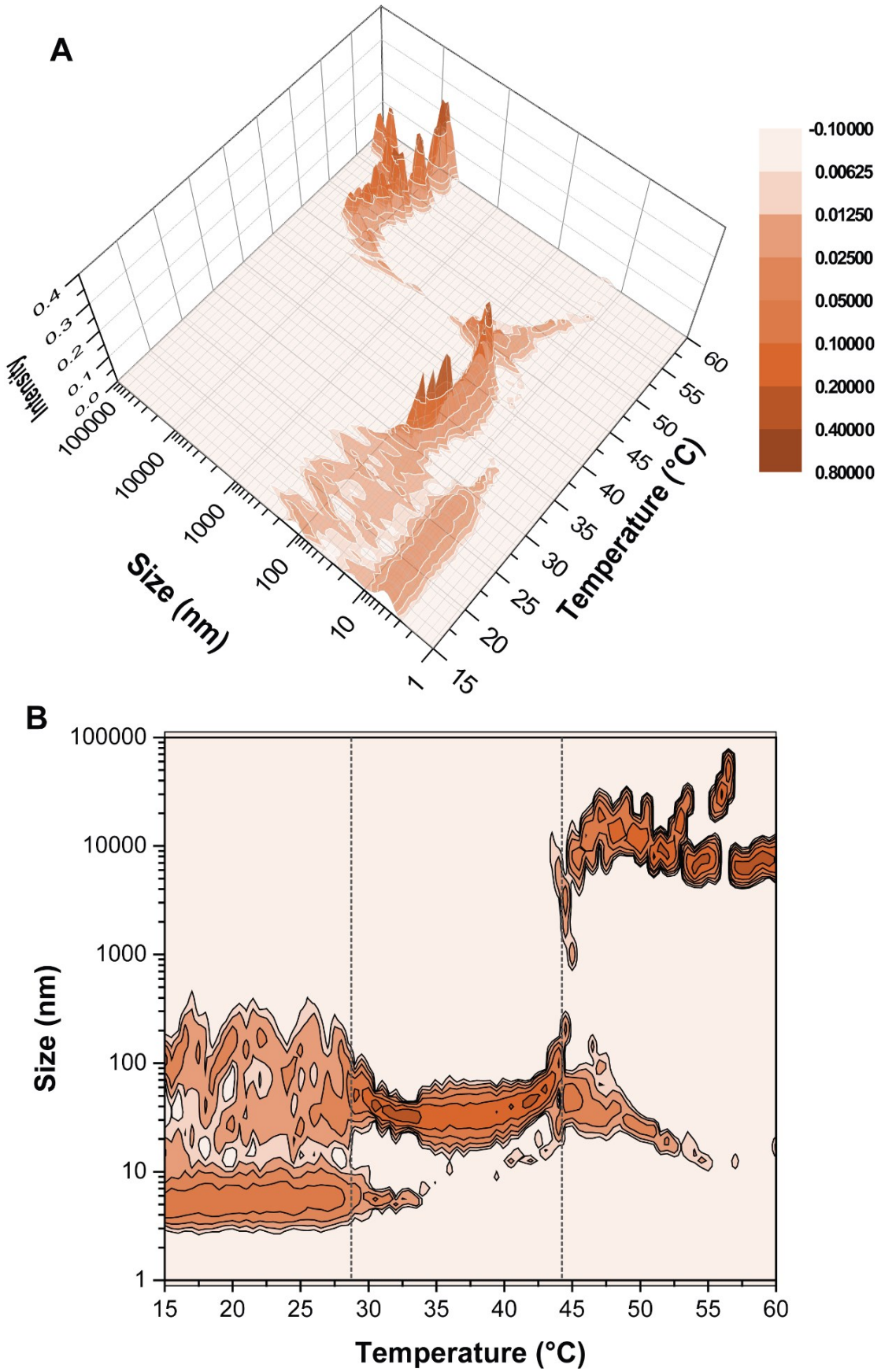

Figure S44. Size distributions of molecular assemblies of polymer **F3** (10 mg/mL in PBS) as a function of temperature; depicted as 3D plot (**A**) and contour graph (**B**). T_{CP1} (dashed lines) was assigned to 28 °C, T_{CP2} was assigned to 44 °C.

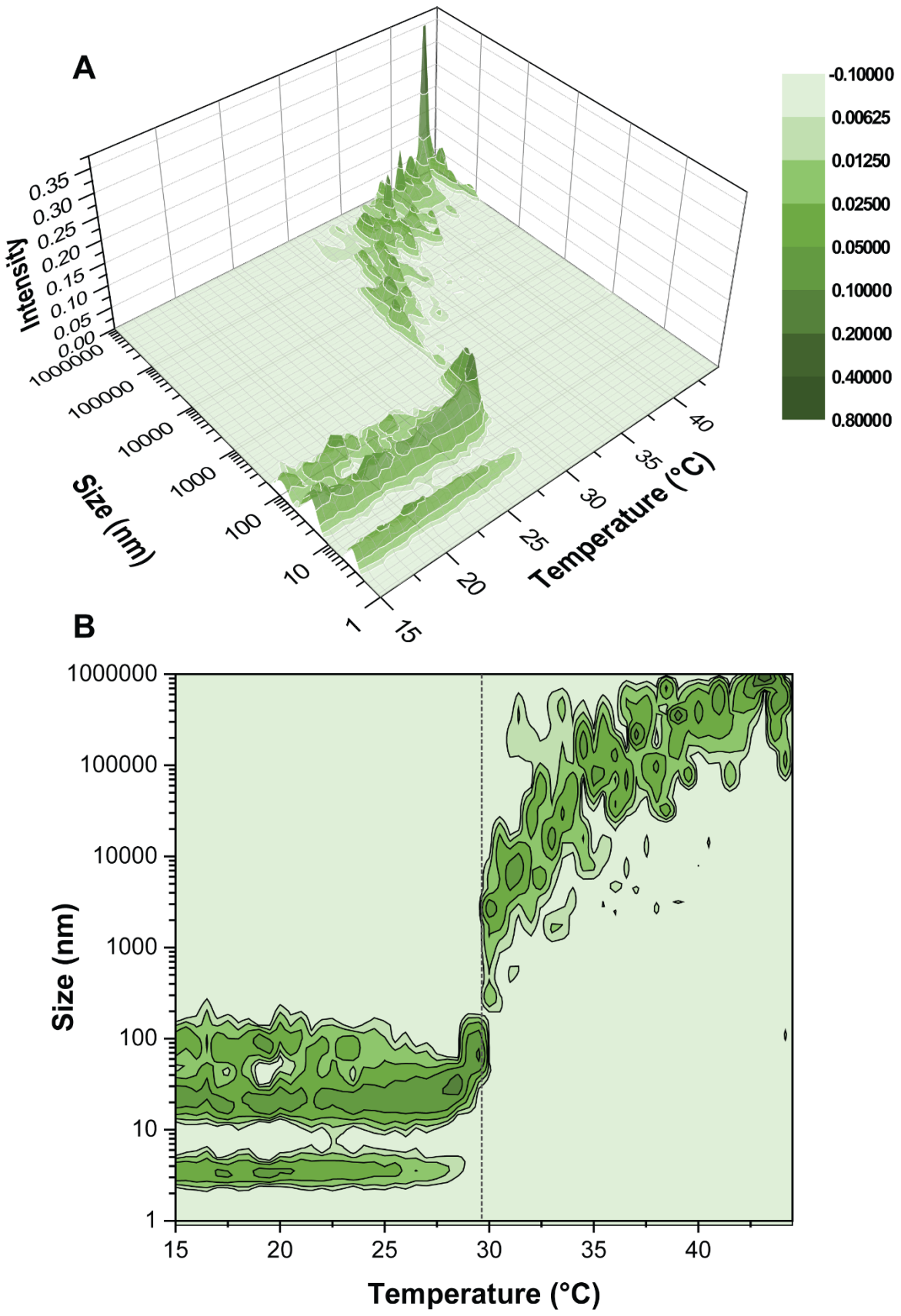

Figure S45. Size distributions of molecular assemblies of polymer **I1** (10 mg/mL in PBS) as a function of temperature; depicted as 3D plot (**A**) and contour graph (**B**). T_{CP} (dashed line) was assigned to 30 °C. The measurement stopped prematurely because the size of the aggregates exceeded the detection limit.

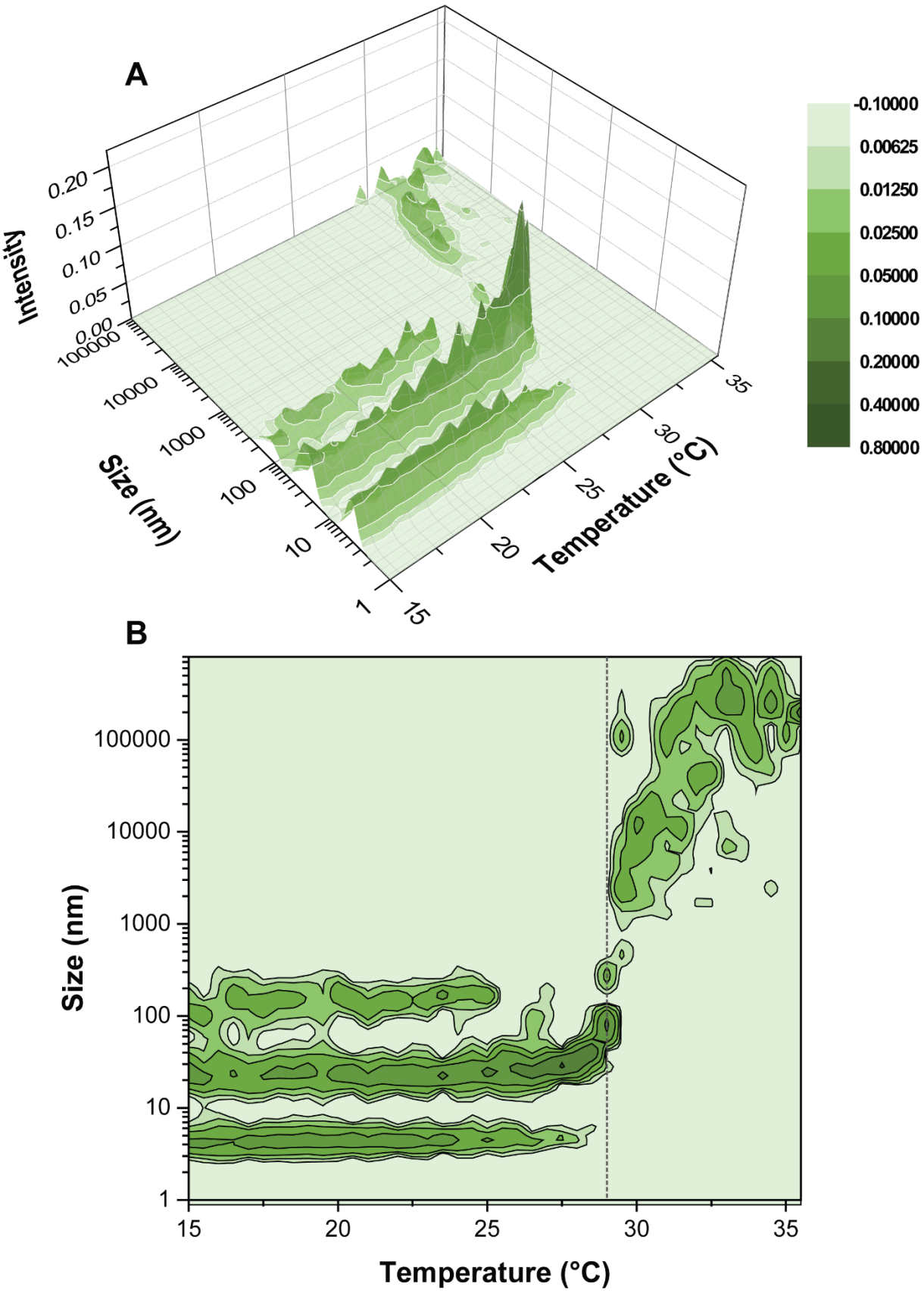

Figure S46. Size distributions of molecular assemblies of polymer **I2** (10 mg/mL in PBS) as a function of temperature; depicted as 3D plot (**A**) and contour graph (**B**). T_{CP} (dashed line) was assigned to 29 °C. The measurement stopped prematurely because the size of the aggregates exceeded the detection limit.

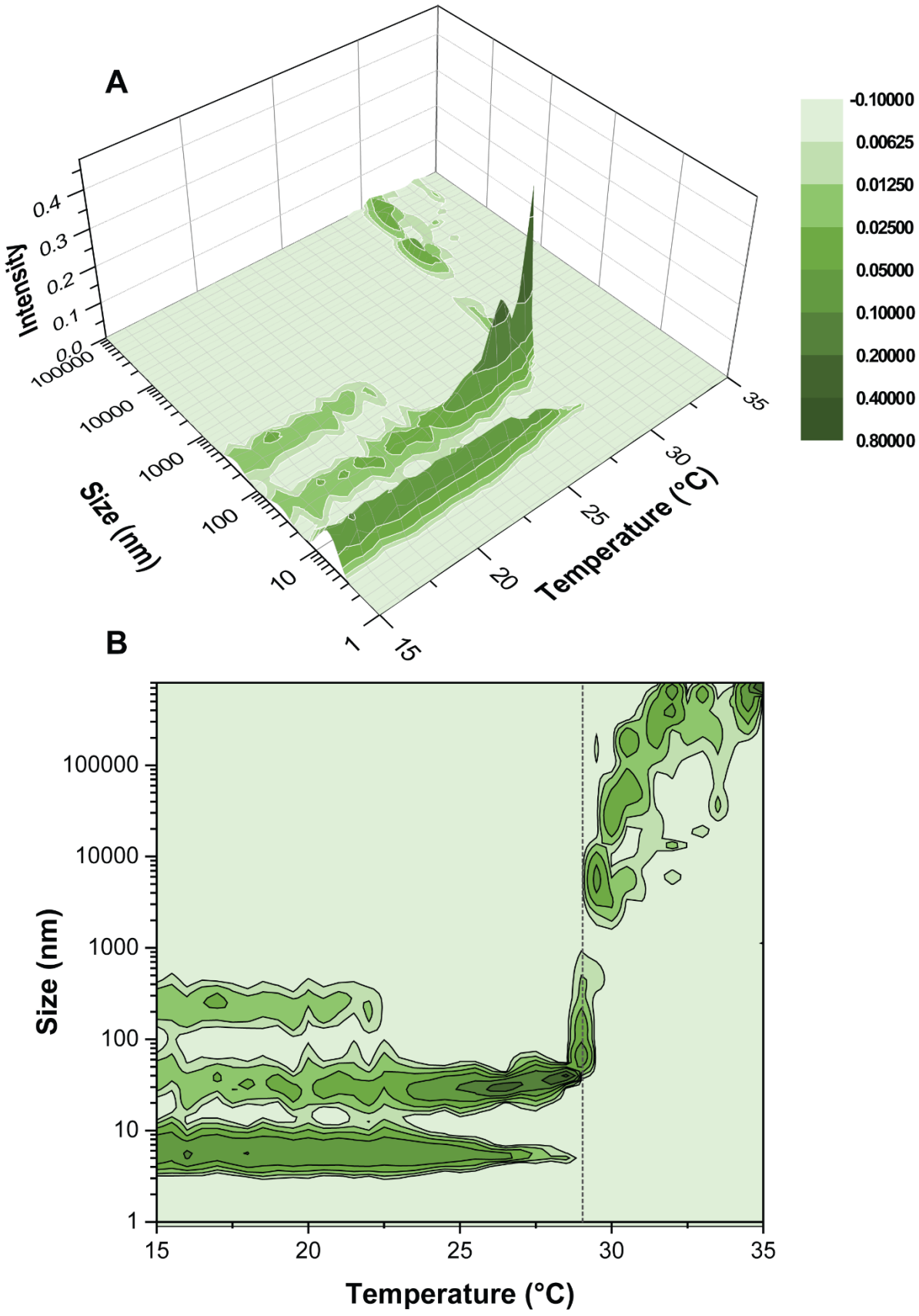

Figure S47. Size distributions of molecular assemblies of polymer **I3** (10 mg/mL in PBS) as a function of temperature; depicted as 3D plot (**A**) and contour graph (**B**). T_{CP} (dashed line) was assigned to 29 °C. The measurement stopped prematurely because the size of the aggregates exceeded the detection limit.

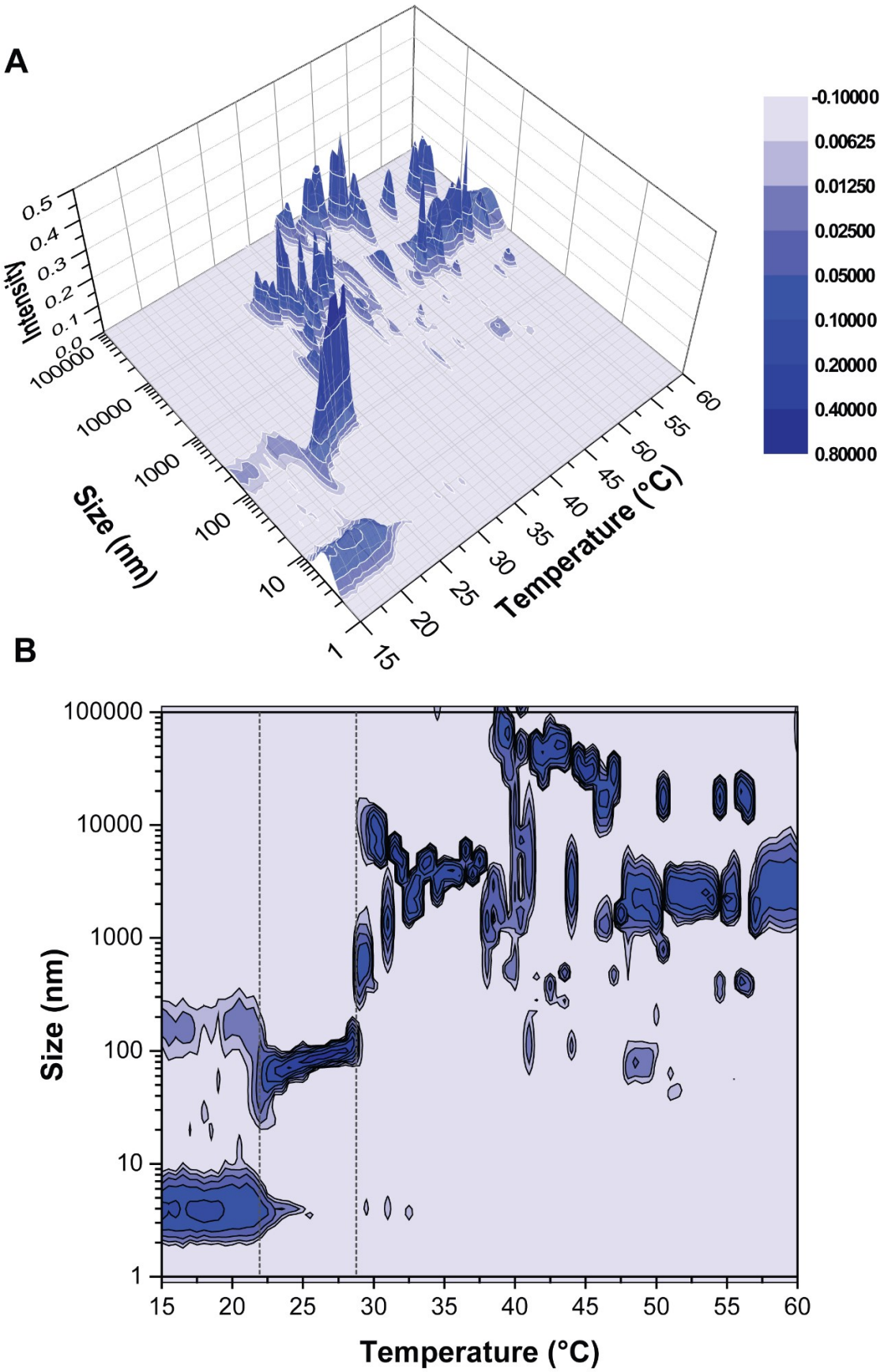

Figure S48. Size distributions of molecular assemblies of polymer **E1** (10 mg/mL in PBS) as a function of temperature; depicted as 3D plot (**A**) and contour graph (**B**). T_{CP1} (dashed lines) was assigned to 22 °C, T_{CP2} was assigned to 28 °C.

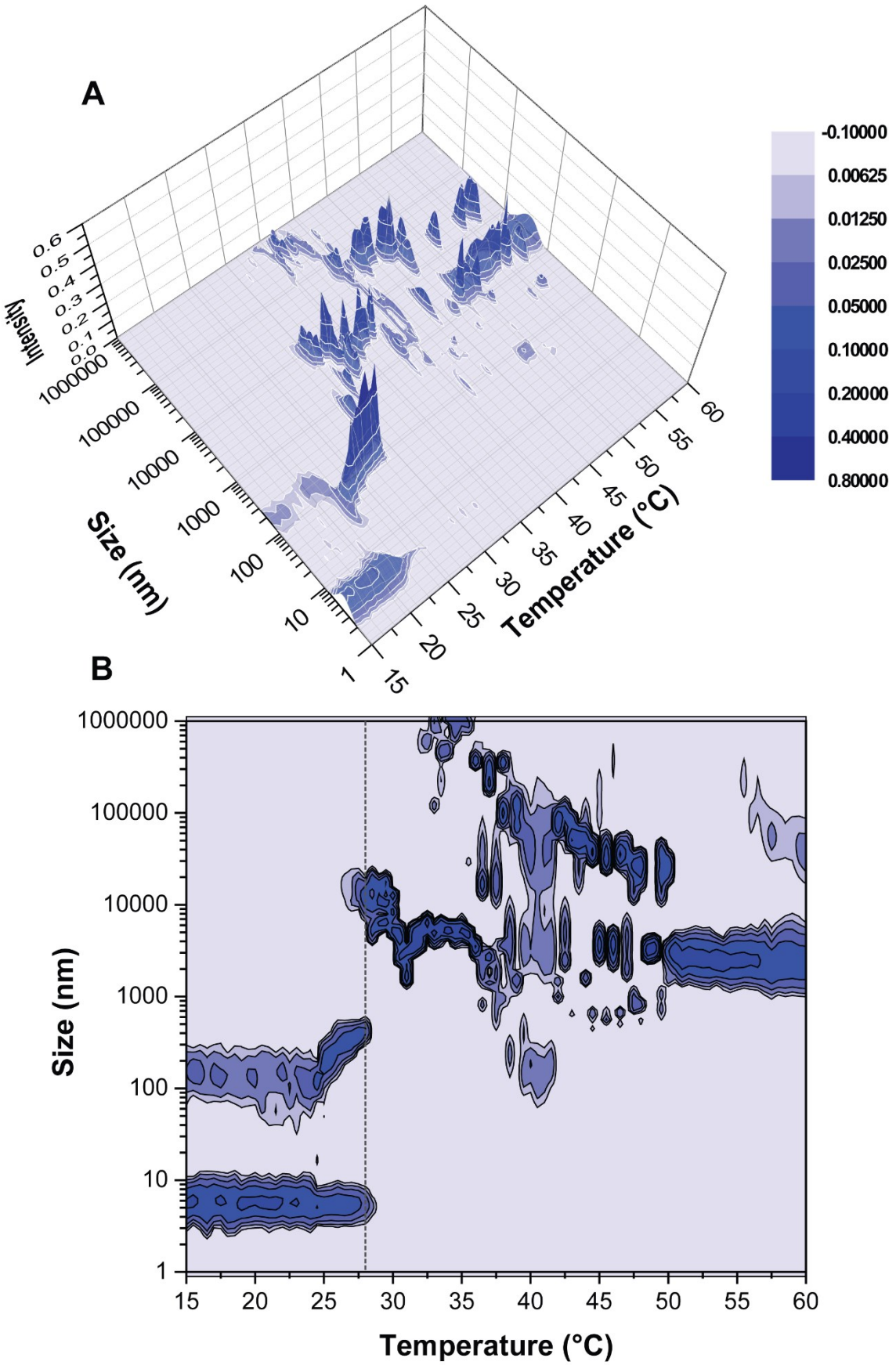

Figure S49. Size distributions of molecular assemblies of polymer **E2** (10 mg/mL in PBS) as a function of temperature; depicted as 3D plot (**A**) and contour graph (**B**). T_{CP} (dashed line) was assigned to 28 °C. The measurement stopped prematurely because the size of the aggregates exceeded the detection limit.

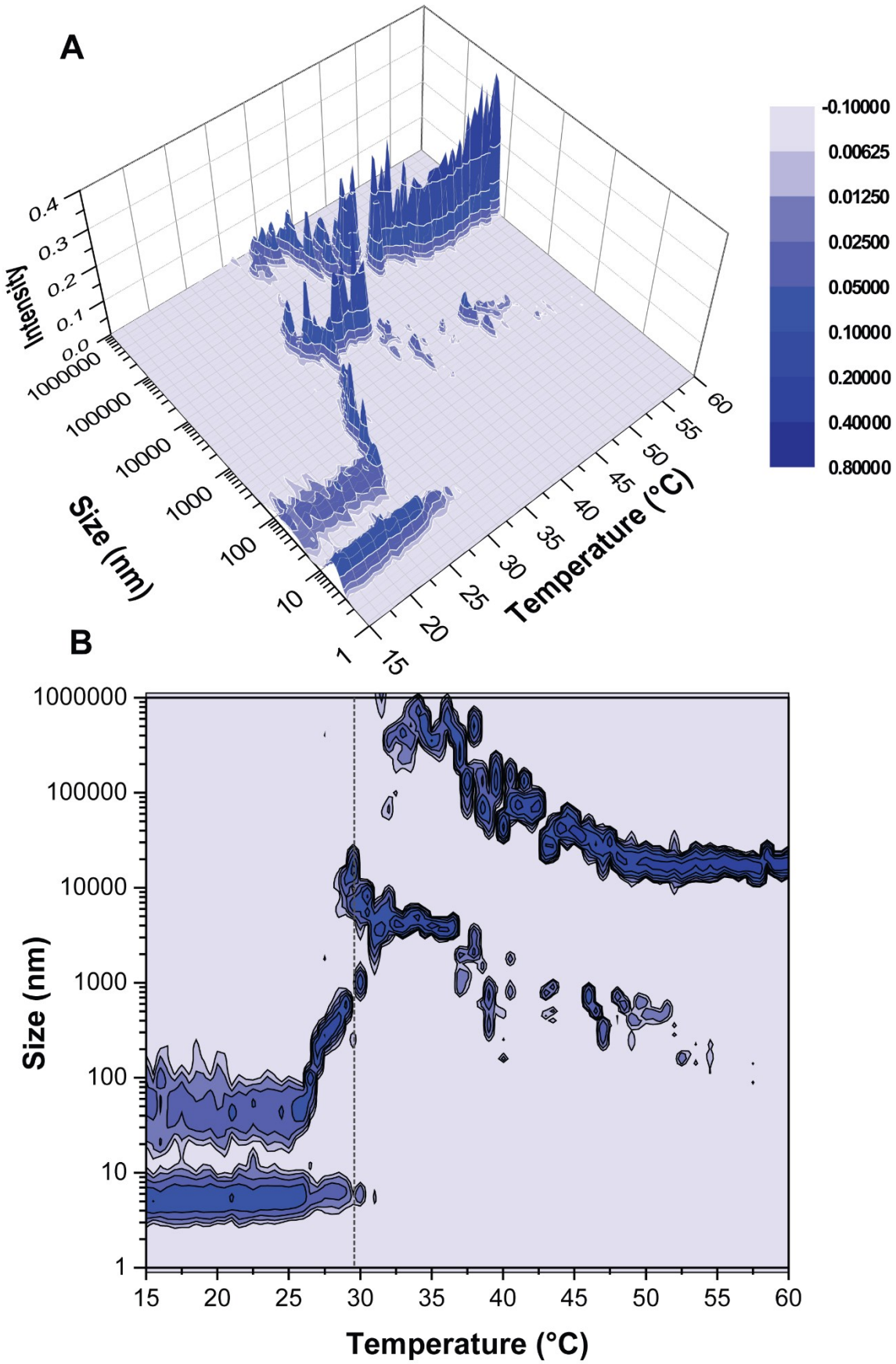

Figure S50. Size distributions of molecular assemblies of polymer **E3** (10 mg/mL in PBS) as a function of temperature; depicted as 3D plot (**A**) and contour graph (**B**). T_{CP} (dashed line) was assigned to 29 °C. The measurement stopped prematurely because the size of the aggregates exceeded the detection limit.

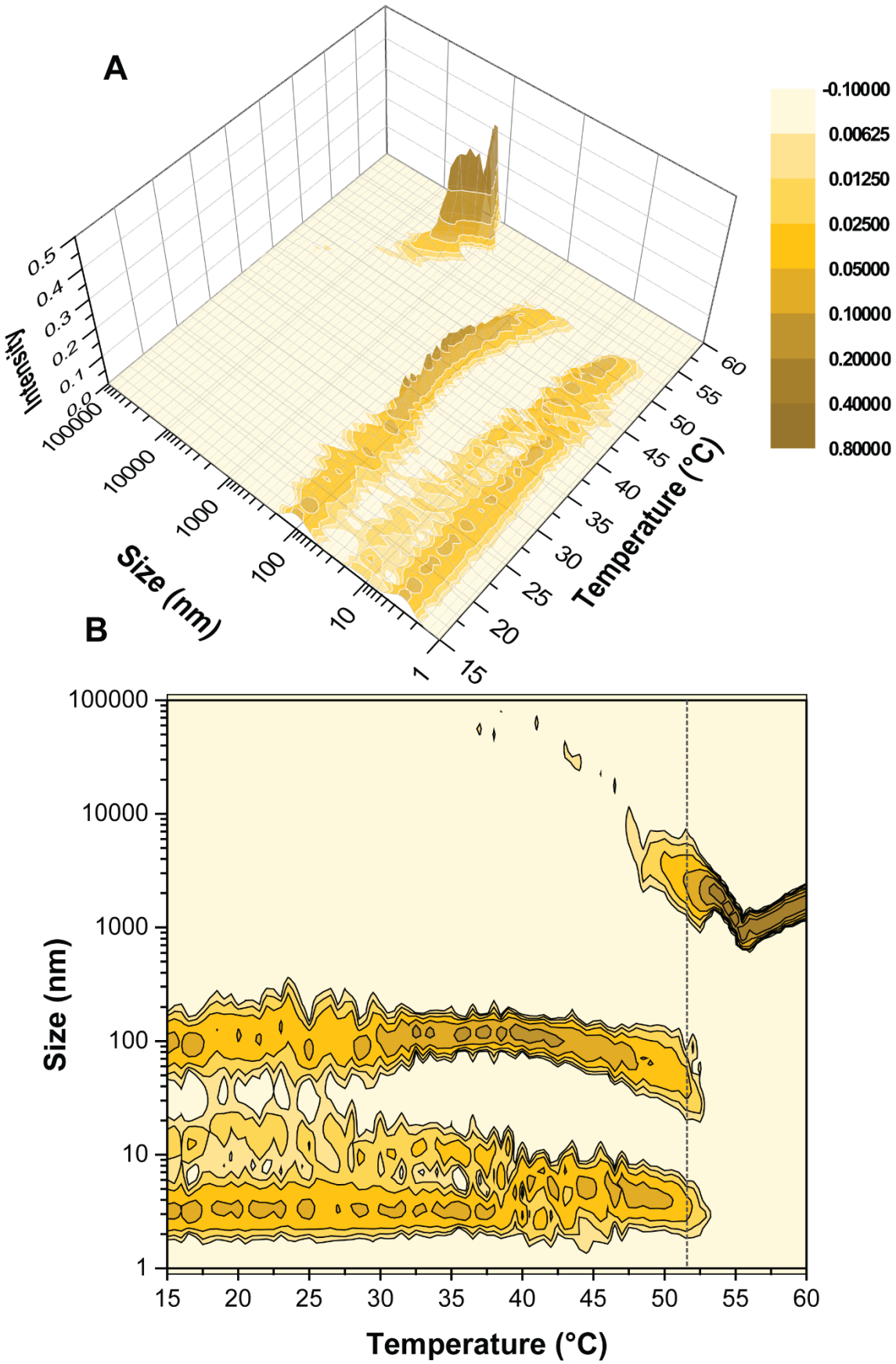

Figure S51. Size distributions of molecular assemblies of polymer **P1** (10 mg/mL in PBS) as a function of temperature; depicted as 3D plot (**A**) and contour graph (**B**). T_{CP} (dashed line) was assigned to 52 °C. The measurement stopped prematurely because the size of the aggregates exceeded the detection limit.

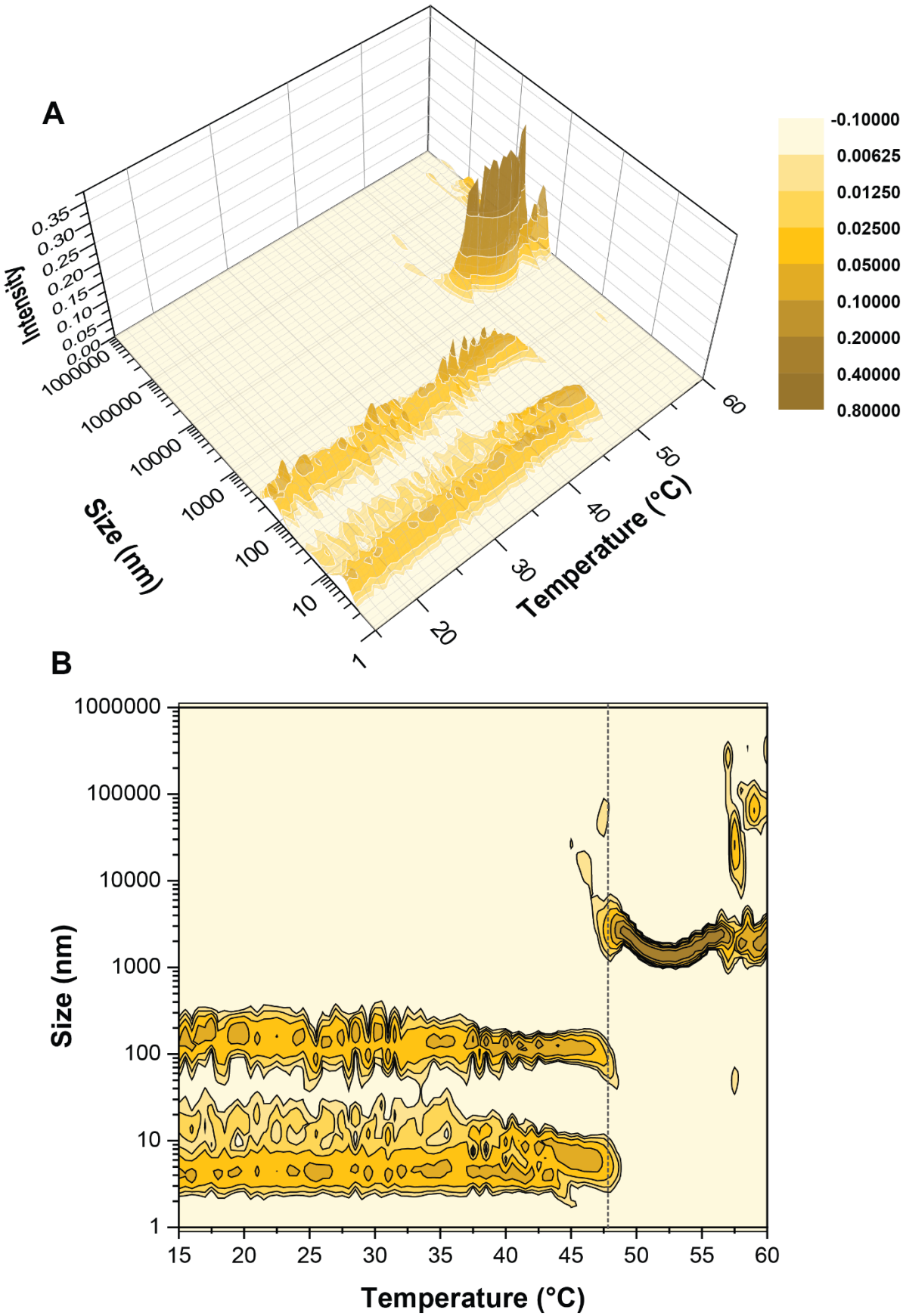

Figure S52. Size distributions of molecular assemblies of polymer **P2** (10 mg/mL in PBS) as a function of temperature; depicted as 3D plot (**A**) and contour graph (**B**). T_{CP} (dashed line) was assigned to 48 °C. The measurement stopped prematurely because the size of the aggregates exceeded the detection limit.

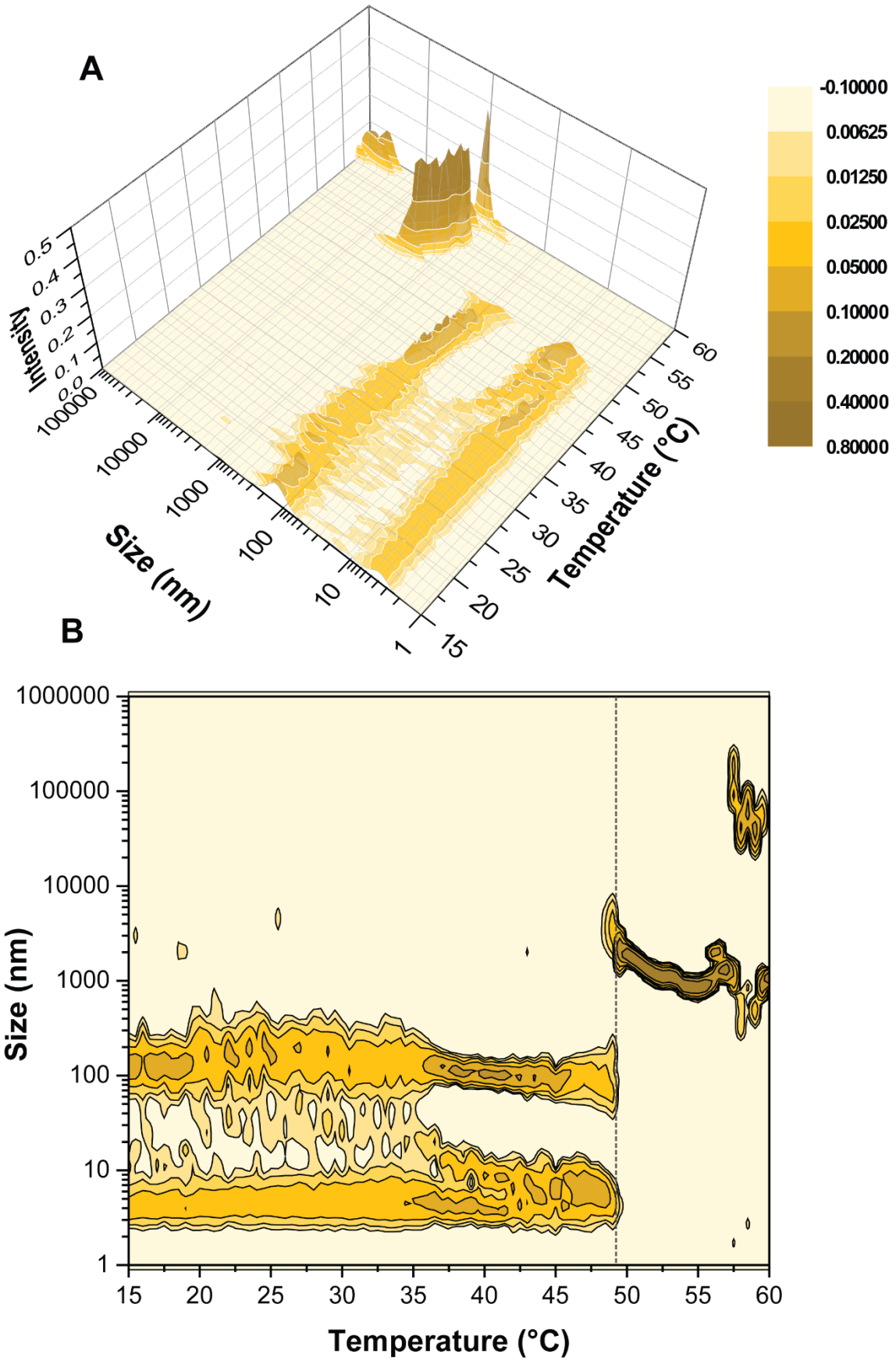

Figure S53. Size distributions of molecular assemblies of polymer **P3** (10 mg/mL in PBS) as a function of temperature; depicted as 3D plot (**A**) and contour graph (**B**). T_{CP} (dashed line) was assigned to 49 °C. The measurement stopped prematurely because the size of the aggregates exceeded the detection limit.

S7. Refractive index increment (d*n*/d*c*)

Brookhaven Instruments Corp.
Differential Refractometer Software Ver. 5.32

Date: Jul 29, 2021
Time: 10:54:38

Sample ID **F1, PBS**
Operator ID **PC**
Notes

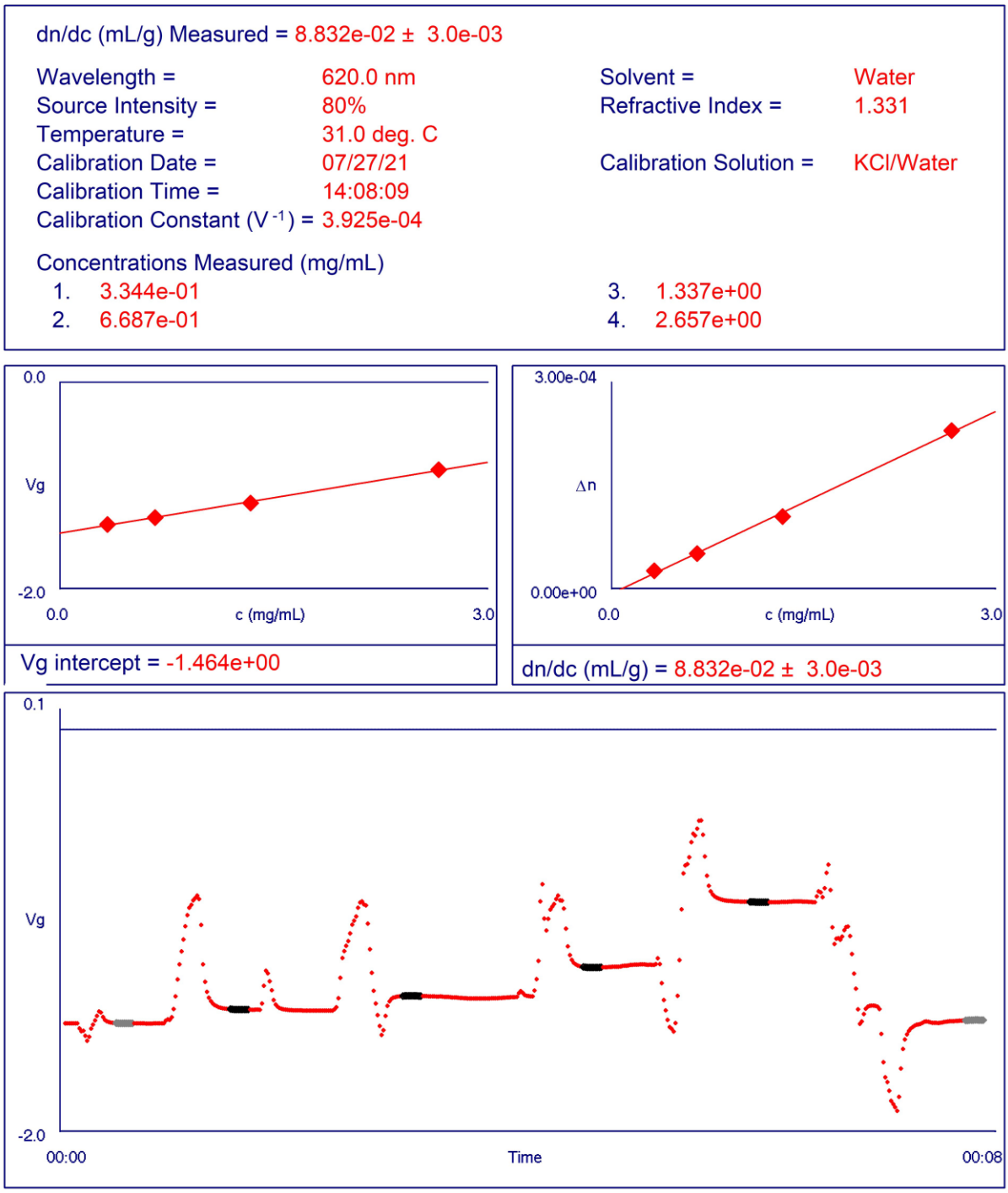

Figure S54. Refractive index increment (d*n*/d*c*) measurement report of **F1** (**pDFEA**) in PBS.

Brookhaven Instruments Corp.
Differential Refractometer Software Ver. 5.32

Date: Jul 29, 2021
Time: 11:06:16

Sample ID **F2, PBS**
Operator ID **PC**
Notes

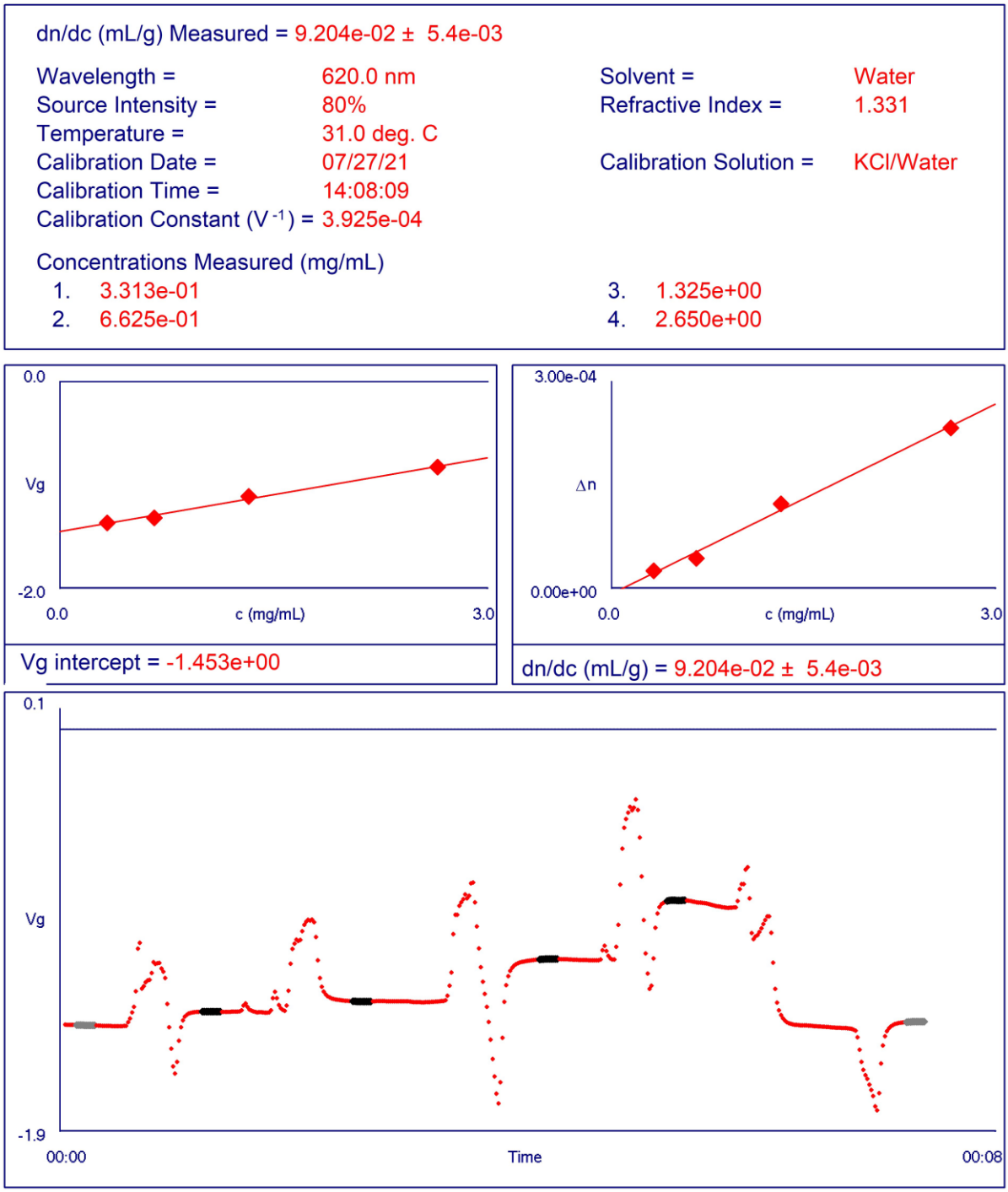

Figure S55. Refractive index increment (d*n*/d*c*) measurement report of **F2** (**pDFEA**) in PBS.

Brookhaven Instruments Corp.
Differential Refractometer Software Ver. 5.32

Date: Jul 29, 2021
Time: 11:15:27

Sample ID **F3, PBS**
Operator ID **PC**
Notes

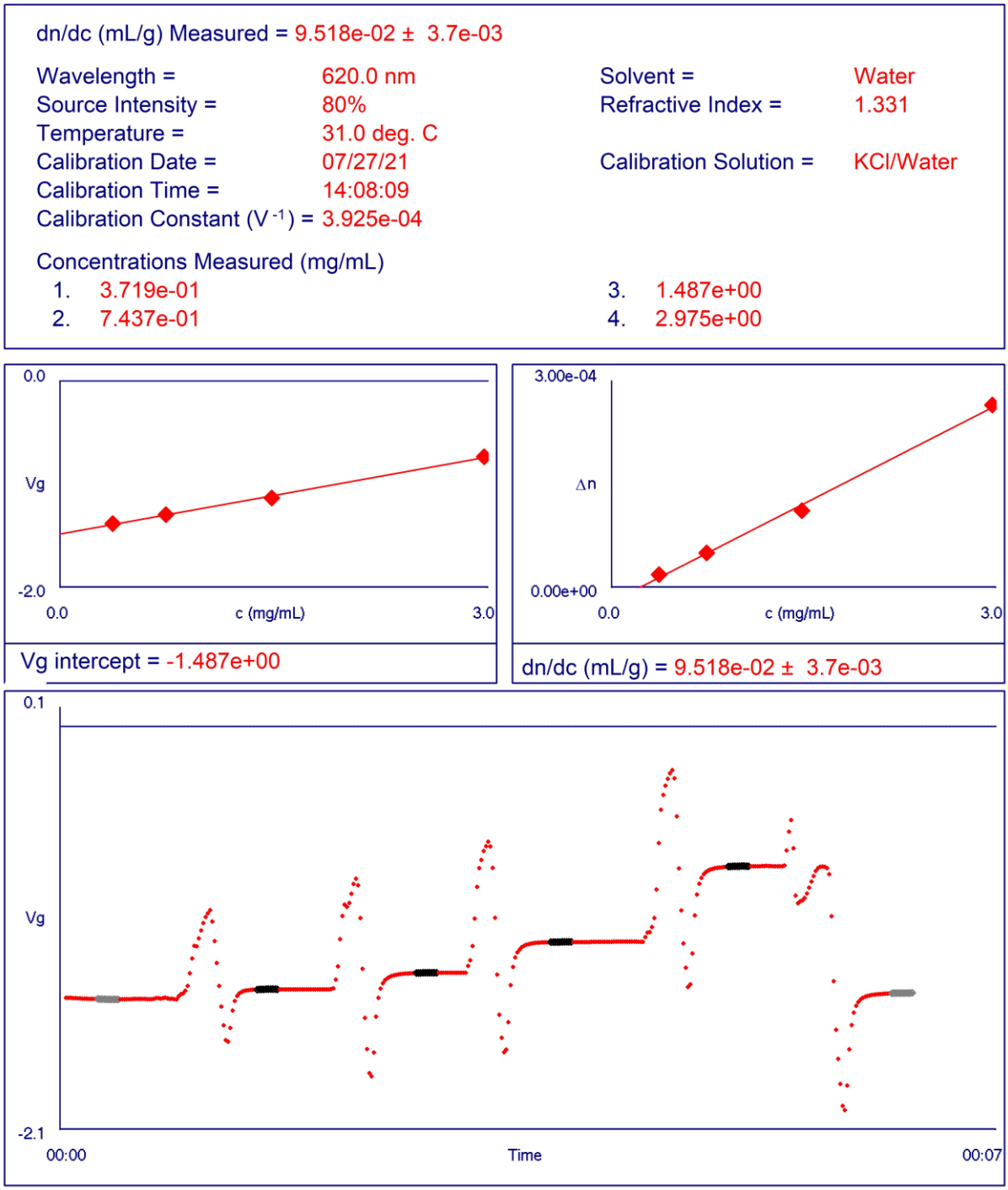

Figure S56. Refractive index increment (d*n*/d*c*) measurement report of **F3** (**pDFEA**) in PBS.

Brookhaven Instruments Corp.
Differential Refractometer Software Ver. 5.32

Date: Jul 29, 2021
Time: 12:14:20

Sample ID **I1, PBS**
Operator ID **PC**
Notes

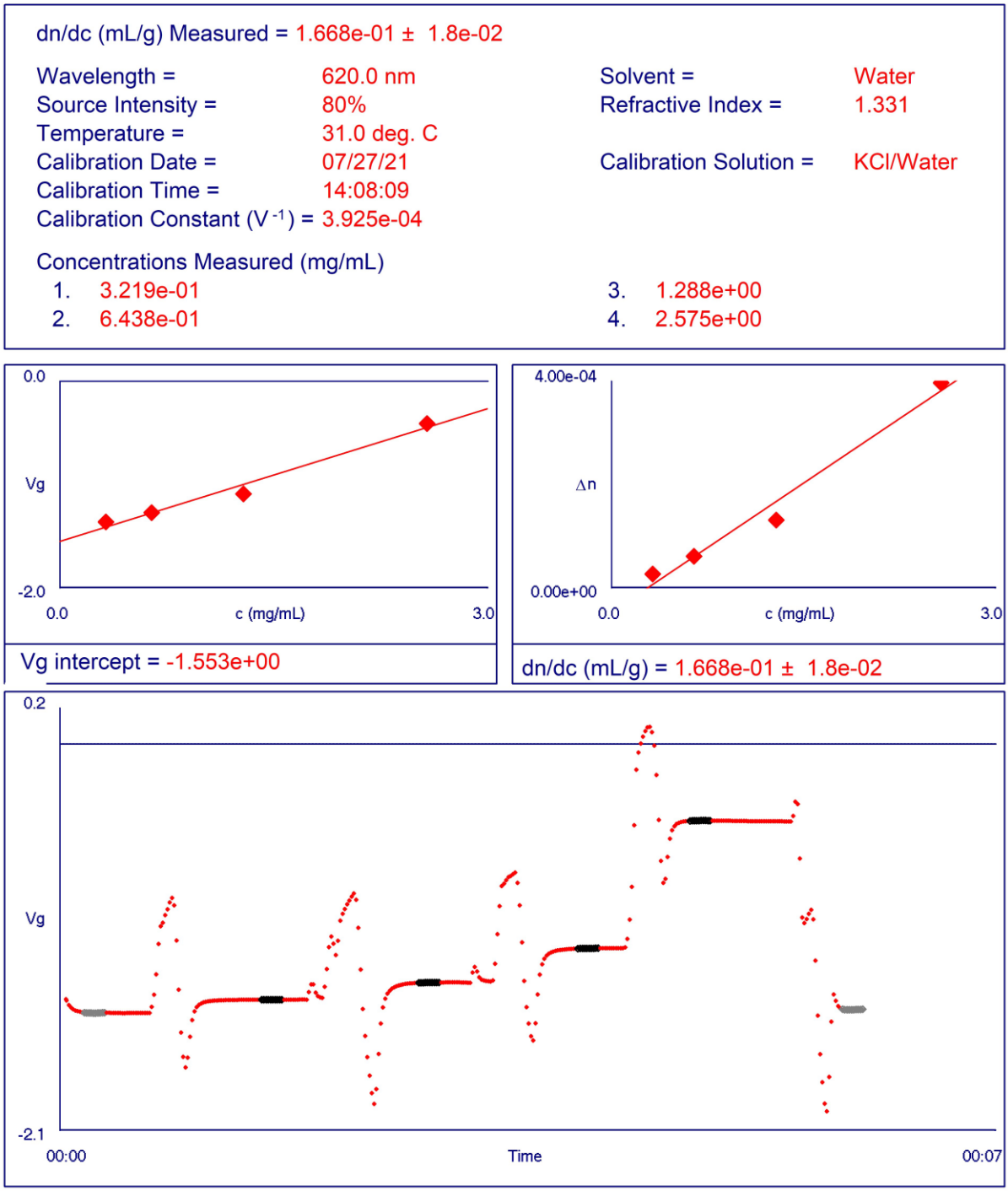

Figure S57. Refractive index increment (d*n*/d*c*) measurement report of **I1** (**pNIPAM**) in PBS.

Brookhaven Instruments Corp.
Differential Refractometer Software Ver. 5.32

Date: Jul 29, 2021
Time: 12:26:10

Sample ID **I2, PBS**
Operator ID **PC**
Notes

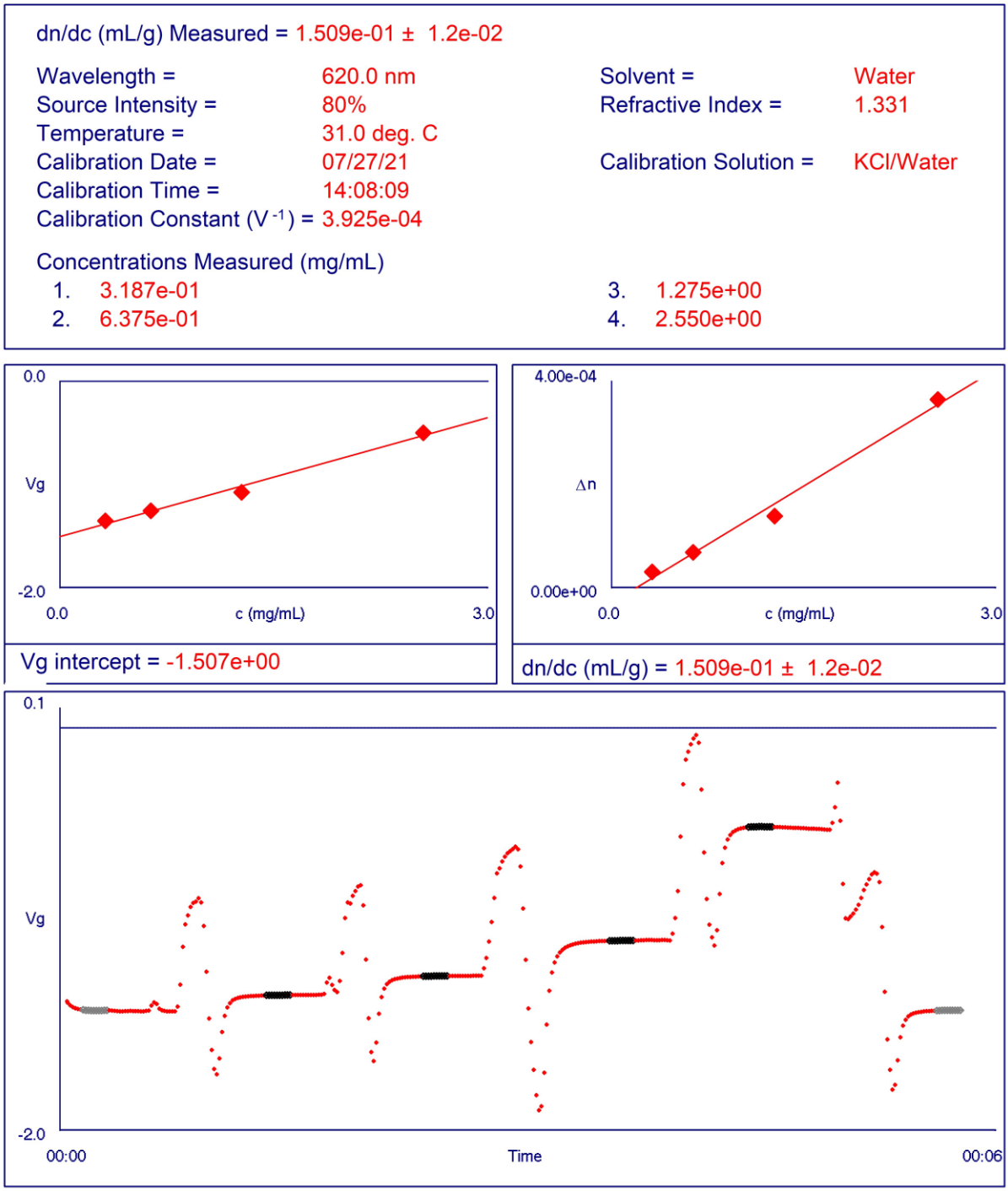

Figure S58. Refractive index increment (d*n*/d*c*) measurement report of **I2** (**pNIPAM**) in PBS.

Brookhaven Instruments Corp.
Differential Refractometer Software Ver. 5.32

Date: Jul 29, 2021
Time: 12:33:07

Sample ID **I3, PBS**
Operator ID **PC**
Notes

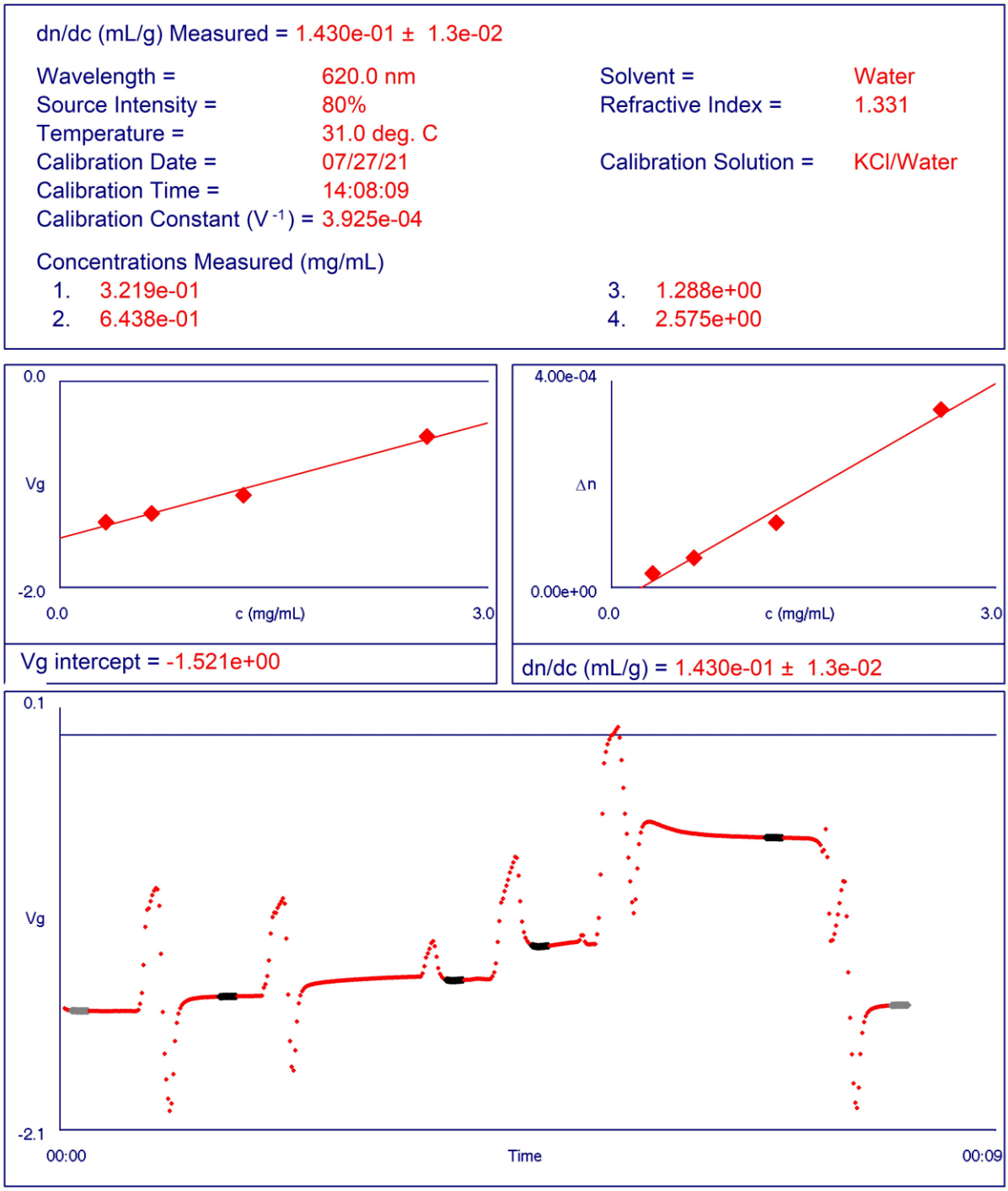

Figure S59. Refractive index increment (d*n*/d*c*) measurement report of **I3** (**pNIPAM**) in PBS.

Brookhaven Instruments Corp.
Differential Refractometer Software Ver. 5.32

Date: Jul 30, 2021
Time: 11:08:22

Sample ID **E1, PBS**
Operator ID **PC**
Notes

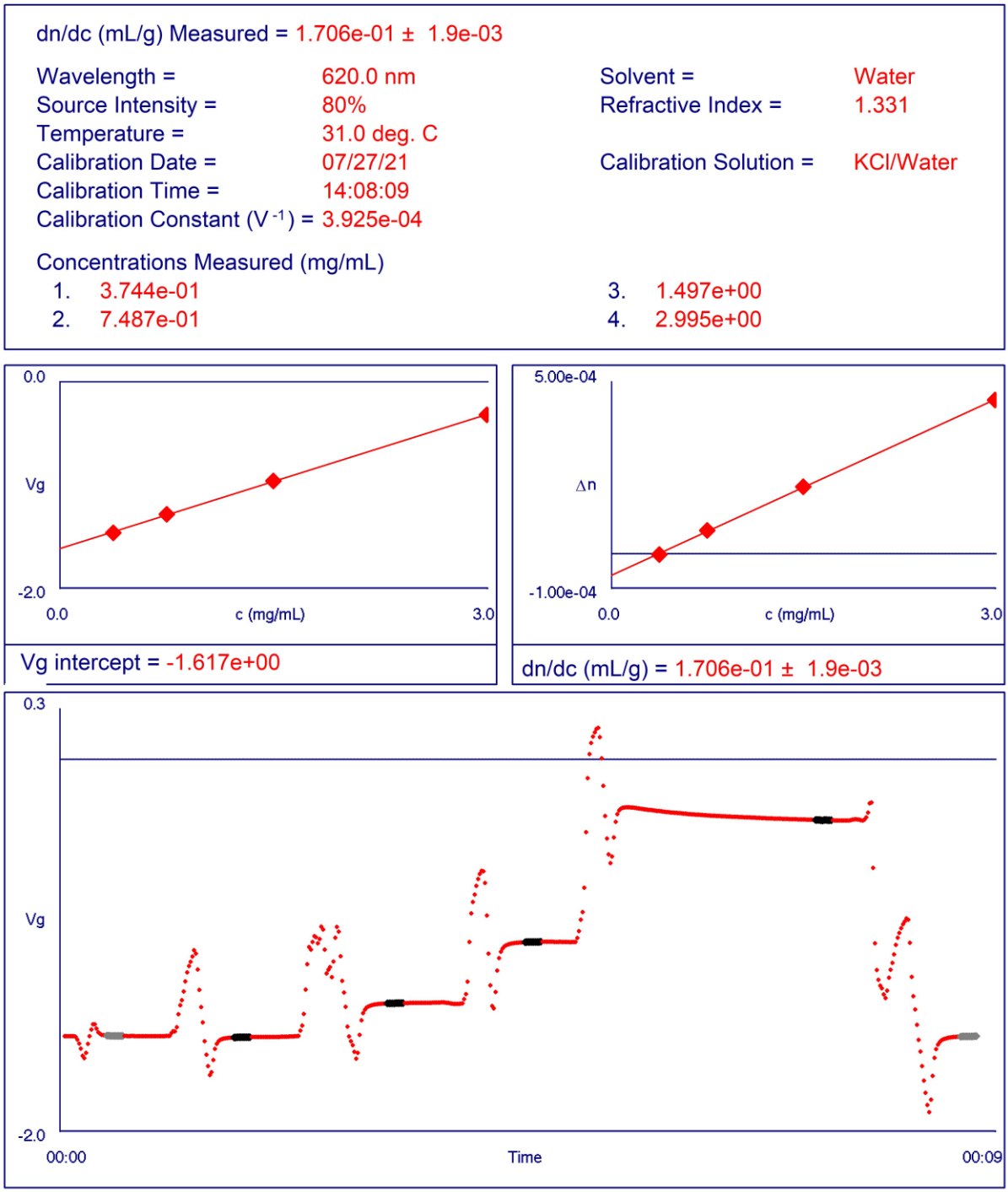

Figure S60. Refractive index increment (d*n*/d*c*) measurement report of **E1** (**pDEA**) in PBS.

Brookhaven Instruments Corp.
Differential Refractometer Software Ver. 5.32

Date: Jul 29, 2021
Time: 11:55:03

Sample ID **E2, PBS**
Operator ID **PC**
Notes

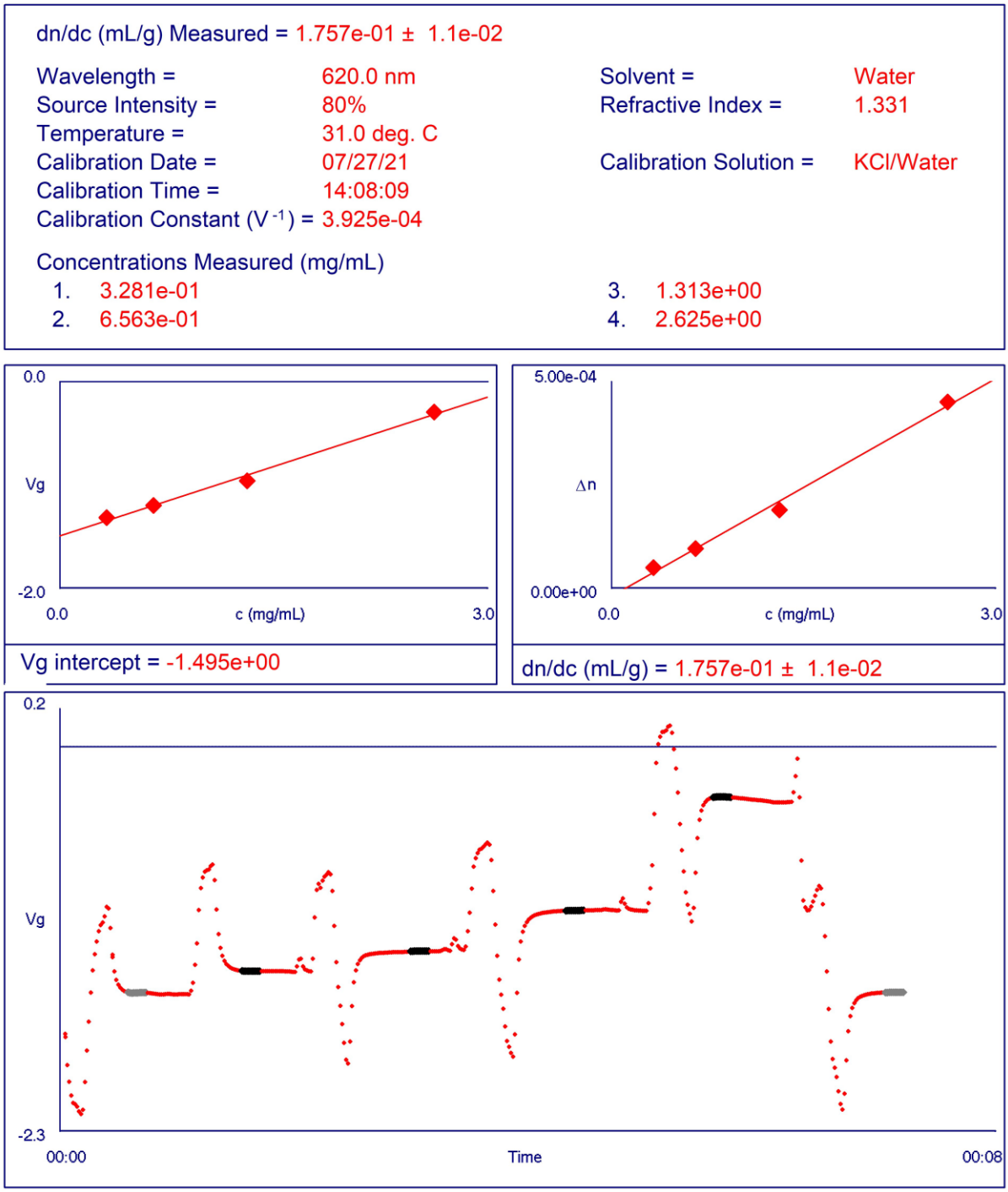

Figure S61. Refractive index increment (d*n*/d*c*) measurement report of **E2** (**pDEA**) in PBS.

Brookhaven Instruments Corp.
Differential Refractometer Software Ver. 5.32

Date: Jul 30, 2021
Time: 11:18:11

Sample ID **E3, PBS**
Operator ID **PC**
Notes

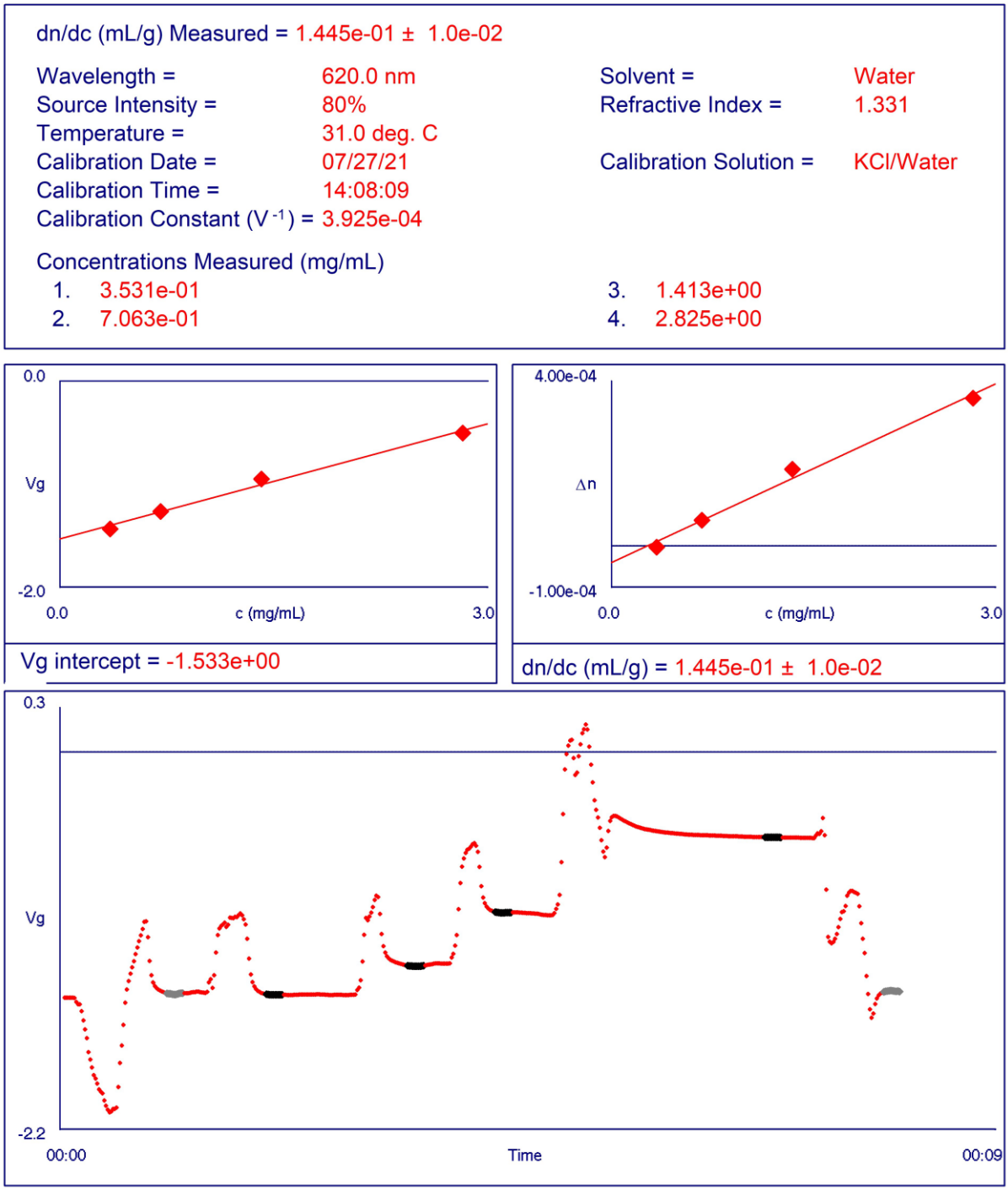

Figure S62. Refractive index increment (d*n*/d*c*) measurement report of **E3** (**pDEA**) in PBS.

Brookhaven Instruments Corp.
Differential Refractometer Software Ver. 5.32

Date: Jul 30, 2021
Time: 11:28:37

Sample ID **P1, PBS**
Operator ID **PC**
Notes

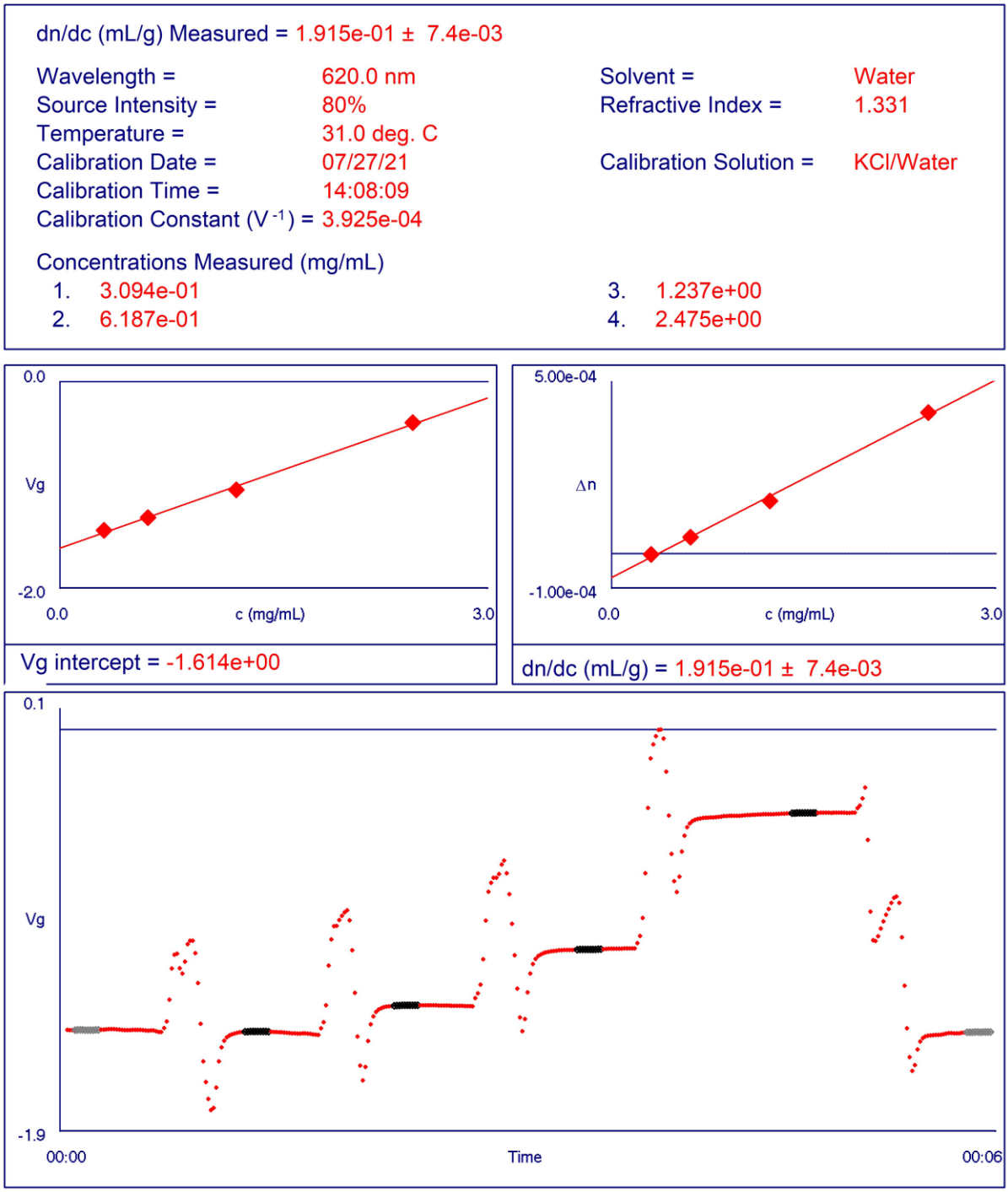

Figure S63. Refractive index increment (d*n*/d*c*) measurement report of **P1** (**pAP**) in PBS.

Brookhaven Instruments Corp.
Differential Refractometer Software Ver. 5.32

Date: Jul 29, 2021
Time: 12:59:10

Sample ID **P2, PBS**
Operator ID **PC**
Notes

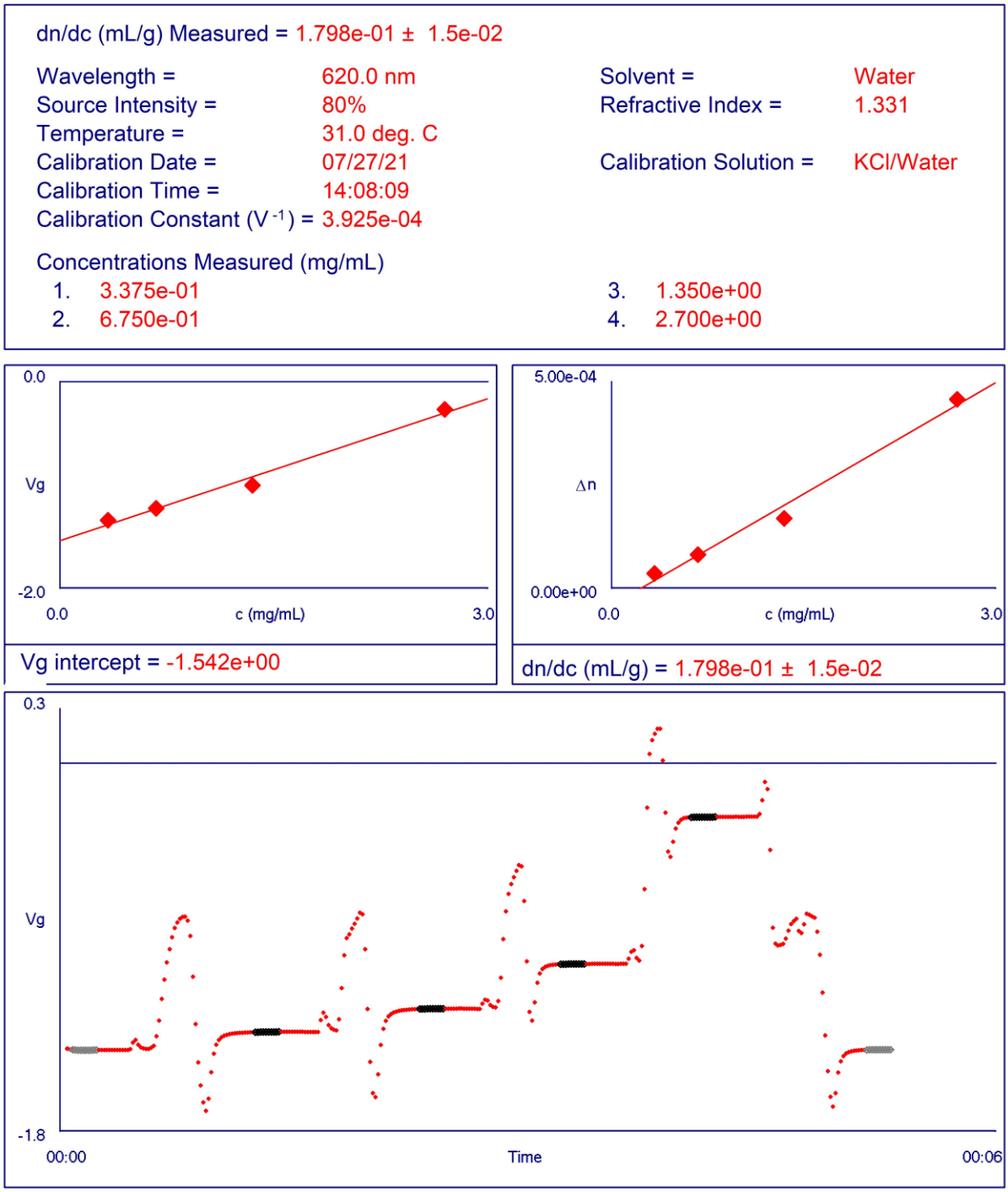

Figure S64. Refractive index increment (d*n*/d*c*) measurement report of **P2** (**pAP**) in PBS.

Brookhaven Instruments Corp.
Differential Refractometer Software Ver. 5.32

Date: Jul 29, 2021
Time: 13:05:54

Sample ID **P3, PBS**
Operator ID **PC**
Notes

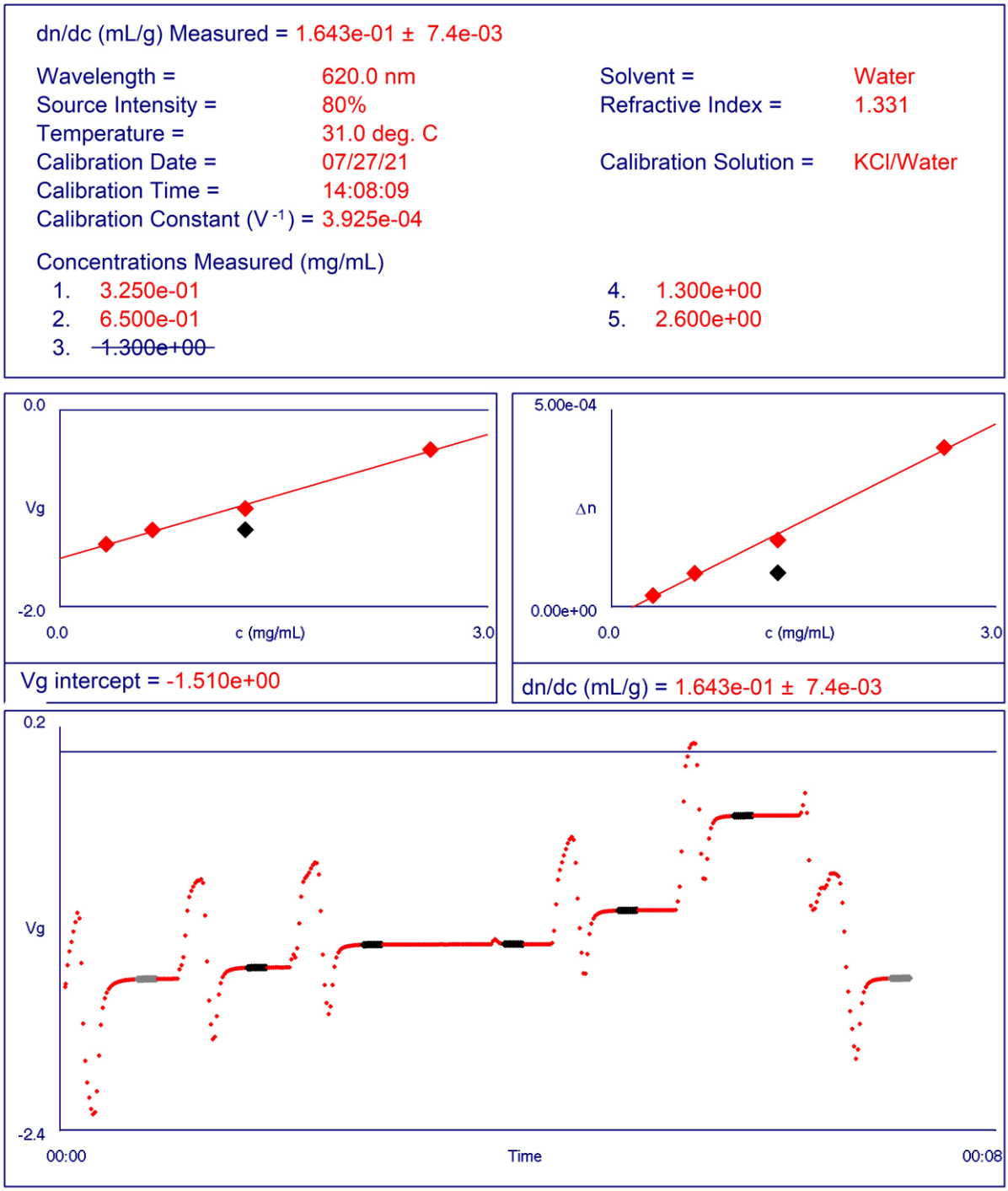

Figure S65. Refractive index increment (d*n*/d*c*) measurement report of **P2** (**pAP**) in PBS.

S8. Additional information

S8.1. Heating/cooling cycles of turbidimetry

Some polymers (particularly **pDFEA** and **pDEA**) tend to coalesce into large particles, which may sink, float, or stick to the cuvette. Coalescence is observed in some heating cycles (see, *e.g.*, **Figure S30**): initially small polymer aggregates are formed, and transmittance decreases. However, upon further heating, these small polymer aggregates may coalesce into large assemblies and (in some cases) move out of the detection area. As a result, transmittance increases again. In some samples, the coalesced assemblies occasionally and temporarily obscure the light beam and thus cause fluctuations in transmittance (caused by sample stirring).

Coalescence and polymer sticking/ floating do not prevent us from determining T_{CP} in the heating cycle: T_{CP} is defined by the initial polymer aggregation. For this reason, such a T_{CP} measurement is well reproducible (inter-run variation was mostly within 0.2 °C; see **Figure 3**). Conversely, T_{CP} measurements during the cooling cycle were unreliable – the polymer may behave as intended but may also float away from the laser beam or stick to the glass and thus hinder proper reading (the T_{CP} values in the cooling cycle varied more than 15 °C). We were unsure whether transmittance increased because the polymer aggregates dissolved or because they moved away from the light beam. Therefore, we decided to disregard these values and focus only on the T_{CP} determined during the heating cycle. The cooling cycle in turbidimetry was used merely as a regeneration phase for subsequent heating cycles; the samples remained at 10 °C for 30 minutes, which reliably ensured that all residual polymer aggregates dissolved.

S8.2. Structure-to-properties relationship

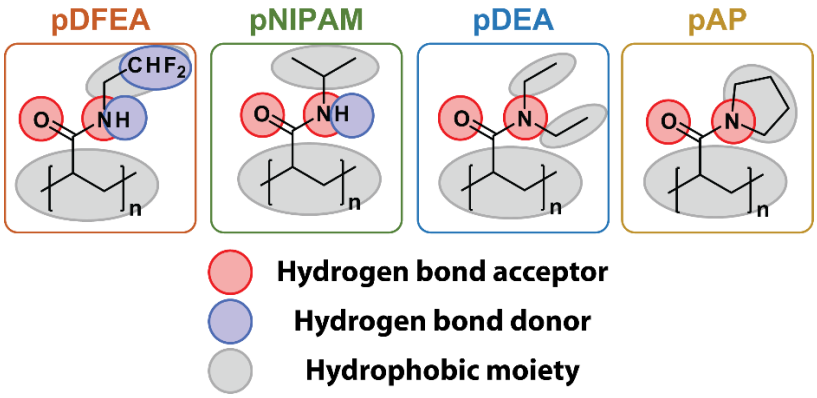

Scheme S1. Hydrogen bond acceptors, donors, and hydrophobic moieties in the molecules.

Zhao *et al.* [S2] suggested, that LCST-type thermoresponsive polymers must be hydrophilic (negative ΔH_m) and that the entropy of mixing (ΔS_m) must be negative as well (see **Scheme S3**). T_{CP} can then be calculated according to **Equation 1**.

$$T_{CP} = \frac{\Delta H_m}{\Delta S_m} \quad (1)$$

The ΔH_m of a polymer correlates with its hydrophilicity. Some researchers rank the hydrophilicity of polymers according to their T_{CP}.[S3] Therefore, the rank of hydrophobicity of the study polymers would be as follows:

pAP ≫ **pNIPAM** ≈ **pDEA** > **pDFEA**

Nevertheless, this approach is most suitable for ranking hydrophilicity of *similar* copolymers (*i.e.* those with *similar* molecular moieties, *e.g.* alkyls). However, **pDFEA** contains -CF_2H moiety, which is somewhat lipophilic, but can also form hydrogen bonds,[S4] decreasing the enthalpy of aggregation and

potentially lowering the T_{CP}. Therefore, we chose a different approach to rank the hydrophilicity of the polymers.

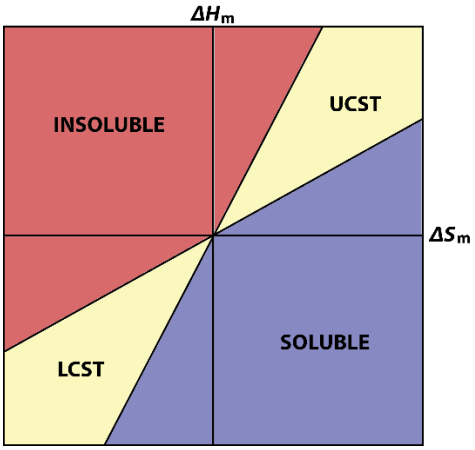

Scheme S2. A thermodynamic map showing the solubility and solution properties of polymers in water, redrawn according to [S2].

Zhao *et al.*[S2] suggests ranking the hydrophilicity of polymers according to the enthalpy of mixing (ΔH_m) of the alkanes (corresponding to the hydrophobic moiety) with water. We were unable to find mixing enthalpy of 1,1-difluoroethane with water in the literature, but the mixing enthalpy should inversely correlate with the solubility of the corresponding alkanes in water, enabling us to estimate the ranks of hydrophilicities of study polymers. The concentration of saturated 1,1-difluoroethane aqueous solution is 50 to 80 mmol/l (0 °C),[S5,S6] ethane 4.2 mmol/l (0 °C),[S6] propane 3.5 mmol/l (4 °C),[S6] and butane 3.1 mmol/l (3 °C).[S6] In this approach, we consider only the "hydrophilicity" of the substituent, and we disregard the effect of ligands on the hydrophilicity of the rest of the acrylamide (due to changes of electron densities on NH). Because 1,1-difluoroethane has (by far) the highest aqueous solubility of all corresponding alkanes, we rank **pDFEA** as the most hydrophilic (contrary to the rank suggested by method in [S3]). Both **pDEA** and **pAP** are di-substituted acrylamides; therefore, we rank them as the least hydrophilic. The cyclic structure of the **pAP** side chain will, however, be more compact, thereby shielding the hydrophilic amide less and being more hydrophilic than pDEA. This approach would suggest the following rank of hydrophilicities of polymers: [note1]

pDFEA ≫ **pNIPAM** > **pAP** > **pDEA**

As shown in the ITC results, **pDFEA** has strong intramolecular interactions, which decrease the aggregation enthalpy, possibly due to its intramolecular hydrogen bonds.[S4] These hydrogen bonds may explain the strong interactions of **pDFEA** with proteins as well.

The ΔS_m is hard to estimate from commonly available material quantities as it is strongly related to the release of 'high energy' hydrating water molecules. In line with this statement, the more hydrophilic **pAP** has a higher T_{CP} as **pDEA** as the hydration ΔS_m will be similar based on the presence of a tertiary amide (**Scheme S2**). Despite the higher hydrophilicity of **pNIPAM** and **pDFEA**, these polymers have a lower T_{CP} than **pAP**, which can be ascribed to the higher ΔS_m resulting from a more efficient hydration thanks to the secondary amide groups (both **pNIPAM** and **pDFEA**) and to the difluoroalkyl group (**pDFEA**).

[note 1] **pDEA** contains two ethyls; therefore, it is considered less hydrophilic than **pNIPAM**. Its monoethyl analogue (poly(ethyl-*N*-acrylamide) would be more hydrophilic than **pNIPAM**; and its T_{CP} is ≈ 73 °C.[2]

S8.3. Detection of terminal moiety

Detecting these terminal moieties in polymers with M_w around/ above 25 kg/mol is notoriously difficult because of their very low content, broad peaks, noise and trace contaminants (see NMR spectra in ESI).[S7] The terminal CH_3O moiety provides ^{1}H NMR signals at ≈ 3.5-3.6 ppm, and -CH_2CH_2- (from acrylate) provides NMR signals at 2.6 to 2.8 ppm.[S8,S9] Unfortunately, these signals are often partly masked by broad peaks from solvents or polymers (NCH_2, 3.2 to 3.9 ppm; acrylamide peak at ≈ 2.3 ppm; see NMR spectra in ESI). Nevertheless, we remeasured ^{1}H NMR spectra of all polymers in higher concentrations and with a higher number of scans (256 scans), now added to ESI as raw files (available for inspection). We were able to detect signals of terminal -CH_2CH_2-, most pronounced in polymers **F1** and **P1**, where the content of end-moiety is the highest and the end-moiety signals are not masked by polymer signals (**Figure S69**). Therefore, the signals of terminal -CH_2CH_2- serve as an indirect evidence of terminal -$CH_2CH_2COOCH_3$ moiety. The remaining peaks in this region can be attributed to low-molecular weight contaminants (mostly solvents; their peaks are narrow, but the overall integral is low).

We measured ^{1}H-NMR spectra in MeOH-4d solutions because polymers dissolve in MeOH, whose residual peak is found at 3.31 ppm, whereas the peak of water is at 4.78 ppm;[S10] therefore, MeOH does not mask these terminal peaks. DMSO-6d has a peak at 2.50 ppm, and water has a peak at 3.33 ppm; thus, the peaks of these solvents would mask the peaks of interest.[S10]

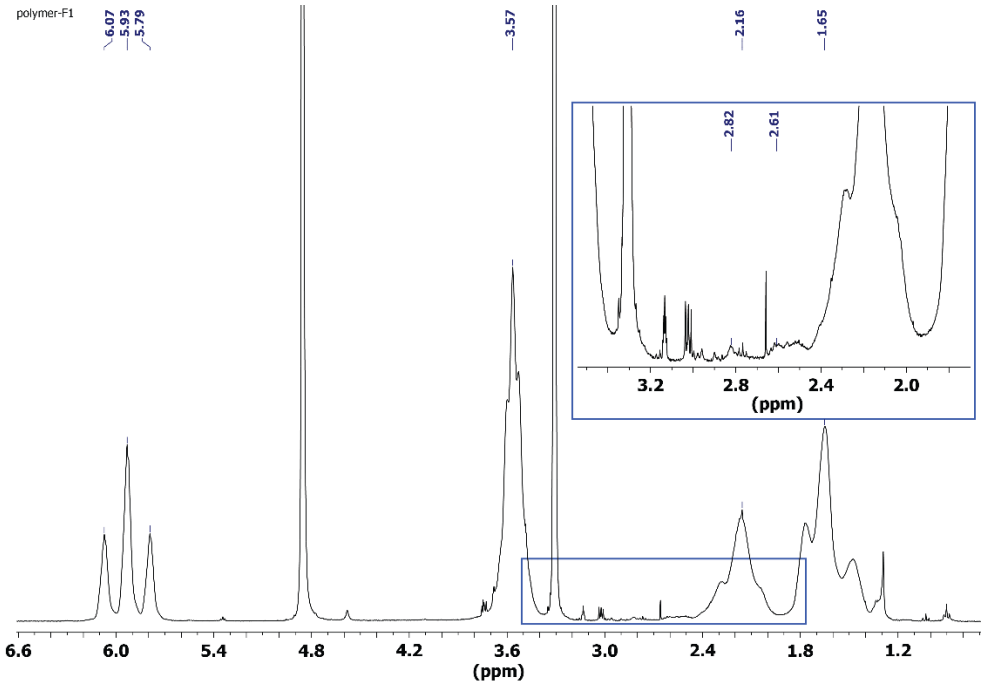

Figure S66. ^{1}H NMR of polymer **F1** in MeOH-4d showing the peaks at 2.6 and 2.8 ppm, corresponding to terminal CH_2CH_2 moieties.[S8,S9] The CH_3O- moiety remained masked by other peaks.

S9. Calibration curves for labelled polymers

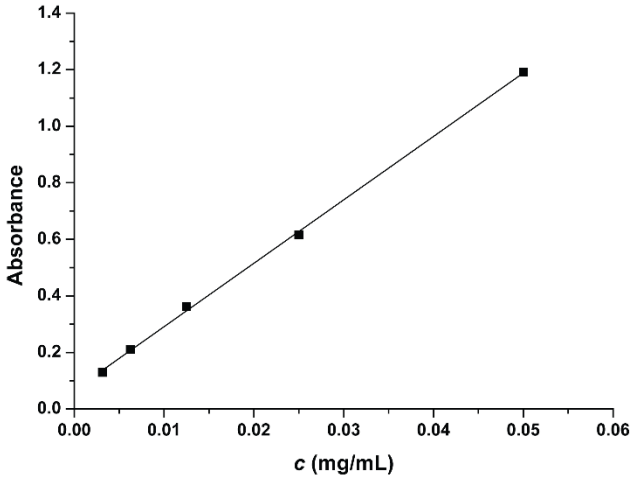

Figure S67. Calibration curve; the absorbance of Cy7-amine as a function concentration (λ = 700 nm) in MeOH, given by the formula $A = 0.0668 \pm 0.0084 + c \cdot (22.429 \pm 0.323)$; $R^2 = 0.9997$.

S10. Size exclusion chromatograms of labelled polymers

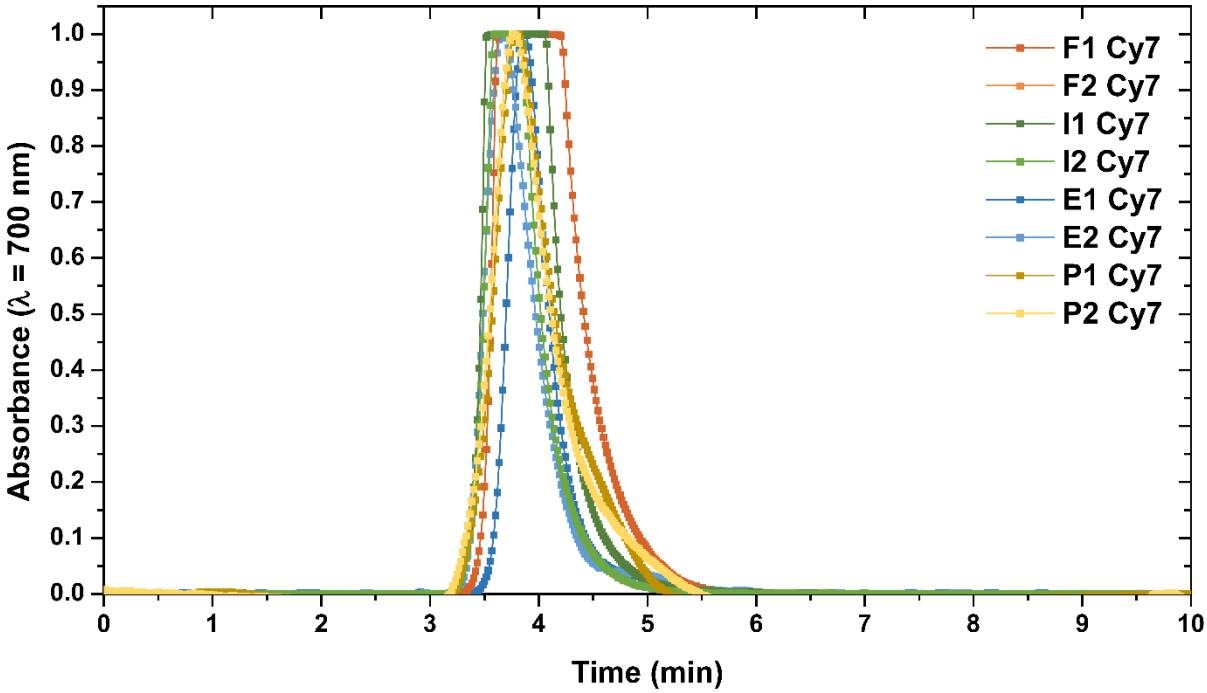

Figure S68. Size exclusion chromatograms (SEC traces) of Cy7-labelled polymers; normalized absorbance at 505 nm as a function of time. The absorbance of polymers in most cases exceeded the detection maximum of the detector. The concentration of low-molecular Cy7 (non-covalently bound) was in most cases below the limit of detection; its concentration was ≥ 0.5%).

S11. *In vivo* experiments

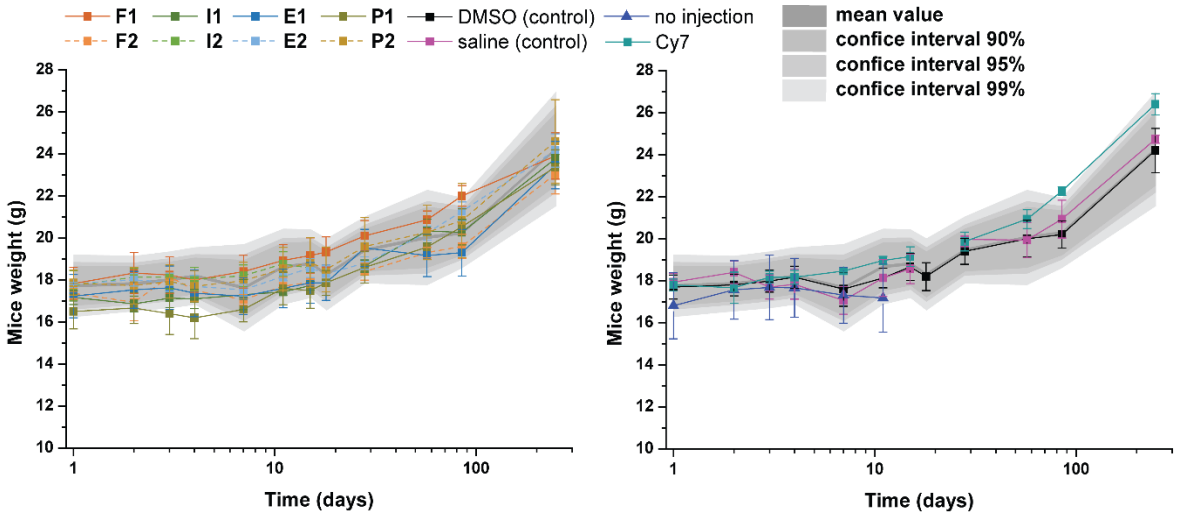

Figure S69. Weights of mice from all groups as a function of time and their comparison with control group (injected with mere DMSO).

S12. Polymer pharmacokinetics - raw data

Table S6. Signal of polymer **F1** (arbitrary units) in mice M1, M2, and M3 as a function of time.

Mouse M1		Mouse M2		Mouse M3	
Time (d)	**Signal**	**Time (d)**	**Signal**	**Time (d)**	**Signal**
0.013461	7553548.5	0.0194213	28789540	0.01521991	31360926
0.015451	8117890.5	0.0218287	31039352	0.01748843	34445812
0.245405	15775586	0.23212963	53403336	0.22951389	64652064
0.247280	16275670	0.23398148	52192068	0.23135417	65437296
1.040648	18469152	1.00384259	46714892	0.98439815	55626292
1.043160	18370780	1.00635417	46124912	0.98690972	53828384
1.992164	17010132	1.9553588	44558780	1.93591435	49688332
1.994664	17324938	1.9578588	42068244	1.93841435	49639340
2.933530	16122334	2.89672454	41400336	2.87728009	44955364
2.936968	16588533	2.90016204	39764792	2.88071759	46544544
6.965347	15363530	6.92854167	35814676	6.90909722	38848812
6.967801	15119886	6.93099537	34991516	6.91155093	38013320
14.961748	9715552	14.9249421	24411188	14.9054977	29248908
14.964178	9733786	14.9273727	24318764	14.9079282	28798778
28.996458	8228305	28.9596528	21997504	28.9402083	24370120
28.999225	8114443.5	28.962419	21839146	28.9429745	24357358
56.111609	6878973	56.0748032	18392500	56.0553588	18631800
56.113819	6900557.5	56.0770139	19244228	56.0575694	18706046
70.259271	5063877.5	70.2224653	12027219	70.2030208	13582575
70.261840	5318400.5	70.2250347	13532210	70.2055903	13935688
86.117326	5881183	86.0805208	16400983	86.0610764	13944691
86.119433	6108106	86.0826273	16605837	86.0631829	13939347
122.075046	4463150.5	122.038241	11754967	122.018796	8767569
122.077396	4765173.5	122.04059	11860858	122.021146	8973079
150.043866	6004102	150.00706	15556560	149.987616	10899622
150.046377	6273049	150.009572	15228101	149.990127	10932180
184.027361	4179011.25	183.990556	10701935	183.971111	6763285.5
184.029525	4357977.5	183.99272	11277099	183.973275	6819046.5
247.073785	4320709.5	**Mouse sacrificed on day 202**		247.017535	5867368.5
247.075775	4238285.5			247.019525	5761552

Table S7. Area of depot of polymer **F1** (pixels) in mice M1, M2, and M3 as a function of time.

Mouse M1		Mouse M2		Mouse M3	
Time (d)	**Area (px)**	**Time (d)**	**Area (px)**	**Time (d)**	**Area (px)**
0.013461	7113	0.0194213	12983	0.01521991	15194
0.015451	7346	0.0218287	13324	0.01748843	15692
0.245405	12878	0.23212963	27028	0.22951389	28771
0.247280	12897	0.23398148	27946	0.23135417	29381
1.040648	17878	1.00384259	30996	0.98439815	34191
1.043160	18410	1.00635417	31069	0.98690972	32400
1.992164	16673	1.9553588	31485	1.93591435	34665
1.994664	16872	1.9578588	31173	1.93841435	34590
2.933530	15699	2.89672454	29728	2.87728009	32840
2.936968	15901	2.90016204	29994	2.88071759	35051
6.965347	14318	6.92854167	28486	6.90909722	31393
6.967801	13887	6.93099537	28515	6.91155093	31205
14.961748	9477	14.9249421	25585	14.9054977	26450
14.964178	9520	14.9273727	25239	14.9079282	26038
28.996458	7961	28.9596528	22404	28.9402083	18563
28.999225	7855	28.962419	22449	28.9429745	18145
56.111609	6344	56.0748032	15517	56.0553588	14194
56.113819	6212	56.0770139	16540	56.0575694	14496
70.259271	4788	70.2224653	11463	70.2030208	12070
70.261840	5154	70.2250347	12956	70.2055903	13058
86.117326	5875	86.0805208	13839	86.0610764	11908
86.119433	6113	86.0826273	14109	86.0631829	11884
122.075046	3844	122.038241	11073	122.018796	9264
122.077396	4161	122.04059	11064	122.021146	9298
150.043866	5238	150.00706	13343	149.987616	10513
150.046377	5513	150.009572	13029	149.990127	10620
184.027361	3309	183.990556	10548	183.971111	7395
184.029525	3540	183.99272	10857	183.973275	7387
247.073785	3662	**Mouse sacrificed on day 202**		247.017535	6218
247.075775	3599			247.019525	6212

Table S8. Signal of polymer **F2** (arbitrary units) in mice M1, M2, and M3 as a function of time.

Mouse M1		Mouse M2		Mouse M3	
Time (d)	**Signal**	**Time (d)**	**Signal**	**Time (d)**	**Signal**
0.010347	54262996	0.0159838	125203992	0.02002315	157183568
0.012211	61030380	0.0177662	133387432	0.02228009	175427376
0.224722	257556048	0.22340278	364630176	0.22635417	330966784
0.226412	265424240	0.22518519	373037920	0.22885417	340889376
1.047130	142496336	1.03324074	220129952	1.01240741	163846848
1.049306	146766496	1.03541667	217174976	1.01458333	155595920
2.045625	111878280	2.03173611	169421696	2.01090278	135859856
2.050220	114271352	2.03633102	169046400	2.01549769	131863624
2.976250	92945104	2.96236111	137816128	2.94152778	116386472
2.978449	98889128	2.96456019	138315120	2.94372685	117224224
7.159144	72358720	7.14525463	103049336	7.1244213	86234424
7.161262	74814096	7.14737269	103634992	7.12653935	85673040
14.950382	48842072	14.9364931	68152000	14.9156597	54715500
14.955000	50066312	14.9411111	67186296	14.9202778	55931768
28.877488	38519392	28.8635995	46626184	28.8427662	38159616
28.880637	39757032	28.8667477	48511032	28.8459144	41520100
56.979942	29742360	56.9660532	37191264	56.9452199	28764126
56.982188	30193790	56.9682986	38076452	56.9474653	30001436
70.180891	15863670	70.1670023	21505322	70.146169	22380846
70.183657	16490397	70.1697685	20601730	70.1489352	21944422
85.974792	18855626	85.9400694	24156698	85.9343866	25128722
85.960903	22300382	85.9552199	28349002	85.9365278	24962034
85.969109	24780614	85.9573611	28949976	122.948773	19910804
85.971250	25026776	122.969606	21052802	122.950926	20359668
122.983495	18948076	122.971759	21255298	149.893275	21743064
122.985648	19395514	149.914109	26752054	149.898021	22090932
149.927998	22636072	149.918854	27206508	183.023657	16337871
149.932743	22618798	183.044491	20172262	183.02831	16523300
183.058380	16835932	183.049144	20732726	247.055856	13095169
183.063032	17176454	**Mouse sacrificed on day 202**		247.062211	13351230
247.090579	12716399				
247.096933	12210013				

Table S9. Area of depot of polymer **F2** (pixels) in mice M1, M2, and M3 as a function of time.

Mouse M1		Mouse M2		Mouse M3	
Time (d)	**Area (px)**	**Time (d)**	**Area (px)**	**Time (d)**	**Area (px)**
0.010347	16378	0.0159838	29436	0.02002315	25347
0.012211	16762	0.0177662	29150	0.02228009	26676
0.224722	57313	0.22340278	74117	0.22635417	69478
0.226412	60470	0.22518519	75451	0.22885417	68387
1.047130	61276	1.03324074	76031	1.01240741	72292
1.049306	63638	1.03541667	74992	1.01458333	67642
2.045625	57793	2.03173611	70070	2.01090278	66796
2.050220	58448	2.03633102	67156	2.01549769	66146
2.976250	52045	2.96236111	61223	2.94152778	61498
2.978449	54150	2.96456019	62252	2.94372685	61795
7.159144	47431	7.14525463	55139	7.1244213	52711
7.161262	46490	7.14737269	56592	7.12653935	52553
14.950382	42139	14.9364931	52632	14.9156597	46269
14.955000	43394	14.9411111	51761	14.9202778	48562
28.877488	39903	28.8635995	45565	28.8427662	41493
28.880637	39630	28.8667477	46000	28.8459144	43524
56.979942	32427	56.9660532	37388	56.9452199	30885
56.982188	32049	56.9682986	38558	56.9474653	34163
70.180891	22960	70.1670023	29409	70.146169	29317
70.183657	22805	70.1697685	29411	70.1489352	28401
85.974792	23213	85.9400694	29090	85.9343866	28015
85.960903	28978	85.9552199	32389	85.9365278	28445
85.969109	26666	85.9573611	33158	122.948773	22181
85.971250	26334	122.969606	25770	122.950926	22153
122.983495	20365	122.971759	26676	149.893275	25797
122.985648	19765	149.914109	32245	149.898021	25390
149.927998	22560	149.918854	32741	183.023657	18403
149.932743	22686	183.044491	26213	183.02831	18752
183.058380	19502	183.049144	26833	247.055856	11868
183.063032	19990	**Mouse sacrificed on day 202**		247.062211	11959
247.090579	14313				
247.096933	14029				

Table S10. Signal of polymer **I1** (arbitrary units) in mice M1, M2, and M3 as a function of time.

Mouse M1		Mouse M2		Mouse M3	
Time (d)	**Area (px)**	**Time (d)**	**Area (px)**	**Time (d)**	**Area (px)**
0.02633102	40819784	0.01673611	36644768	0.01299769	64834648
0.02996528	44773180	0.01873843	38908120	0.01515046	73464312
0.22190972	90299304	0.22025463	89767080	0.22270833	195998768
0.22383102	95070320	0.2259838	90036632	0.22454861	202969536
1.02435185	103279472	1.02292824	105543352	1.03050926	168052912
1.02648148	102399920	1.02537037	96409176	1.03290509	166631664
2.03247685	112248640	2.0019213	132527464	1.98108796	175614352
2.0350463	120344688	2.00449074	133243152	1.98365741	177275344
3.0316088	111311000	3.00105324	115107552	2.98021991	170138112
3.03372685	107239544	3.0031713	115683040	2.98233796	172770032
7.21012731	98133752	7.17957176	105373544	7.15873843	169507056
7.21243056	100931640	7.181875	101545024	7.16104167	166734912
14.9954051	74861344	14.9648495	73298632	14.9440162	128718520
14.9974769	76377616	14.9669213	74637264	14.946088	127076672
28.9281713	67346872	28.8976157	61217040	28.8767824	104246528
28.9306597	67641416	28.9001042	63226592	28.8792708	104403656
57.0315972	35490684	57.0010417	40205780	56.9802083	63406312
57.0342361	36121528	57.0036806	41205004	56.9828472	63892100
70.1842824	11815777	70.1537269	16556711	70.1328935	37086536
70.187581	10599304	70.1570255	16804756	70.1361921	36601864
85.9946065	19913270	85.9737731	38267076	85.9685417	43776440
86.0199306	20589960	85.989375	23767526	85.9707986	43463804
86.0221875	20231838	85.9916319	23795058	122.990764	4934739.5
86.025162	15257848	123.011597	11812462	122.99338	4977021
123.042153	10225124	123.014213	11842725	123.143553	21010404
123.044769	10180461	123.164387	1684026	123.145579	20460130
123.194942	1675300.5	123.166412	1642069.25	149.929352	21444948
123.196968	1620633.63	149.950185	16974868	183.063484	14851167
149.980741	11585462	183.084317	11152629	183.065741	15068273
183.114873	7154293.5	183.086574	11154938	247.094583	10037237
183.11713	7015475	247.115417	7451302.5	247.096771	9839475
Mouse sacrificed on day 202		247.117604	7722107		

Table S11. Area of depot of polymer **I1** (pixels) in mice M1, M2, and M3 as a function of time.

Mouse M1		Mouse M2		Mouse M3	
Time (d)	**Signal**	**Time (d)**	**Signal**	**Time (d)**	**Signal**
0.02633102	14356	0.01673611	14561	0.01299769	17818
0.02996528	15407	0.01873843	15327	0.01515046	19355
0.22190972	24857	0.22025463	28558	0.22270833	35973
0.22383102	26085	0.2259838	28648	0.22454861	36739
1.02435185	27779	1.02292824	31557	1.03050926	41403
1.02648148	30106	1.02537037	30886	1.03290509	41239
2.03247685	34890	2.0019213	39366	1.98108796	47599
2.0350463	35763	2.00449074	41604	1.98365741	47514
3.0316088	32411	3.00105324	38578	2.98021991	43929
3.03372685	34431	3.0031713	37271	2.98233796	45866
7.21012731	31717	7.17957176	34210	7.15873843	38580
7.21243056	32353	7.181875	34000	7.16104167	38861
14.9954051	25996	14.9648495	32427	14.9440162	35054
14.9974769	26919	14.9669213	32789	14.946088	35706
28.9281713	22132	28.8976157	28257	28.8767824	30733
28.9306597	22596	28.9001042	29916	28.8792708	32798
57.0315972	17099	57.0010417	23847	56.9802083	21825
57.0342361	17524	57.0036806	23899	56.9828472	21839
70.1842824	10293	70.1537269	15661	70.1328935	17257
70.187581	9443	70.1570255	16199	70.1361921	17323
85.9946065	16913	85.9737731	15650	85.9685417	16225
86.0199306	13563	85.989375	18251	85.9707986	16790
86.0221875	13435	85.9916319	18335	122.990764	2960
86.025162	12212	123.011597	12906	122.99338	2965
123.042153	9379	123.014213	12722	123.143553	12276
123.044769	9363	123.164387	258	123.145579	11647
123.194942	93	123.166412	260	149.929352	11415
123.196968	91	149.950185	16431	183.063484	8843
149.980741	9758	183.084317	13395	183.065741	8911
183.114873	7005	183.086574	13071	247.094583	7464
183.11713	7043	247.115417	10132	247.096771	7195
Mouse sacrificed on day 202		247.117604	10836		

Table S12. Signal of polymer **I2** (arbitrary units) in mice M1, M2, and M3 as a function of time.

Mouse M1		Mouse M2		Mouse M3	
Time (d)	**Signal**	**Time (d)**	**Signal**	**Time (d)**	**Signal**
0.032778	18719762	0.01844907	33847708	0.01446759	51774700
0.035521	18982692	0.02033565	35520840	0.01644676	57045540
0.242720	36602796	0.26974537	51685164	0.25232639	104401752
0.244618	34985852	0.2718287	50911232	0.25450231	101315544
1.073611	46416612	1.03125	65149736	0.99930556	84368520
1.075903	46315612	1.03354167	54239184	1.00159722	89002648
2.035255	43738808	1.99289352	54652188	1.96094907	89313928
2.037593	46241268	1.99523148	59481224	1.96328704	89875296
3.026563	48850688	2.98420139	65064300	2.95225694	94513128
3.029097	48543836	2.98673611	65080808	2.95479167	93729056
7.055336	45888696	7.01297454	63067996	6.98103009	96953496
7.057593	45574720	7.01523148	61650760	6.98328704	95358432
15.047234	34346584	15.0048727	50252372	14.9729282	75662992
15.050243	35257972	15.0078819	45221096	14.9759375	81280568
29.182743	25249454	29.1403819	48598280	29.1084375	72847080
29.185405	25436142	29.143044	49131672	29.1110995	73792056
56.171192	17100800	56.128831	31848922	56.0968866	45324592
56.175382	18043014	56.1330208	33270792	56.1010764	48038380
70.350521	11047815	70.3081597	25482802	70.2762153	32795702
70.353565	10768138	70.3112037	25107712	70.2792593	33140768
86.211505	10611325	86.1691435	22572650	86.1371991	28086168
86.213646	11582647	86.1712847	23184970	86.1393403	27958440
122.168889	7938186	122.126528	13841878	122.094583	15355841
122.171273	8030185	122.128912	14988715	122.096968	15831957
150.137176	9159573	150.094815	15772427	150.06287	15523631
150.139375	8933243	150.097014	14240340	150.065069	15354183
184.123391	5963470.5	184.08103	11065047	184.049086	9364890
184.128218	6446911	184.085856	10279452	184.053912	9416439
247.167245	4623424	**Mouse sacrificed on day 202**		247.09294	7858573.5
247.169271	4684578			247.094965	7599768

Table S13. Area of depot of polymer **I2** (pixels) in mice M1, M2, and M3 as a function of time.

Mouse M1		Mouse M2		Mouse M3	
Time (d)	**Signal**	**Time (d)**	**Signal**	**Time (d)**	**Signal**
0.032778	18719762	0.01844907	33847708	0.01446759	51774700
0.035521	18982692	0.02033565	35520840	0.01644676	57045540
0.242720	36602796	0.26974537	51685164	0.25232639	104401752
0.244618	34985852	0.2718287	50911232	0.25450231	101315544
1.073611	46416612	1.03125	65149736	0.99930556	84368520
1.075903	46315612	1.03354167	54239184	1.00159722	89002648
2.035255	43738808	1.99289352	54652188	1.96094907	89313928
2.037593	46241268	1.99523148	59481224	1.96328704	89875296
3.026563	48850688	2.98420139	65064300	2.95225694	94513128
3.029097	48543836	2.98673611	65080808	2.95479167	93729056
7.055336	45888696	7.01297454	63067996	6.98103009	96953496
7.057593	45574720	7.01523148	61650760	6.98328704	95358432
15.047234	34346584	15.0048727	50252372	14.9729282	75662992
15.050243	35257972	15.0078819	45221096	14.9759375	81280568
29.182743	25249454	29.1403819	48598280	29.1084375	72847080
29.185405	25436142	29.143044	49131672	29.1110995	73792056
56.171192	17100800	56.128831	31848922	56.0968866	45324592
56.175382	18043014	56.1330208	33270792	56.1010764	48038380
70.350521	11047815	70.3081597	25482802	70.2762153	32795702
70.353565	10768138	70.3112037	25107712	70.2792593	33140768
86.211505	10611325	86.1691435	22572650	86.1371991	28086168
86.213646	11582647	86.1712847	23184970	86.1393403	27958440
122.168889	7938186	122.126528	13841878	122.094583	15355841
122.171273	8030185	122.128912	14988715	122.096968	15831957
150.137176	9159573	150.094815	15772427	150.06287	15523631
150.139375	8933243	150.097014	14240340	150.065069	15354183
184.123391	5963470.5	184.08103	11065047	184.049086	9364890
184.128218	6446911	184.085856	10279452	184.053912	9416439
247.167245	4623424	**Mouse sacrificed on day 202**		247.09294	7858573.5
247.169271	4684578			247.094965	7599768

Table S14. Signal of polymer **E1** (arbitrary units) in mice M1, M2, and M3 as a function of time.

Mouse M1		Mouse M2		Mouse M3	
Time (d)	**Signal**	**Time (d)**	**Signal**	**Time (d)**	**Signal**
0.011493	100759712	0.01586806	78106272	0.02699074	131686488
0.013692	107975536	0.0177662	85563992	0.02877315	142938224
0.225417	230897776	0.22773148	200423840	0.22833333	233372432
0.227512	236489648	0.2300463	201566368	0.2308912	226985744
1.035475	295543264	1.02158565	301522240	1.01047454	272491008
1.037512	298796448	1.02362269	298698880	1.01251157	296743424
2.032593	272779808	2.0187037	303773312	2.00759259	275909664
2.035069	265408608	2.02118056	296266272	2.01006944	267746992
2.910428	285479424	2.89653935	308300864	2.88542824	281708160
2.912407	289008064	2.89851852	294158240	2.88740741	261369760
7.093634	253235968	7.07974537	258022960	7.06863426	248822416
7.095995	259362800	7.08210648	263048128	7.07099537	246230640
14.888090	110368880	14.8742014	117601776	14.8630903	104723224
14.890556	111002744	14.8766667	121179648	14.8655556	106058088
28.838588	42676336	28.8246991	50589816	28.813588	42154000
28.841157	42855020	28.8272685	51638080	28.8161574	42306628
56.961609	17888342	56.9477199	22021410	56.9366088	16956844
56.963611	18067414	56.9497222	22271998	56.9386111	17774838
70.226042	5628809.5	70.2121528	7461319	70.2010417	7186982
70.238461	5454129	70.2245718	7895244	70.2134606	6957034
85.996516	4200149.5	85.9715162	6304246	85.9663542	6664610
85.982627	6300436	85.9774653	8394923	85.9687616	6727956
85.991354	6659401	85.9798727	8309783	122.899873	4031186
85.993762	6966501	122.910984	4256246	122.902014	4166084
122.924873	3950179	122.913125	4335072	149.843137	4071684
122.927014	4066735.75	149.854248	4202816	149.845949	3960995
149.868137	4045237.75	149.85706	4208418	182.97081	2743187
149.870949	4079474.5	182.981921	2945409	182.974109	2769228
182.995810	2932700.25	182.98522	2940675	**Mouse sacrificed on day 202**	
182.999109	2934117	247.951123	2938057		
Mouse sacrificed on day 202		247.953171	2883426		

Table S15. Area of depot of polymer **E1** (pixels) in mice M1, M2, and M3 as a function of time.

Mouse M1		Mouse M2		Mouse M3	
Time (d)	Area (px)	Time (d)	Area (px)	Time (d)	Area (px)
0.011493	21086	0.01586806	19759	0.02699074	22934
0.013692	22278	0.0177662	19683	0.02877315	24553
0.225417	36334	0.22773148	33197	0.22833333	34148
0.227512	36973	0.2300463	33321	0.2308912	34740
1.035475	107895	1.02158565	113291	1.01047454	84471
1.037512	110202	1.02362269	115791	1.01251157	84720
2.032593	105167	2.0187037	112384	2.00759259	82002
2.035069	104788	2.02118056	111906	2.01006944	79910
2.910428	103571	2.89653935	119053	2.88542824	80793
2.912407	104028	2.89851852	113431	2.88740741	80503
7.093634	86480	7.07974537	98786	7.06863426	65515
7.095995	88091	7.08210648	102514	7.07099537	65542
14.888090	34810	14.8742014	32588	14.8630903	30464
14.890556	36009	14.8766667	36399	14.8655556	30954
28.838588	23023	28.8246991	24098	28.813588	23183
28.841157	23052	28.8272685	24255	28.8161574	22170
56.961609	15460	56.9477199	15560	56.9366088	14291
56.963611	15627	56.9497222	15770	56.9386111	14743
70.226042	8735	70.2121528	8458	70.2010417	9033
70.238461	8525	70.2245718	9109	70.2134606	9070
85.996516	5326	85.9715162	7445	85.9663542	8400
85.982627	7292	85.9774653	9457	85.9687616	8629
85.991354	8483	85.9798727	9480	122.899873	3184
85.993762	8861	122.910984	4153	122.902014	3500
122.924873	3195	122.913125	4104	149.843137	1972
122.927014	3407	149.854248	3231	149.845949	1914
149.868137	2574	149.85706	3200	182.97081	244
149.870949	2568	182.981921	86	182.974109	273
182.995810	61	182.98522	106	**Mouse sacrificed on day 202**	
182.999109	94	247.951123	6		
Mouse sacrificed on day 202		247.953171	4		

Table S16. Signal of polymer **E2** (arbitrary units) in mice M1, M2, and M3 as a function of time.

Mouse M1		**Mouse M2**		**Mouse M3**	
Time (d)	**Area (px)**	**Time (d)**	**Area (px)**	**Time (d)**	**Area (px)**
0.014248	85746872	0.023438	47450956	0.03496528	94031336
0.016308	90715736	0.025266	53224272	0.03700231	101594424
0.233553	224295040	0.255868	89545808	0.24475694	116376224
0.237211	221386736	0.257917	84671288	0.24680556	113001568
1.078912	66576880	1.066412	89433784	1.05530093	106334560
1.081262	68607304	1.068762	89428480	1.05765046	96833936
2.060162	65122096	2.047662	85086280	2.03655093	97769640
2.062292	67881624	2.049792	86090368	2.03868056	97225376
3.051863	65181180	3.039363	82204560	3.02825231	96996560
3.054572	65996256	3.042072	82188040	3.03096065	93691632
7.079803	62955308	7.067303	76157904	7.05619213	85718328
7.082315	62609716	7.069815	75010088	7.0587037	86282680
15.116968	134638784	15.104468	129166072	15.0933565	197852384
15.119954	136148720	15.107454	121394072	15.0963426	195390480
29.195035	59214444	29.182535	41696132	29.1714236	80526160
29.197188	59814280	29.184688	44500948	29.1735764	85674392
56.193160	25166426	56.180660	21042212	56.1695486	45022580
56.195787	24914136	56.183287	21373730	56.1721759	47373124
70.366667	9485862	70.354167	9283645	70.3430556	24444674
70.370995	9145668	70.358495	10110350	70.3473843	25011100
86.182789	7787146	86.170289	8015856	86.1591782	15740525
86.184942	7985573.5	86.172442	8161466.5	86.161331	16655944
122.196285	3591569	122.183785	3532736.25	122.172674	7394382
122.198391	3650486	122.185891	3685406.25	122.17478	7428091
150.162384	4211164.5	150.149884	4408554.5	150.138773	7468021
150.164688	4231040	150.152188	4435089	150.141076	7369665
184.150914	2643604.5	184.138414	2989652.25	184.127303	4401534
184.153461	2730022	184.140961	3009296.25	184.12985	4590717
Mouse sacrificed on day 202		247.182743	3069384	247.171632	4306085
		247.185266	3170592.25	247.174155	4399593

Table S17. Area of depot of polymer **E2** (pixels) in mice M1, M2, and M3 as a function of time.

Mouse M1		Mouse M2		Mouse M3	
Time (d)	**Signal**	**Time (d)**	**Signal**	**Time (d)**	**Signal**
0.014248	18587	0.023438	12176	0.03496528	21179
0.016308	17720	0.025266	13545	0.03700231	22494
0.233553	35972	0.255868	24664	0.24475694	28795
0.237211	34494	0.257917	24437	0.24680556	27192
1.078912	24504	1.066412	27293	1.05530093	27509
1.081262	24612	1.068762	29235	1.05765046	27690
2.060162	22141	2.047662	26749	2.03655093	27688
2.062292	22419	2.049792	27293	2.03868056	27951
3.051863	21958	3.039363	24684	3.02825231	27081
3.054572	21391	3.042072	25440	3.03096065	26024
7.079803	20236	7.067303	22940	7.05619213	25383
7.082315	20608	7.069815	24505	7.0587037	25985
15.116968	45451	15.104468	50284	15.0933565	44809
15.119954	42850	15.107454	46837	15.0963426	44838
29.195035	22831	29.182535	23254	29.1714236	29500
29.197188	22499	29.184688	22632	29.1735764	31735
56.193160	15237	56.180660	16188	56.1695486	22387
56.195787	14947	56.183287	16564	56.1721759	22849
70.366667	9778	70.354167	9861	70.3430556	15940
70.370995	9252	70.358495	11961	70.3473843	16891
86.182789	8165	86.170289	9090	86.1591782	12595
86.184942	8113	86.172442	9129	86.161331	13227
122.196285	2876	122.183785	2071	122.172674	7558
122.198391	2894	122.185891	2099	122.17478	7596
150.162384	2444	150.149884	2051	150.138773	7083
150.164688	2558	150.152188	2109	150.141076	7052
184.150914	217	184.138414	679	184.127303	4395
184.153461	280	184.140961	581	184.12985	4603
Mouse sacrificed on day 202		247.182743	165	247.171632	3696
		247.185266	186	247.174155	3690

Table S18. Signal of polymer **P1** (arbitrary units) in mice M1, M2, and M3 as a function of time.

Mouse M1		Mouse M2		Mouse M3	
Time (d)	**Signal**	**Time (d)**	**Signal**	**Time (d)**	**Signal**
0.012836	154887312	0.0287037	108204912	0.05402778	125653488
0.015046	161041872	0.03050926	99065472	0.05605324	128814272
0.236042	279881120	0.21969907	456556032	0.21454861	132311896
0.237963	282674464	0.22186343	457324992	0.21667824	133418048
1.058287	229188256	1.00898148	275546688	0.98814815	305203936
1.060428	222781312	1.01112269	283785824	0.99028935	313983584
1.934028	251478208	1.88472222	292941216	1.86388889	329541184
1.936377	252007584	1.88707176	305490752	1.86623843	332254976
2.874641	234527392	2.82533565	307356768	2.80450231	313274080
2.876829	246496880	2.82752315	303854784	2.80668981	330575296
6.907106	225847744	6.85780093	322972160	6.83696759	306682784
6.909606	239675344	6.86030093	315422464	6.83946759	319124512
14.919120	106640712	14.8698148	142372480	14.8489815	160397536
14.921794	108571584	14.8724884	140454416	14.8516551	163068608
28.941736	72051984	28.8924306	88760312	28.8715972	97913776
28.944757	73080744	28.8954514	95740256	28.8746181	104045736
56.025822	20177468	55.9765162	24346508	55.9556829	32669470
56.029977	20624290	55.9806713	26945896	55.959838	31215204
70.203449	8089560.5	70.1541435	10222686	70.1333102	14021357
70.206343	8043254.5	70.157037	10068751	70.1362037	14013940
87.048657	7717418	86.9993519	9669622	86.9785185	12588132
87.051551	7956233	87.0022454	9926090	86.981412	12678964
122.015833	3377739	121.966528	4191970.5	121.945694	5518841
122.018137	3546953	121.968831	4105463	121.947998	5639853
149.986389	4013929	149.937083	4324199.5	149.91625	5295717
149.988553	3868657.5	149.939248	4452572.5	149.918414	5060149
183.973345	2477204.5	183.924039	2619053.25	183.903206	3103979
183.975544	2403427	183.926238	2497420.25	183.905405	3024662
Mouse sacrificed on day 202		246.964363	2673012.75	246.94353	2820044
		246.966736	2674293.75	246.945903	2801602

Table S19. Area of depot of polymer **P1** (pixels) in mice M1, M2, and M3 as a function of time.

Mouse M1		Mouse M2		Mouse M3	
Time (d)	**Area (px)**	**Time (d)**	**Area (px)**	**Time (d)**	**Area (px)**
0.012836	33001	0.0287037	29802	0.05402778	30537
0.015046	33814	0.03050926	28614	0.05605324	31256
0.236042	55447	0.21969907	89576	0.21454861	33509
0.237963	54178	0.22186343	88394	0.21667824	34371
1.058287	95713	1.00898148	118664	0.98814815	84112
1.060428	102888	1.01112269	112544	0.99028935	87542
1.934028	116166	1.88472222	125396	1.86388889	91508
1.936377	120024	1.88707176	125418	1.86623843	94016
2.874641	107495	2.82533565	117667	2.80450231	91365
2.876829	116111	2.82752315	126101	2.80668981	94134
6.907106	106528	6.85780093	120682	6.83696759	88482
6.909606	111629	6.86030093	125123	6.83946759	90682
14.919120	45010	14.8698148	53007	14.8489815	52000
14.921794	46265	14.8724884	57117	14.8516551	50815
28.941736	34296	28.8924306	37080	28.8715972	35563
28.944757	35406	28.8954514	38632	28.8746181	39915
56.025822	23269	55.9765162	26198	55.9556829	27103
56.029977	23282	55.9806713	28077	55.959838	26709
70.203449	9016	70.1541435	16023	70.1333102	15224
70.206343	9112	70.157037	14672	70.1362037	15406
87.048657	7308	86.9993519	12316	86.9785185	13034
87.051551	7769	87.0022454	12191	86.981412	12377
122.015833	2042	121.966528	3085	121.945694	5620
122.018137	2405	121.968831	2765	121.947998	5652
149.986389	2105	149.937083	2313	149.91625	5067
149.988553	1877	149.939248	2487	149.918414	4598
183.973345	21	183.924039	124	183.903206	1515
183.975544	14	183.926238	50	183.905405	1505
Mouse sacrificed on day 202		246.964363	8	246.94353	380
		246.966736	9	246.945903	445

Table S20. Area of depot of polymer **P2** (pixels) in mice M1, M2, and M3 as a function of time.

Mouse M1		Mouse M2		Mouse M3	
Time (d)	**Area (px)**	**Time (d)**	**Area (px)**	**Time (d)**	**Area (px)**
0.015718	54501	0.015266	35564	0.01445602	39366
0.017488	55192	0.017002	38378	0.0162037	41140
0.228264	52261	0.230995	36413	0.22918981	62368
0.230139	53669	0.997037	108688	0.23116898	61648
1.010926	103085	0.999329	125795	0.98175926	85180
1.013218	113268	2.011065	127918	0.98405093	86875
2.024954	118307	2.013414	129939	1.99578704	91598
2.027303	123054	2.928044	121229	1.99813657	97601
2.941933	118956	2.930139	123391	2.9127662	92423
2.944028	113727	7.108056	122998	2.91486111	92356
7.121944	107826	7.112905	117699	7.09277778	82523
7.126794	111763	14.904560	59488	7.09762731	86213
14.918449	54274	14.907685	56496	14.8892824	51213
14.921574	53514	28.851331	37850	14.8924074	49447
28.865220	35588	28.855197	37633	28.8360532	31997
28.869086	35498	56.939838	29109	28.839919	32429
56.953727	26663	56.942627	29636	56.9245602	18311
56.956516	26909	70.237604	18027	56.9273495	19818
70.251493	1847	70.240197	17982	70.2223264	10467
70.254086	3738	85.926921	7381	70.224919	10077
85.942199	12575	85.936134	17797	85.9208565	7515
85.950023	5308	85.939190	18140	85.923912	7556
85.953079	5214	122.939815	5205	122.924537	1841
85.956088	1016	122.941944	5306	122.926667	1882
122.953704	3	149.881215	3917	149.865938	793
122.955833	16	149.884109	3983	149.868831	757
149.895104	2	183.014711	523	182.999433	277
149.897998	6	183.017002	541	183.001725	244
183.028600	9	247.984745	4	247.969468	232
183.030891	0	247.986771	14	247.971493	293
247.998634	0				
248.00066	0				

Table S21. Area of depot of polymer **P2** (pixels) in mice M1, M2, and M3 as a function of time.

Mouse M1		Mouse M2		Mouse M3	
Time (d)	**Signal**	**Time (d)**	**Signal**	**Time (d)**	**Signal**
0.015718	182731056	0.015266	222033440	0.01445602	247837232
0.017488	182161360	0.017002	250553952	0.0162037	252251376
0.228264	231932272	0.230995	140752112	0.22918981	372584832
0.230139	233438608	0.997037	336779296	0.23116898	390281312
1.010926	219447040	0.999329	354007904	0.98175926	277054944
1.013218	230945264	2.011065	388713664	0.98405093	288075168
2.024954	224264352	2.013414	392865824	1.99578704	279141600
2.027303	237709264	2.928044	377100576	1.99813657	293722336
2.941933	209337056	2.930139	382994560	2.9127662	292883840
2.944028	221618032	7.108056	370583008	2.91486111	275523488
7.121944	218936160	7.112905	379360480	7.09277778	259383216
7.126794	210496480	14.904560	211303552	7.09762731	266491488
14.918449	110368408	14.907685	207180224	14.8892824	124180472
14.921574	103478080	28.851331	83511440	14.8924074	122191904
28.865220	40770040	28.855197	85220440	28.8360532	43586332
28.869086	40270200	56.939838	35206748	28.839919	45037324
56.953727	17189172	56.942627	35357748	56.9245602	16478573
56.956516	17766150	70.237604	12564073	56.9273495	16265671
70.251493	4388745.5	70.240197	12670079	70.2223264	8342033.5
70.254086	4885701	85.926921	6374145.5	70.224919	8143282.5
85.942199	9523845	85.936134	12588164	85.9208565	6207786
85.950023	6139817	85.939190	12786431	85.923912	6189218.5
85.953079	6027451.5	122.939815	5542673.5	122.924537	3662393
85.956088	4199413.5	122.941944	5626556.5	122.926667	3672003.5
122.953704	3148978.25	149.881215	5052904.5	149.865938	3815709.5
122.955833	3333047	149.884109	4931006.5	149.868831	3669871.25
149.895104	3355014.75	183.014711	3272383.5	182.999433	2666931.75
149.897998	3296004.25	183.017002	3236646	183.001725	2545537.5
183.028600	2565520.75	247.984745	3141866.25	247.969468	2958416.5
183.030891	2509487.75	247.986771	3238033.25	247.971493	3089208.25
247.998634	2853189.75				
248.00066	2896543.75				

Table S22. Signal of **Cy7-amine** (arbitrary units) in mice M1, M2, and M3 as a function of time.

Mouse M1		Mouse M2		Mouse M3	
Time (d)	**Signal**	**Time (d)**	**Signal**	**Time (d)**	**Signal**
0.021204	70673272	0.02197917	283337376	0.01547454	54470576
0.023160	71270424	0.02417824	290718112	0.01768519	52146660
0.230845	250990432	0.22875	104115808	0.23915509	46086672
0.232801	250163152	0.23070602	97453512	0.2409838	45629548
1.045174	78536712	1.01809028	123167424	1.00003472	11619925
1.047720	79967232	1.02063657	116126248	1.00258102	11844664
2.042720	73382144	2.01563657	110531032	1.99758102	9142454
2.044769	68012648	2.01768519	106823080	1.99962963	8607974
5.342083	167414752	5.315	286664448	5.29694444	25349484
5.344514	171695296	5.31743056	286676256	5.299375	24623624
6.083484	152731424	6.05640046	259348048	6.03834491	23052426
6.086042	156788176	6.05895833	260531408	6.04090278	22903890
15.167164	26948396	15.140081	45813784	15.1220255	5871099.5
15.170266	27082226	15.1431829	46255968	15.1251273	5971087
29.280613	6551659	29.2535301	11326173	29.2354745	2688971
29.283438	6809372.5	29.2563542	11593822	29.2382986	2564405.25
57.314549	2625429.75	57.2874653	3791530.25	57.2694097	1901502.63
57.317106	2612183.25	57.2900231	3733947	57.2719676	1905894.25
69.454954	1998970	69.4278704	2380125.75	69.4098148	1881207.25
69.457512	1949823.25	69.4304282	2370743.5	69.4123727	1751782.5
85.189363	2128030.5	85.1622801	2449296.75	85.1442245	1968201.75
85.191597	2107862.5	85.1645139	2421435.25	85.1464583	1869644.88
121.100891	2127014.25	121.073808	2201486.5	121.055752	2141068.5
121.107928	2102814	121.080845	2235757	121.062789	2173531.75
149.266551	2271334.25	149.239468	2404249.25	149.221412	2523788
183.249641	1860027.63	183.222558	1911268.25	183.204502	1907063.63
183.252072	1839011.5	183.224988	1915366.38	183.206933	1869627.5
246.272627	2097062.63	246.245544	2160823.25	**Mouse sacrificed on day 202**	
246.274444	2164975.5	246.247361	2182537.75		

Table S23. Area of depot of **Cy7-amine** (pixels) in mice M1, M2, and M3 as a function of time.

Mouse M1		**Mouse M2**		**Mouse M3**	
Time (d)	**Area (px)**	**Time (d)**	**Area (px)**	**Time (d)**	**Area (px)**
0.021204	23262	0.02197917	42521	0.01547454	17312
0.023160	27387	0.02417824	43265	0.01768519	17649
0.230845	37918	0.22875	24964	0.23915509	18295
0.232801	38691	0.23070602	24946	0.2409838	18506
1.045174	30763	1.01809028	29751	1.00003472	8019
1.047720	30183	1.02063657	29626	1.00258102	7980
2.042720	29685	2.01563657	27639	1.99758102	6376
2.044769	29593	2.01768519	27268	1.99962963	6121
5.342083	58033	5.315	65657	5.29694444	18866
5.344514	58838	5.31743056	67382	5.299375	18081
6.083484	54428	6.05640046	59868	6.03834491	15890
6.086042	54337	6.05895833	61511	6.04090278	15688
15.167164	21840	15.140081	20619	15.1220255	3228
15.170266	22148	15.1431829	20274	15.1251273	3233
29.280613	7624	29.2535301	10313	29.2354745	466
29.283438	7865	29.2563542	10269	29.2382986	307
57.314549	371	57.2874653	4108	57.2694097	494
57.317106	413	57.2900231	4042	57.2719676	527
69.454954	0	69.4278704	878	69.4098148	470
69.457512	2	69.4304282	960	69.4123727	320
85.189363	1	85.1622801	270	85.1442245	328
85.191597	4	85.1645139	290	85.1464583	231
121.100891	0	121.073808	1	121.055752	151
121.107928	0	121.080845	0	121.062789	172
149.266551	0	149.239468	1	149.221412	581
183.249641	0	183.222558	2	183.204502	262
183.252072	3	183.224988	1	183.206933	254
246.272627	0	246.245544	4	**Mouse sacrificed on day 202**	
246.274444	1	246.247361	1		

S13. Polymer pharmacokinetics - fitting curves

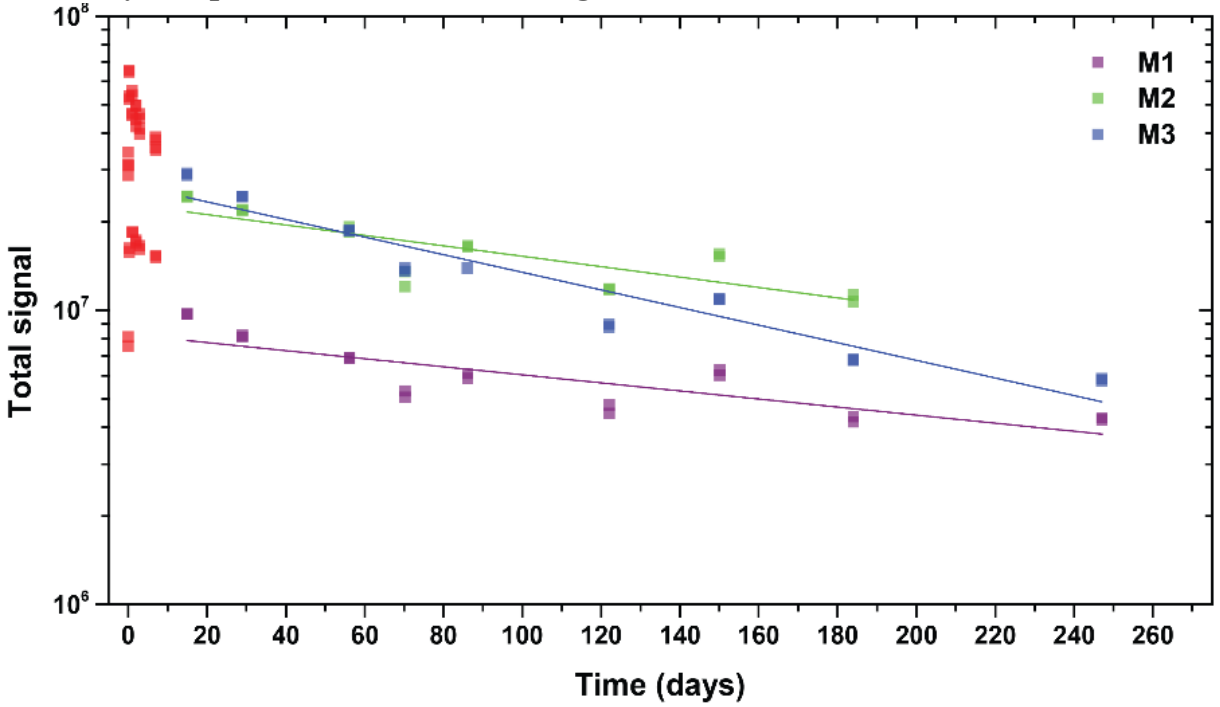

Equation	y = a + b*x		
Weight	No Weighting		
Residual Sum of Squares	0.078	0.0715	0.08004
Pearson's r	-0.83147	-0.8253	-0.95523
Adj. R-Square	0.67205	0.65834	0.90699
		Value	Standard Error
M1	Intercept	6.91766	0.02943
M1	Slope	-0.00137	2.28796E-4
M2	Intercept	7.36081	0.03391
M2	Slope	-0.00177	3.23681E-4
M3	Intercept	7.42854	0.0298
M3	Slope	-0.00299	2.31772E-4

Figure S70. Signal of **F1** (arbitrary units) in mice M1, M2, and M3 as a function of time. Both outlier points and points in **Phase 1** and **Phase 3** are marked in red.

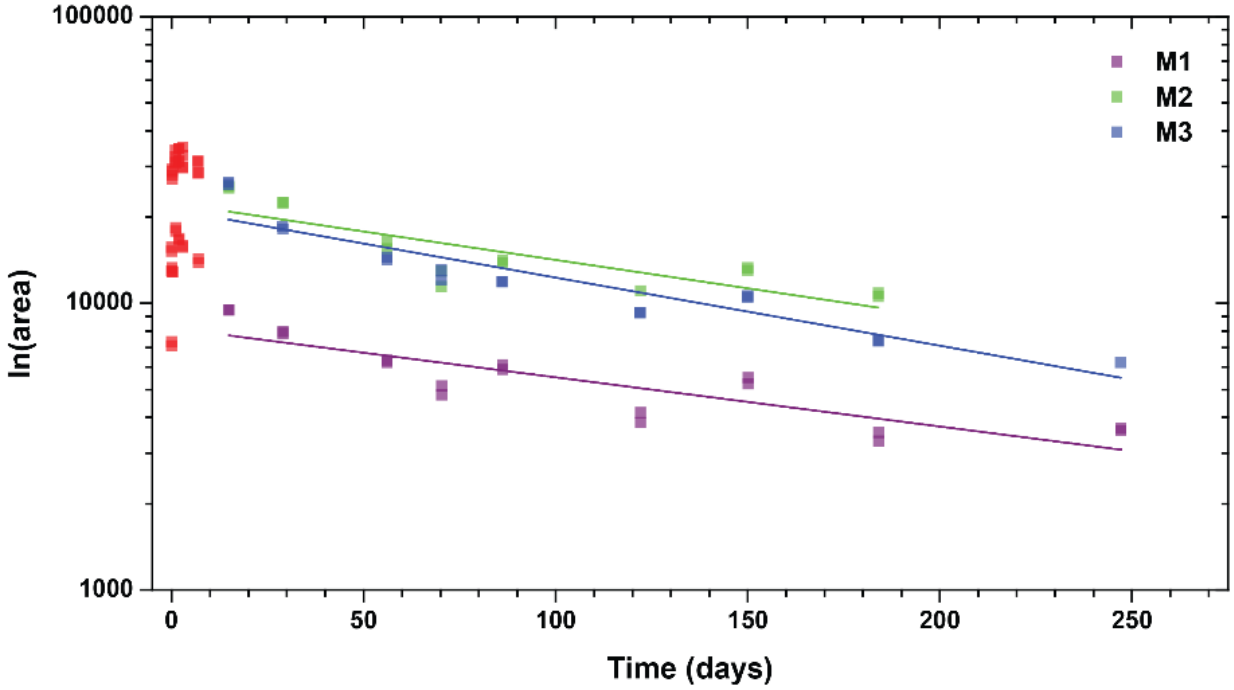

Equation	y = a + b*x		
Weight	No Weighting		
Residual Sum of Squares	0.09008	0.08012	0.06991
Pearson's r	-0.86762	-0.83967	-0.93942
Adj. R-Square	0.73732	0.68398	0.87516
		Value	Standard Error
M1	Intercept	3.91342	0.03163
M1	Slope	-0.00172	2.45875E-4
M2	Intercept	4.34964	0.03589
M2	Slope	-0.00198	3.42632E-4
M3	Intercept	4.32721	0.02785
M3	Slope	-0.00237	2.16612E-4

Figure S71. Area of depot of **F1** (pixels) in mice M1, M2, and M3 as a function of time. Both outlier points and points in **Phase 1** and **Phase 3** are marked in red.

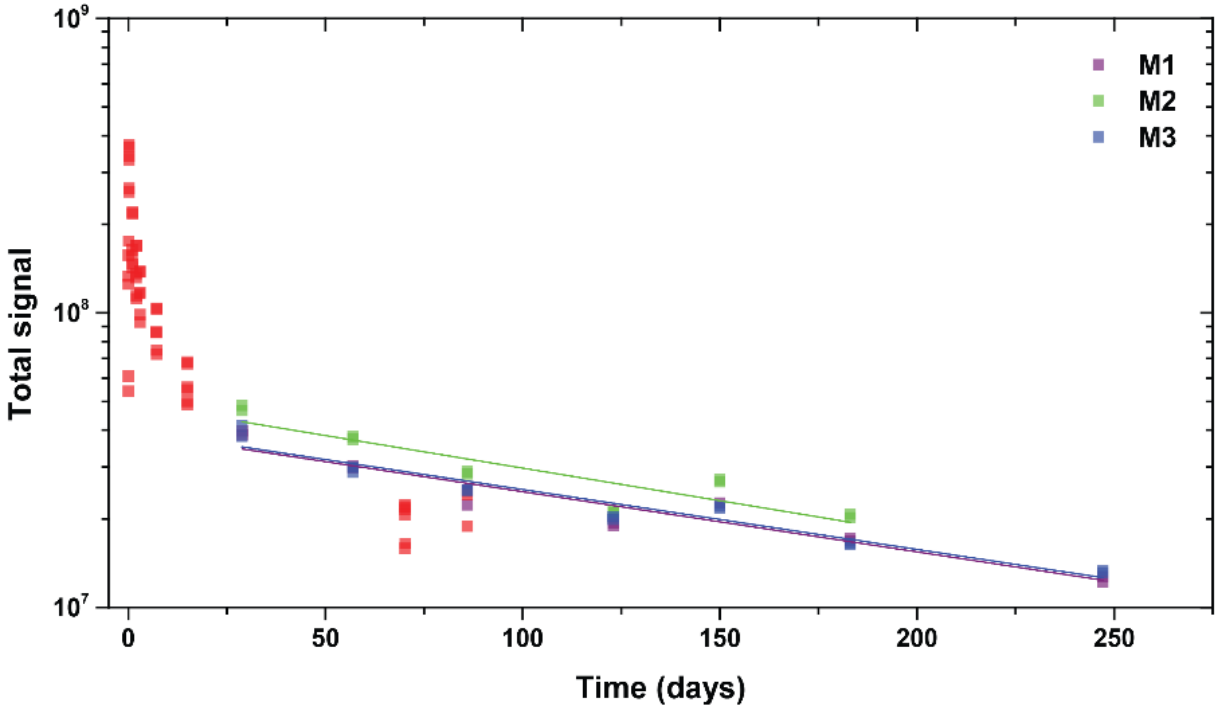

Equation	y = a + b*x		
Weight	No Weighting		
Residual Sum of Squares	0.02923	0.03829	0.01937
Pearson's r	-0.95344	-0.90121	-0.96758
Adj. R-Square	0.90205	0.7934	0.93089
		Value	Standard Error
M1	Intercept	7.59708	0.02512
M1	Slope	-0.00204	1.79219E-4
M2	Intercept	7.6944	0.03949
M2	Slope	-0.00221	3.36596E-4
M3	Intercept	7.60412	0.02197
M3	Slope	-0.00204	1.53406E-4

Figure S72. Signal of **F2** (arbitrary units) in mice M1, M2, and M3 as a function of time. Both outlier points and points in **Phase 1** and **Phase 3** are marked in red.

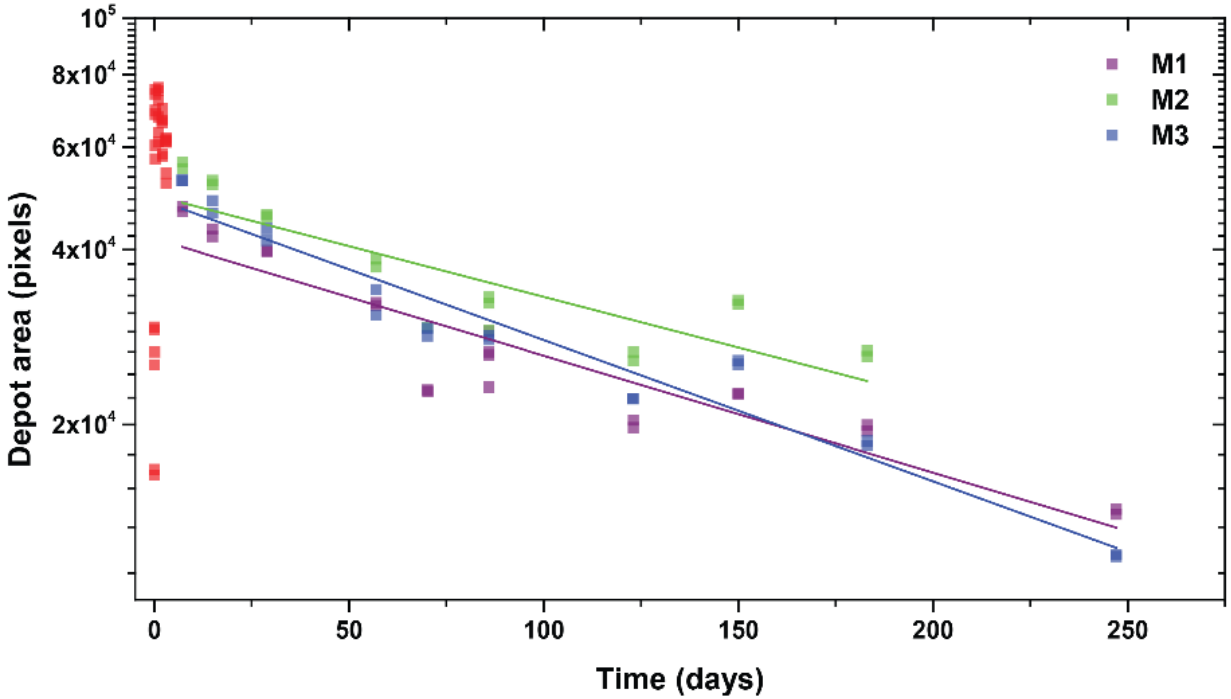

Equation	y = a + b*x		
Weight	No Weighting		
Residual Sum of Squares	0.06965	0.06909	0.0387
Pearson's r	-0.93039	-0.85231	-0.97164
Adj. R-Square	0.85891	0.71035	0.94098
		Value	Standard Error
M1	Intercept	4.62094	0.02113
M1	Slope	-0.00201	1.77285E-4
M2	Intercept	4.69523	0.02546
M2	Slope	-0.00174	2.59444E-4
M3	Intercept	4.6897	0.01701
M3	Slope	-0.00243	1.39435E-4

Figure S73. Area of depot of **F2** (pixels) in mice M1, M2, and M3 as a function of time. Both outlier points and points in **Phase 1** and **Phase 3** are marked in red.

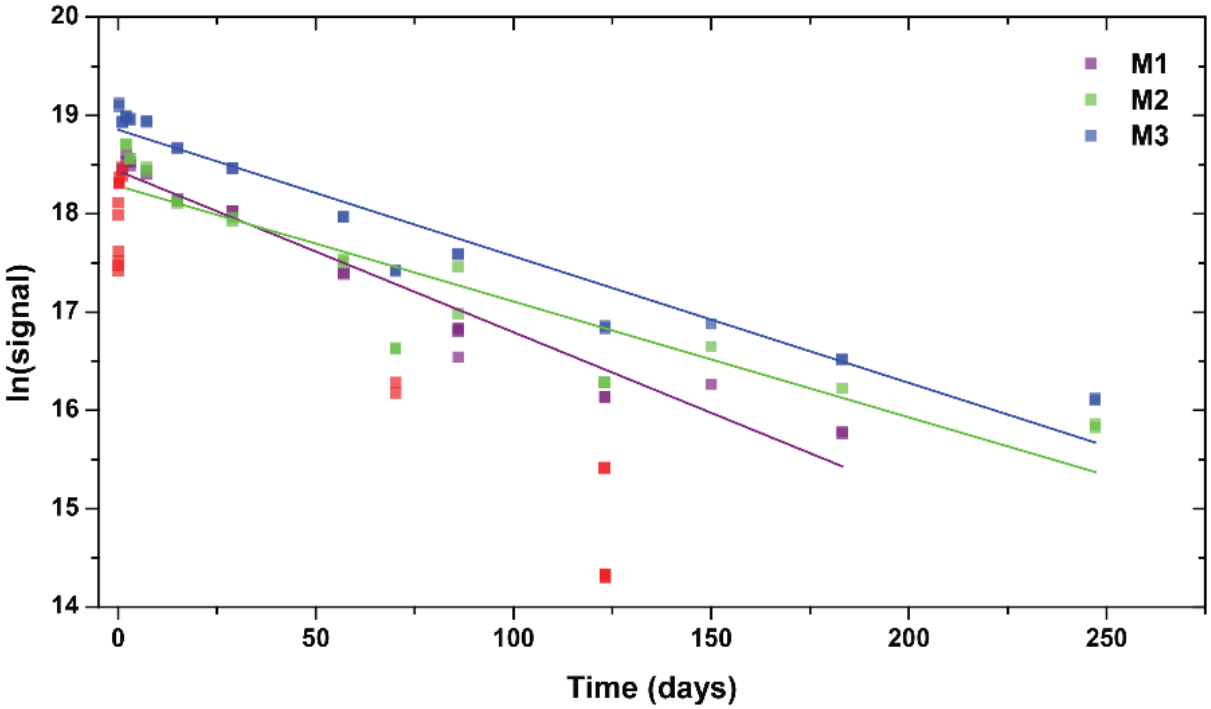

Equation	y = a + b*x		
Weight	No Weighting		
Residual Sum of Squares	0.97849	3.39305	1.70982
Pearson's r	-0.97821	-0.92025	-0.96844
Adj. R-Square	0.95484	0.8399	0.93539
		Value	Standard Error
M1	Intercept	18.43524	0.06301
M1	Slope	-0.0164	7.59771E-4
M2	Intercept	18.28392	0.11587
M2	Slope	-0.01178	0.00107
M3	Intercept	18.85464	0.06693
M3	Slope	-0.01288	6.62791E-4

Figure S74. Signal of **I1** (arbitrary units) in mice M1, M2, and M3 as a function of time. Both outlier points and points in **Phase 1** and **Phase 3** are marked in red.

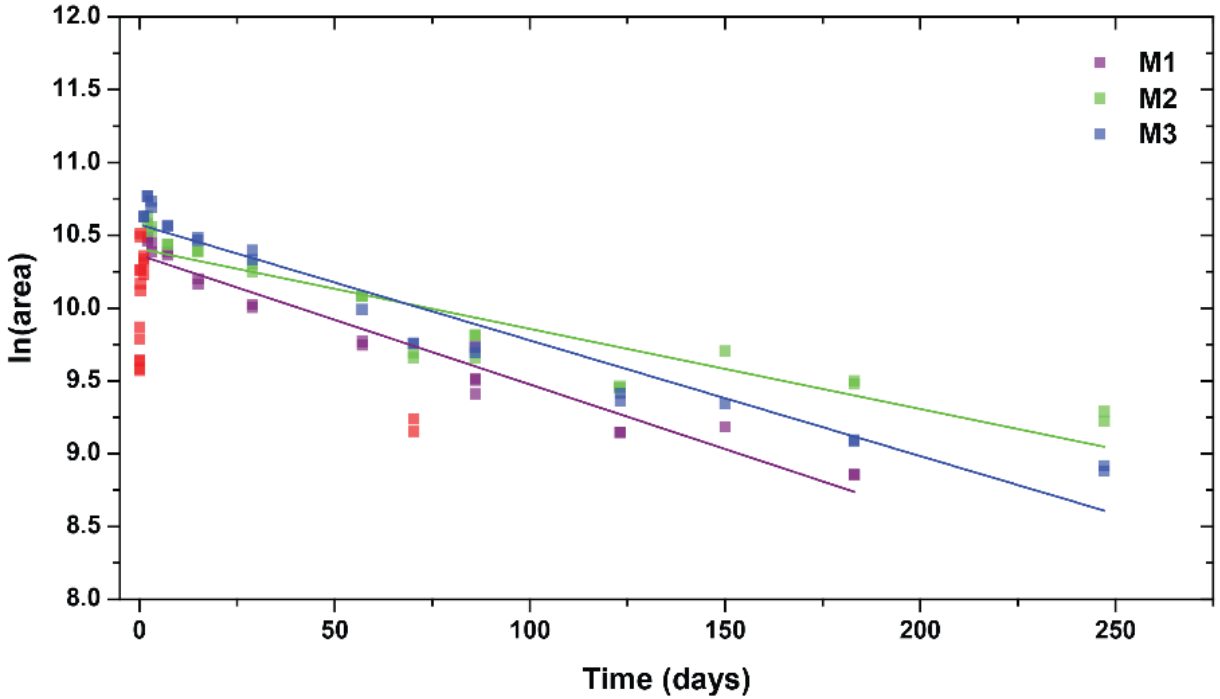

Equation	y = a + b*x		
Weight	No Weighting		
Residual Sum of Squares	0.25436	0.77567	0.64913
Pearson's r	-0.97877	-0.91697	-0.96661
Adj. R-Square	0.95577	0.8336	0.93148
		Value	Standard Error
M1	Intercept	10.36334	0.03702
M1	Slope	-0.00888	4.26491E-4
M2	Intercept	10.40771	0.0554
M2	Slope	-0.0055	5.10464E-4
M3	Intercept	10.57331	0.04611
M3	Slope	-0.00795	4.39392E-4

Figure S75. Area of depot of **I1** (pixels) in mice M1, M2, and M3 as a function of time. Both outlier points and points in **Phase 1** and **Phase 3** are marked in red.

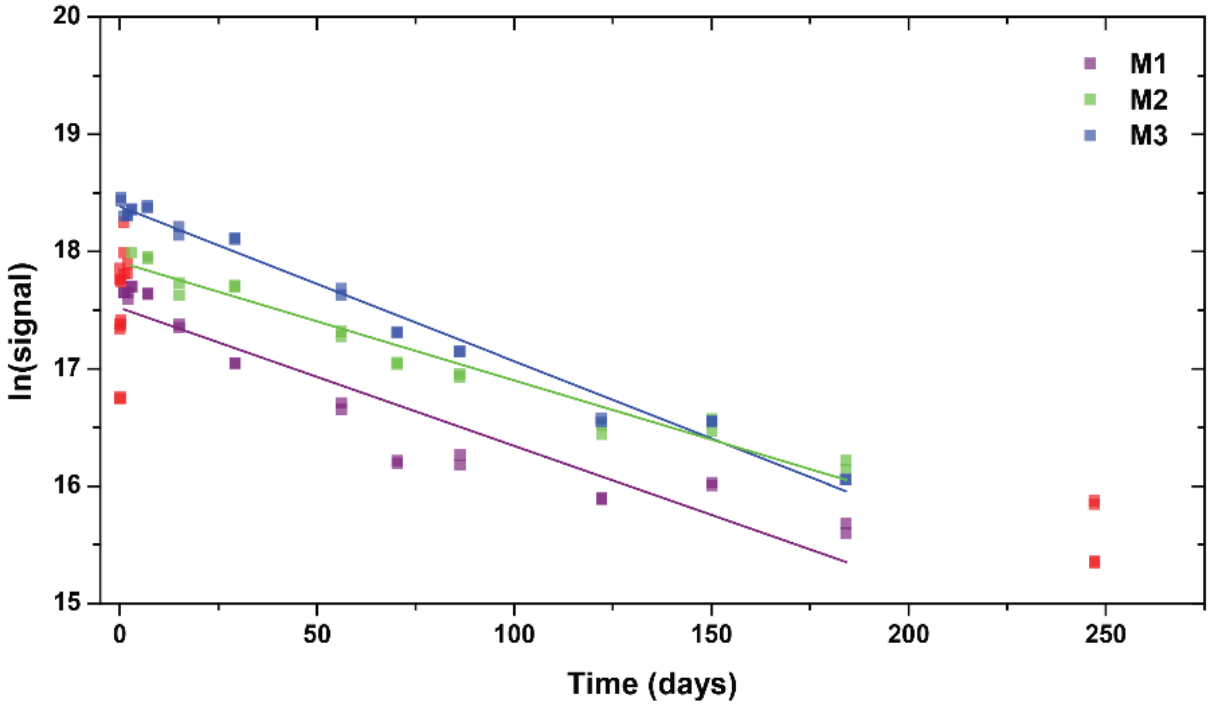

Equation	y = a + b*x		
Weight	No Weighting		
Residual Sum of Squares	0.28	0.30677	1.36916
Pearson's r	-0.99133	-0.97951	-0.94821
Adj. R-Square	0.98198	0.95719	0.89451
		Value	Standard Error
M3	Intercept	18.38342	0.03057
M3	Slope	-0.01318	3.64409E-4
M2	Intercept	17.90918	0.04583
M2	Slope	-0.01008	4.88561E-4
M1	Intercept	17.51956	0.07199
M1	Slope	-0.01177	8.40448E-4

Figure S76. Signal of **I2** (arbitrary units) in mice M1, M2, and M3 as a function of time. Both outlier points and points in **Phase 1** and **Phase 3** are marked in red.

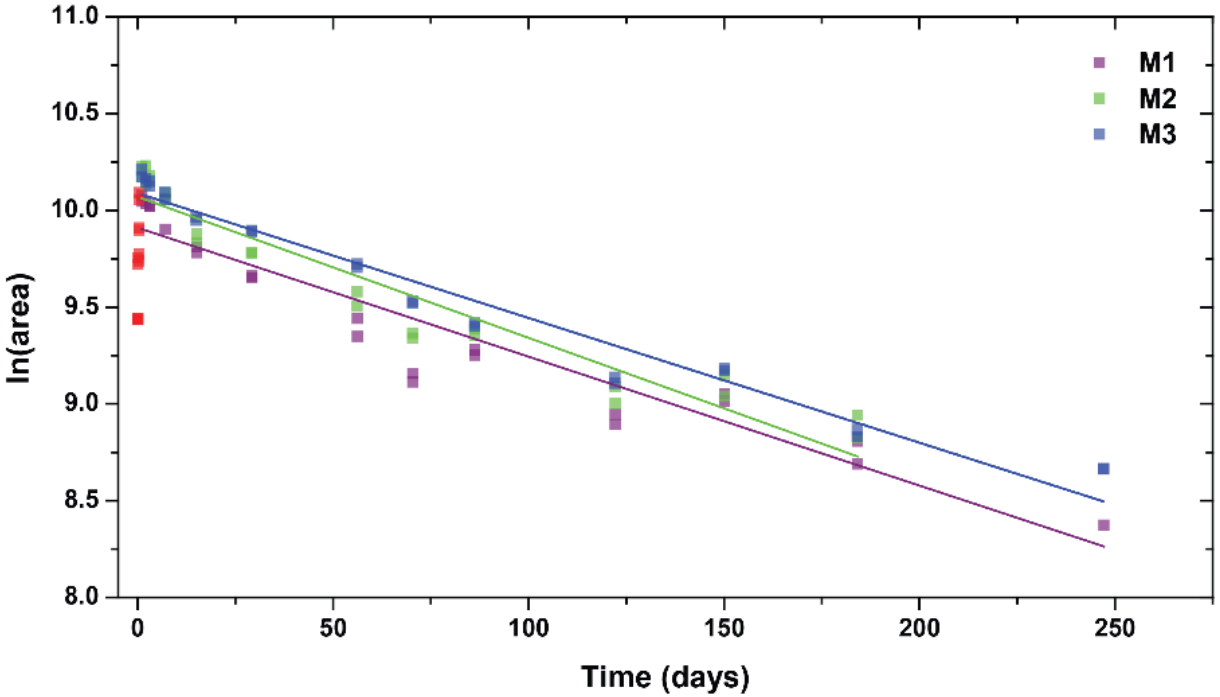

Equation	y = a + b*x		
Weight	No Weighting		
Residual Sum of Squares	0.51047	0.39975	0.24329
Pearson's r	-0.96429	-0.9598	-0.98133
Adj. R-Square	0.92694	0.91764	0.96147
		Value	Standard Error
M1	Intercept	9.91035	0.04001
M1	Slope	-0.00666	3.73579E-4
M2	Intercept	10.06964	0.03889
M2	Slope	-0.00728	4.54127E-4
M3	Intercept	10.08867	0.02761
M3	Slope	-0.00645	2.57907E-4

Figure S77. Area of depot of **I2** (pixels) in mice M1, M2, and M3 as a function of time. Both outlier points and points in **Phase 1** and **Phase 3** are marked in red.

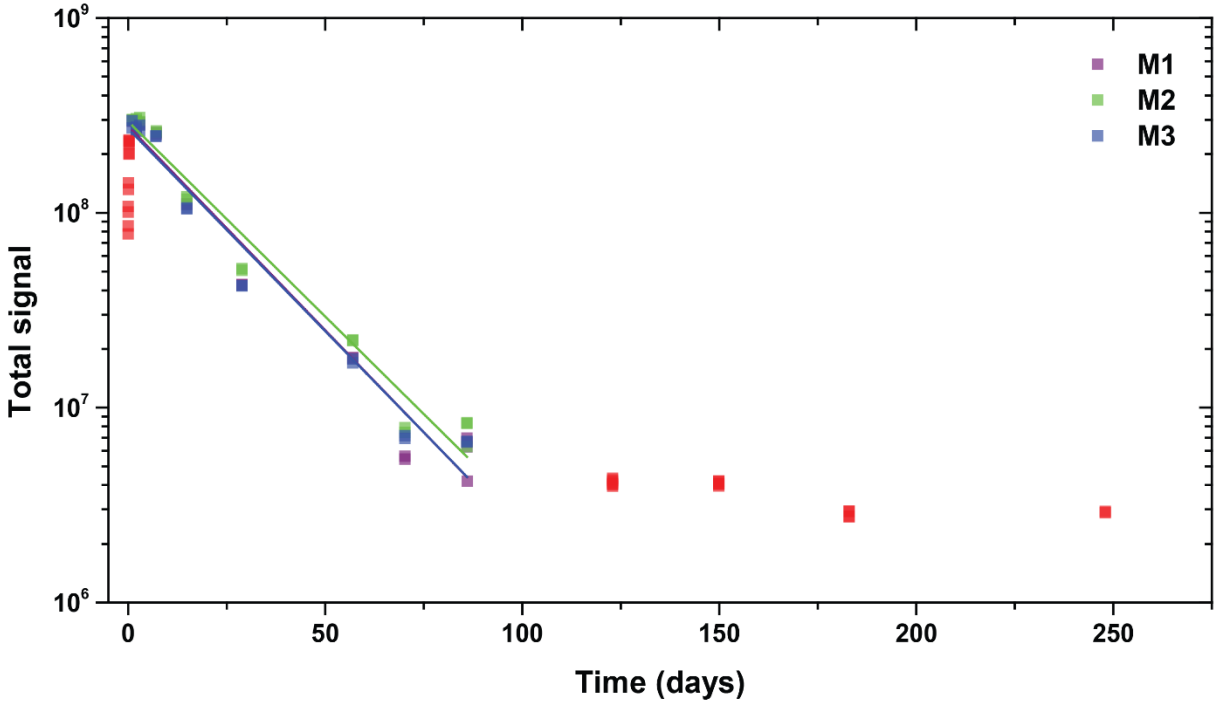

Equation	y = a + b*x		
Weight	No Weighting		
Residual Sum of Squares	0.34951	0.24436	0.24234
Pearson's r	-0.98299	-0.9852	-0.98406
Adj. R-Square	0.96439	0.96888	0.96639
		Value	Standard Error
M1	Intercept	8.44436	0.04527
M1	Slope	-0.02094	9.22377E-4
M2	Intercept	8.46817	0.03912
M2	Slope	-0.02001	8.44617E-4
M3	Intercept	8.43159	0.04042
M3	Slope	-0.02078	9.38946E-4

Figure S78. Signal of **E1** (arbitrary units) in mice M1, M2, and M3 as a function of time. Both outlier points and points in **Phase 1** and **Phase 3** are marked in red.

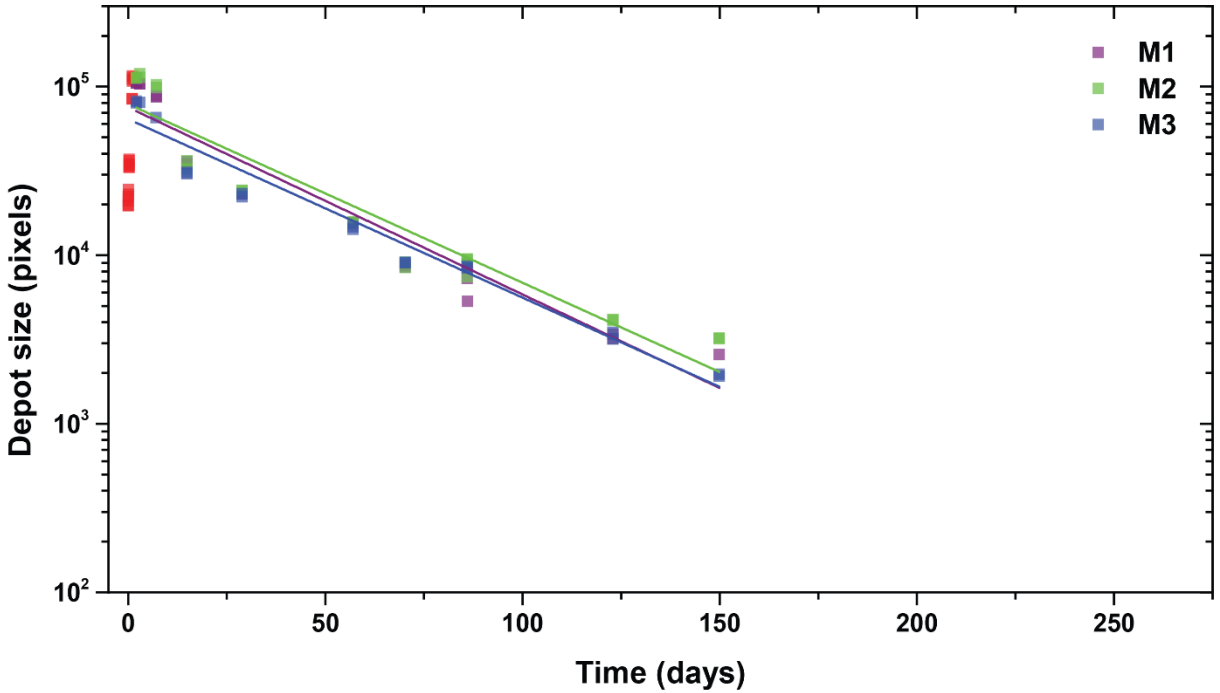

Equation	y = a + b*x		
Weight	No Weighting		
Residual Sum of Squares	0.4621	0.5757	0.21362
Pearson's r	-0.96556	-0.95301	-0.98141
Adj. R-Square	0.92892	0.9034	0.96111
		Value	Standard Error
M1	Intercept	4.87688	0.05007
M1	Slope	-0.0111	6.68762E-4
M2	Intercept	4.89561	0.05738
M2	Slope	-0.01059	7.72421E-4
M3	Intercept	4.80676	0.03594
M3	Slope	-0.01059	4.88066E-4

Figure S79. Area of depot of **E1** (pixels) in mice M1, M2, and M3 as a function of time. Both outlier points and points in **Phase 1** and **Phase 3** are marked in red.

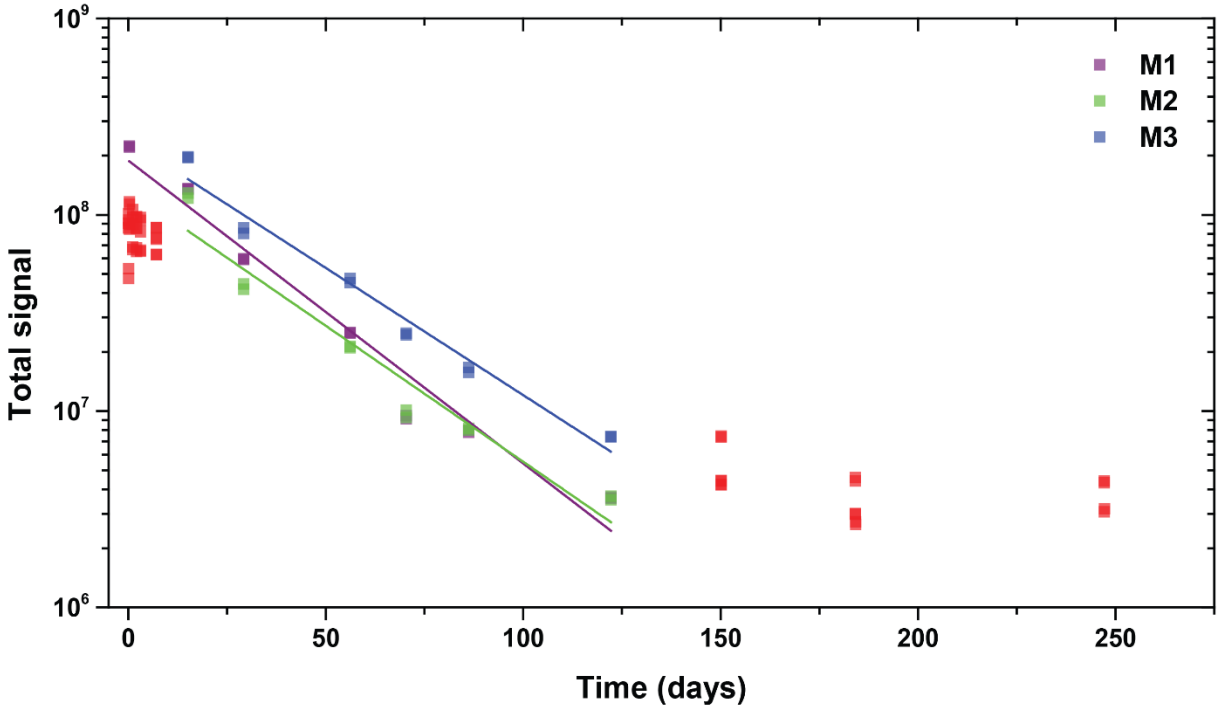

Equation	y = a + b*x		
Weight	No Weighting		
Residual Sum of Squares	0.19215	0.16977	0.06657
Pearson's r	-0.98211	-0.97204	-0.98717
Adj. R-Square	0.96159	0.93934	0.97196
		Value	Standard Error
M1	Intercept	8.27622	0.05734
M1	Slope	-0.01543	8.54039E-4
M2	Intercept	8.12718	0.07674
M2	Slope	-0.01385	0.00106
M3	Intercept	8.37714	0.04805
M3	Slope	-0.01296	6.62761E-4

Figure S80. Signal of E2 (arbitrary units) in mice M1, M2, and M3 as a function of time. Both outlier points and points in **Phase 1** and **Phase 3** are marked in red.

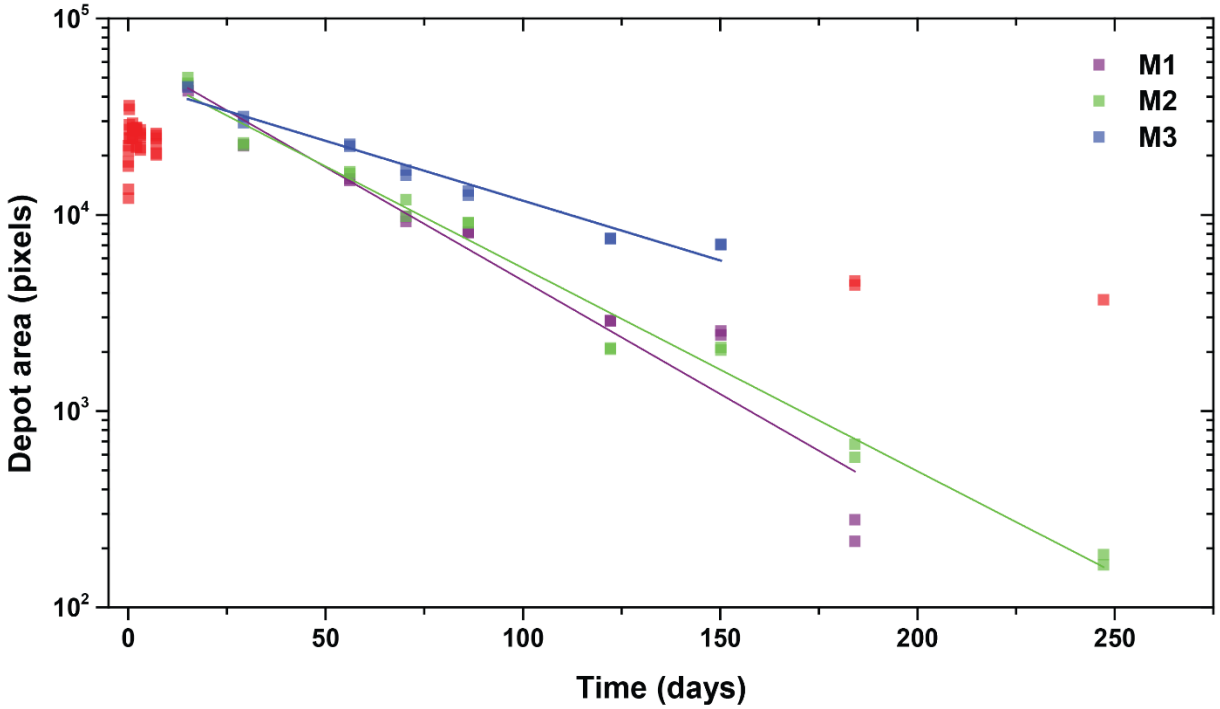

Equation	y = a + b*x		
Weight	No Weighting		
Residual Sum of Squares	0.43804	0.15641	0.03719
Pearson's r	-0.96795	-0.99225	-0.98265
Adj. R-Square	0.93242	0.98361	0.96274
		Value	Standard Error
M1	Intercept	4.82041	0.08405
	Slope	-0.01156	8.01336E-4
M2	Intercept	4.76452	0.04171
	Slope	-0.01035	3.24027E-4
M3	Intercept	4.68167	0.02918
	Slope	-0.00609	3.32019E-4

Figure S81. Area of depot of **E2** (pixels) in mice M1, M2, and M3 as a function of time. Both outlier points and points in **Phase 1** and **Phase 3** are marked in red.

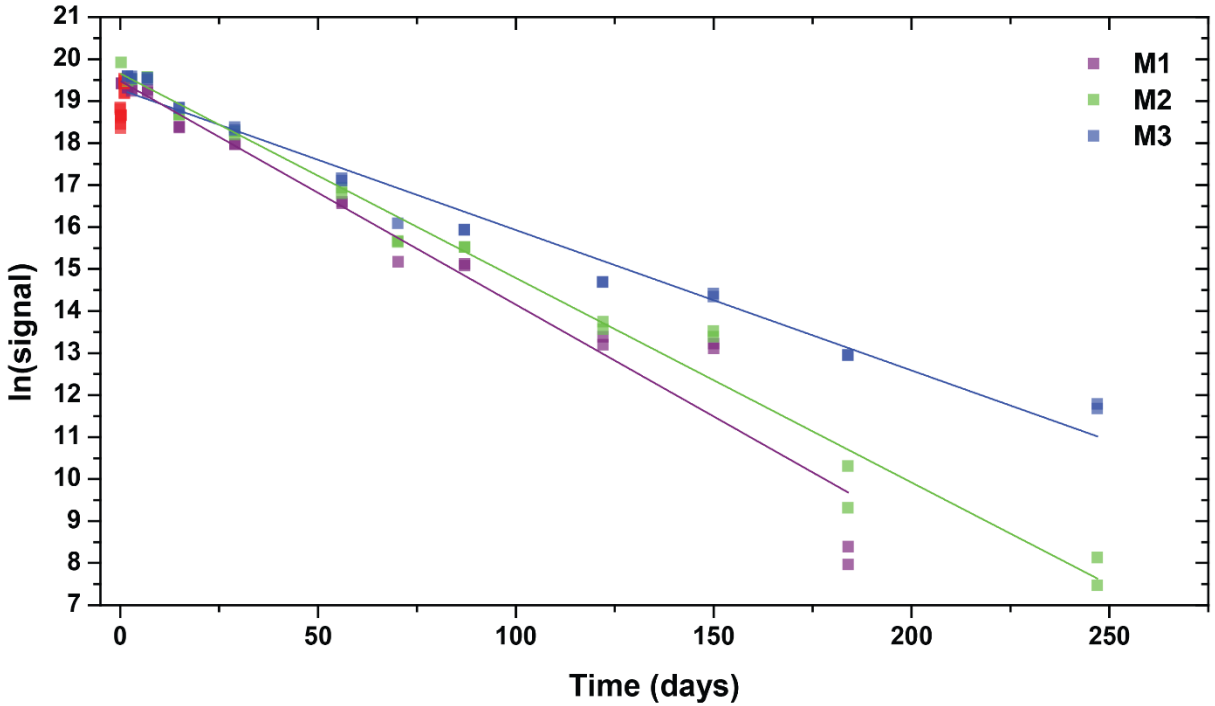

Equation	y = a + b*x		
Weight	No Weighting		
Residual Sum of Squares	4.62769	5.90797	11.46087
Pearson's r	-0.98559	-0.99193	-0.97789
Adj. R-Square	0.97009	0.98326	0.95427
		Value	Standard Error
M3	Intercept	19.2735	0.13624
M3	Slope	-0.03343	0.00122
M2	Intercept	19.65653	0.13592
M2	Slope	-0.04868	0.00127
M1	Intercept	19.47858	0.20792
M1	Slope	-0.05325	0.00243

Figure S82. Signal of **P1** (arbitrary units) in mice M1, M2, and M3 as a function of time. Both outlier points and points in **Phase 1** and **Phase 3** are marked in red.

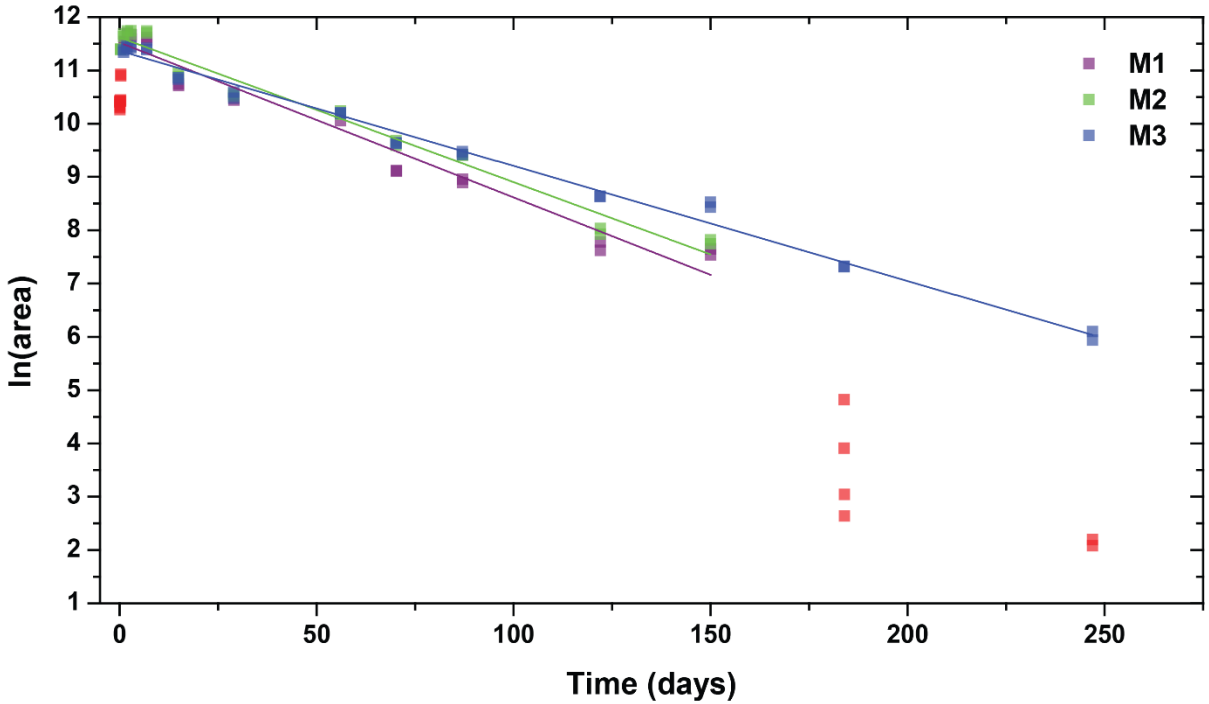

Equation	y = a + b*x		
Weight	No Weighting		
Residual Sum of Squares	1.55791	1.16603	0.69752
Pearson's r	-0.9836	-0.98691	-0.99512
Adj. R-Square	0.96585	0.97282	0.98986
		Value	Standard Error
M1	Intercept	11.52105	0.08357
M1	Slope	-0.02905	0.00119
M2	Intercept	11.61656	0.06347
M2	Slope	-0.02714	9.45354E-4
M3	Intercept	11.36476	0.04673
M3	Slope	-0.02158	4.36694E-4

Figure S83. Area of depot of **P1** (pixels) in mice M1, M2, and M3 as a function of time. Both outlier points and points in **Phase 1** and **Phase 3** are marked in red.

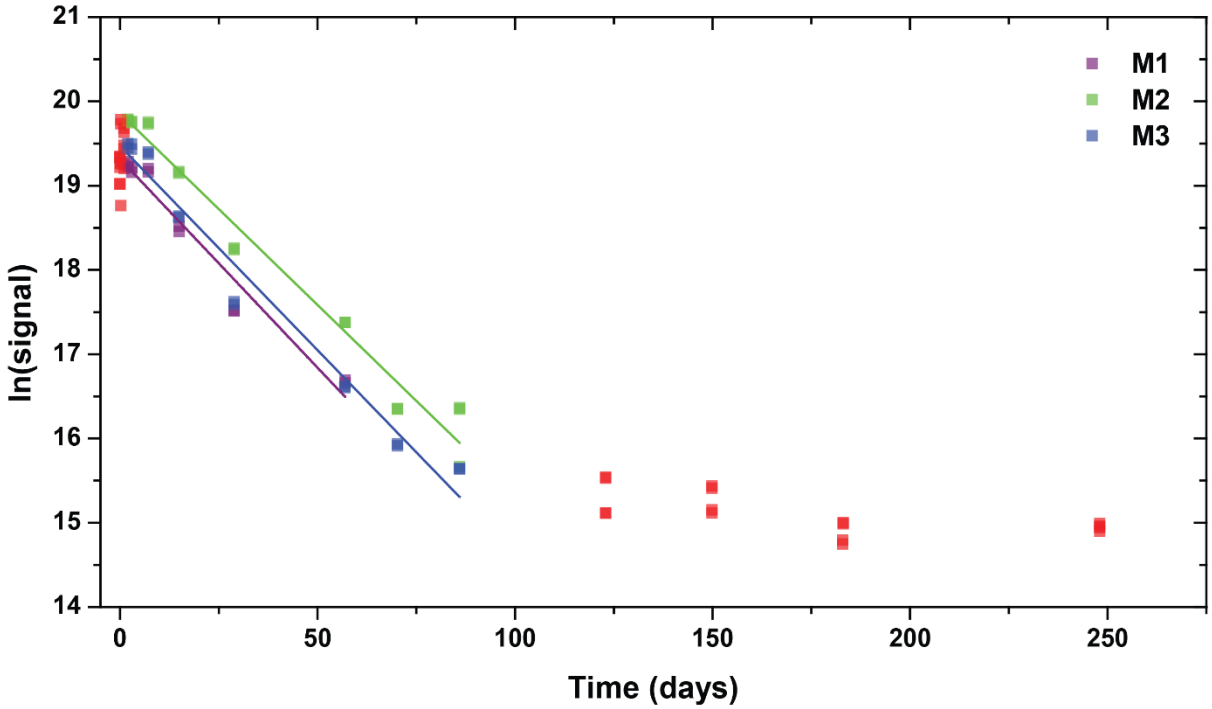

Equation	y = a + b*x		
Weight	No Weighting		
Residual Sum of Squares	0.46314	0.89546	0.94342
Pearson's r	-0.97959	-0.9881	-0.9871
Adj. R-Square	0.95556	0.97477	0.97253
		Value	Standard Error
M1	Intercept	19.31672	0.08668
M1	Slope	-0.04954	0.00321
M2	Intercept	19.85913	0.08952
M2	Slope	-0.0455	0.00183
M3	Intercept	19.46979	0.09587
M3	Slope	-0.04844	0.0021

Figure S84. Signal of **P2** (arbitrary units) in mice M1, M2, and M3 as a function of time. Both outlier points and points in **Phase 1** and **Phase 3** are marked in red.

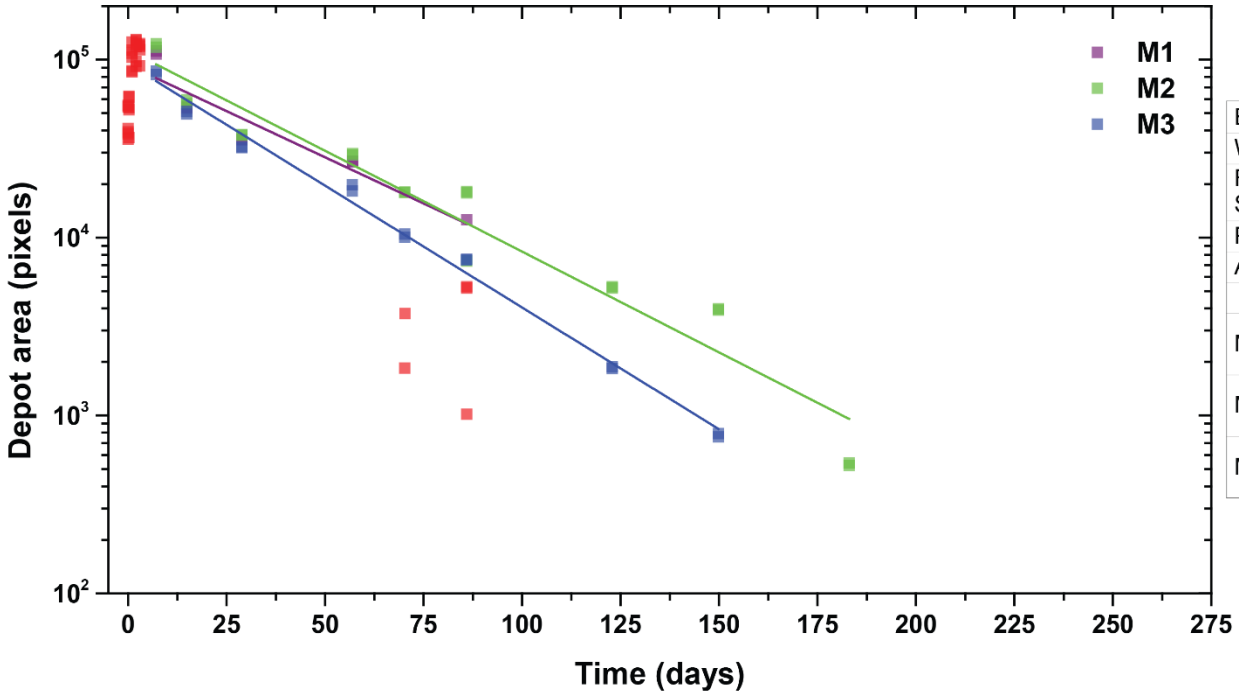

Equation	y = a + b*x		
Weight	No Weighting		
Residual Sum of Squares	0.08976	0.46378	0.05577
Pearson's r	-0.93677	-0.97135	-0.99594
Adj. R-Square	0.86003	0.9402	0.99132
		Value	Standard Error
M1	Intercept	4.97009	0.06194
	Slope	-0.01038	0.00146
M2	Intercept	5.05435	0.06595
	Slope	-0.01133	6.72234E-4
M3	Intercept	4.97622	0.02722
	Slope	-0.01369	3.30576E-4

Figure S85. Area of depot of **P2** (pixels) in mice M1, M2, and M3 as a function of time. Both outlier points and points in **Phase 1** and **Phase 3** are marked in red.

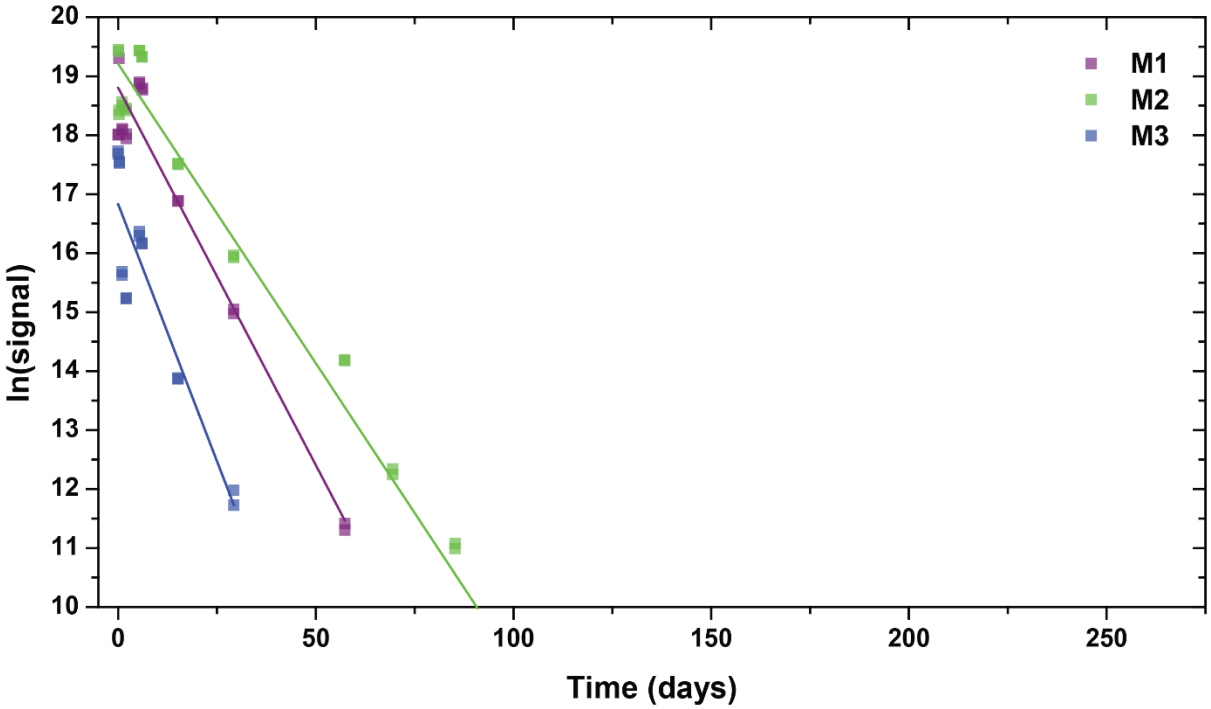

Equation	y = a + b*x		
Weight	No Weighting		
Residual Sum of Squares	9.16116	5.43752	8.68797
Pearson's r	-0.9848	-0.97286	-0.91332
Adj. R-Square	0.96839	0.9431	0.8223
		Value	Standard Error
M2	Intercept	19.20711	0.17791
M2	Slope	-0.10152	0.00391
M1	Intercept	18.8024	0.16908
M1	Slope	-0.12796	0.00761
M3	Intercept	16.8295	0.24947
M3	Slope	-0.17436	0.02078

Figure S86. Signal of **Cy7-amine** (arbitrary units) in mice M1, M2, and M3 as a function of time. Both outlier points and points in **Phase 1** and **Phase 3** are marked in red.

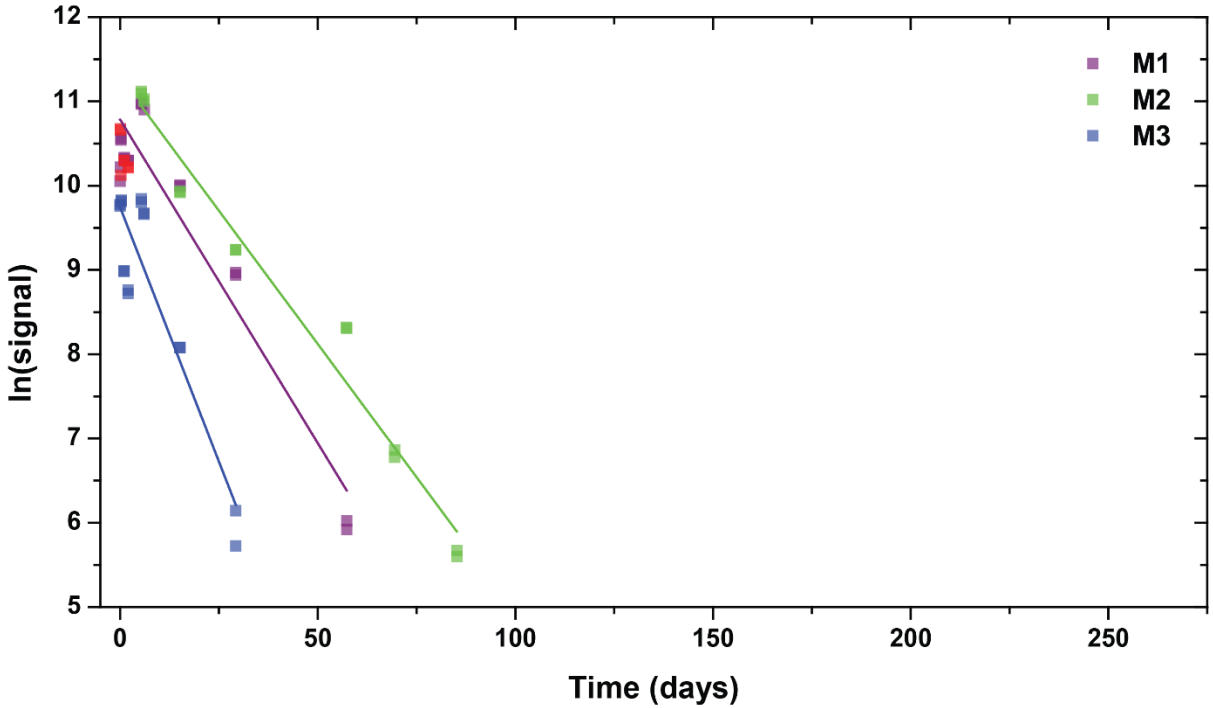

Equation	y = a + b*x		
Weight	No Weighting		
Residual Sum of Squares	4.17941	3.84536	1.47839
Pearson's r	-0.91305	-0.94871	-0.98558
Adj. R-Square	0.82178	0.8938	0.96898
		Value	Standard Error
M3	Intercept	9.74248	0.17302
M3	Slope	-0.12072	0.01441
M1	Intercept	10.78498	0.14219
M1	Slope	-0.07681	0.0064
M2	Intercept	11.28257	0.15218
M2	Slope	-0.06324	0.00313

Figure S87. Area of depot of **Cy7-amine** (pixels) in mice M1, M2, and M3 as a function of time. Both outlier points and points in **Phase 1** and **Phase 3** are marked in red.

S14. Polymer pharmacokinetics - results

Table S24. Calculated parameters of polymer release: time of maximum signal (T_{max}), biological half-lives ($T_{1/2}$), and fitting R^2; all parameters were calculated both from signal and depot size as a function of time.

Polymer; mouse			Total signal (*I*)			Depot area (*S*)		
			T_{max} (d)	$T_{1/2,I}$ (d)	R^2	T_{max} (d)	$T_{1/2,S}$ (d)	R^2
pDFEA	F1	M1	≈ 1	179 ± 26	0.670	2 ± 1	180 ± 26	0.737
		M2	≈ 1	158 ± 27	0.658	2 ± 1	157 ± 27	0.684
		M3	≈ 1	128 ± 12	0.907	2 ± 1	128 ± 12	0.875
	F2	M1	2 ± 1	149 ± 13	0.902	2 ± 1	151 ± 13	0.859
		M2	2 ± 1	139 ± 21	0.793	2 ± 1	177 ± 26	0.710
		M3	2 ± 1	149 ± 11	0.931	2 ± 1	124 ± 7	0.941
pNIPAM	I1	M1	2 ± 1	42 ± 2	0.955	2 ± 1	78 ± 4	0.956
		M2	2 ± 1	59 ± 5	0.840	2 ± 1	127 ± 12	0.834
		M3	2 ± 1	54 ± 3	0.935	2 ± 1	87 ± 5	0.935
	I2	M1	2 ± 1	53 ± 2	0.982	2 ± 1	104 ± 6	0.927
		M2	2 ± 1	69 ± 3	0.957	2 ± 1	96 ± 6	0.918
		M3	2 ± 1	59 ± 4	0.895	2 ± 1	108 ± 4	0.961
pDEA	E1	M1	2 ± 1	14 ± 1	0.964	2 ± 1	27 ± 2	0.929
		M2	2 ± 1	15 ± 1	0.969	2 ± 1	29 ± 2	0.903
		M3	2 ± 1	14 ± 1	0.966	2 ± 1	28 ± 1	0.961
	E2	M1	2 ± 1	20 ± 1	0.961	2 ± 1	26 ± 2	0.932
		M2	2 ± 1	22 ± 2	0.939	2 ± 1	29 ± 1	0.963
		M3	2 ± 1	23 ± 1	0.972	2 ± 1	50 ± 3	0.983
pAP	P1	M1	2 ± 1	13 ± 1	0.970	2 ± 1	24 ± 1	0.966
		M2	2 ± 1	14 ± 1	0.957	2 ± 1	26 ± 1	0.973
		M3	2 ± 1	21 ± 1	0.954	2 ± 1	32 ± 1	0.990
	P2	M1	2 ± 1	14 ± 1	0.956	2 ± 1	30 ± 4	0.860
		M2	2 ± 1	15 ± 1	0.975	2 ± 1	27 ± 2	0.940
		M3	2 ± 1	14 ± 1	0.973	2 ± 1	22 ± 1	0.991
Cy7		M1	< 0.5	6.8 ± 0.3	0.968	< 0.5	9 ± 1	0.894
		M2	< 0.5	5.4 ± 0.3	0.943	< 0.5	11 ± 1	0.969
		M3	< 0.5	4.0 ± 0.5	0.822	< 0.5	6 ± 1	0.822

S15. Staining protocols in histological examination.

Table S25. The report detailed description of haematoxylin & eosin staining protocol. Asterisk (*) indicates that a solution from staining kit (H&E FastStaining KitArt. No. 9194) was used without.

Haematoxylin & Eosin Staining Protocol		
step	compound/procedure (concentration %)	approximate time
1	Xylene (100%)	5 min
2	Xylene (100%)	5 min
3	Ethanol (100%)	2 min
4	Ethanol (100%)	2 min
5	Ethanol (95%)	2 min
6	Distilled water wash	2 min
7	**Haematoxylin (< 0.5%)***	3 min
8	Distilled water wash	30 s
9	Hydrochloric acid in ethanol (0.5%)	2 s
10	Running water washing	1 min
11	Ethanol (95%)	1 min
12	**Eosin (1%)***	90 s
13	Ethanol (95%)	1 min
14	Ethanol (95%)	1 min
15	Ethanol (100%)	1 min
16	Acetone (100%)	5 min
17	Xylene (100%)	5 min
18	Xylene (100%)	5 min
19	Mounting: Canada balsam	-

Table S26. The report detailed description of haematoxylin & eosin staining protocol. Asterisk (*) indicates that a solution from staining kit (Van Gieson Trichrome Staining Kit 9193.1) was used without.

Van Gieson Trichrome Staining Protocol		
step	compound/procedure (concentration %)	approximate time
1	Xylene (100%)	5 min
2	Xylene (100%)	5 min
3	Ethanol (100%)	2 min
4	Ethanol (96%)	2 min
5	Ethanol (80%)	2 min
6	Ethanol (70%)	2 min
7	**Solution A+B (1:1)***	5 min
8	Destilled water wash	2 min
9	Hydrochloric acid in ethanol (0.5%)	2 s
10	Running water washing	10 min
11	**Van Gieson solution***	2 min
12	Ethanol (70%)	2 s
13	Ethanol (80%)	2 s
14	Ethanol (96%)	2 s
15	Ethanol (95%)	2 s
16	Ethanol (100%)	2 s
17	Xylene (100%)	5 min
18	Xylene (100%)	5 min
19	Mounting: Canada balsam	-

S16. Histopathological findings

Table S27. List of all findings from autopsy and subsequent histopathological examination.

Polymer	Autopsy finding (macroscopic)	Spleen	Liver	Kidney	Injected muscle	Control muscle
F1	**Liver**: size normal; darker than in DMSO **Kidney**: Larger than in F2 or DMSO, colour normal **Spleen**: normal size and colour **Lungs**: normal size and colour **Heart**: normal size and colour **Pancreas**: minor haemorrhage, normal size and colour **Muscles**: normal size and colour	No sign of chronic congestion, fibrosis, or hemosiderin accumulation; well developed white and red pulp, no sign of presence of foreign material	No sign of steatosis, fibrosis, or ischemia; no sign of pathologic Kupffer cell proliferation; mild autolysis	No sign of fibrosis or any other pathologic change; mild autolysis	No sign of fibrosis or chronic inflammation. Cells are basophilic, cytoplasm is slightly granular; presence of mast cells.	No sign of fibrosis or chronic inflammation. Cells are basophilic, cytoplasm is slightly granular; presence of mast cells.
F2	**Liver**: Smaller than F1 or DMSO, colour normal **Kidney**: Larger than in DMSO, colour normal **Spleen**: normal size and colour **Lungs**: normal size and colour **Heart**: normal size and colour **Pancreas**: darker than in F1 or DMSO. **Muscle**: normal colour	No sign of chronic congestion, fibrosis, or hemosiderin accumulation; well developed white and red pulp, no sign of presence of foreign material	No sign of steatosis, fibrosis, or ischemia; no sign of pathologic Kupffer cell proliferation; mild autolysis	No sign of fibrosis or any other pathologic change; mild autolysis	No sign of fibrosis or chronic inflammation. Cells are basophilic, cytoplasm is slightly granular; presence of mast cells.	No sign of fibrosis or chronic inflammation. Cells are basophilic, cytoplasm is slightly granular; presence of mast cells.
P1	**Liver**: Larger than DMSO, colour normal. Small haemorrhage in the capsule **Kidney**: larger and lighter than P2 and DMSO, one haemorrhage. **Spleen**: normal size and colour **Lungs**: small fibrotic fusions with pleura **Heart**: Larger than in P2 and DMSO, one haemorrhage **Pancreas**: smaller than in DMSO. **Muscle**: normal colour	No sign of chronic congestion, fibrosis, or hemosiderin accumulation; well developed white and red pulp, no sign of presence of foreign material	No sign of steatosis, fibrosis, or ischemia; no sign of pathologic Kupffer cell proliferation; mild autolysis	No sign of fibrosis or any other pathologic change; mild autolysis	No sign of fibrosis or chronic inflammation. Cells are basophilic, cytoplasm is slightly granular; presence of mast cells.	No sign of fibrosis or chronic inflammation. Cells are basophilic, cytoplasm is slightly granular; presence of mast cells.
P2	**Liver**: smaller than in P1 and DMSO, lighter than in DMSO; capsule enlargement in one lobe. **Kidneys**: Normal size and colour; visible vein **Spleen**: normal size and colour	No sign of chronic congestion, fibrosis, or hemosiderin	No sign of steatosis, fibrosis, or ischemia; no	No sign of fibrosis or any other pathologic	No sign of fibrosis or chronic inflammation. Cells are basophilic,	No sign of fibrosis or chronic inflammation. Cells are basophilic,

	Lungs: normal size and colour **Heart**: normal size and colour **Pankreas**: N/A **Muscle**: normal colour	accumulation; well developed white and red pulp, no sign of presence of foreign material	sign of pathologic Kupffer cell proliferation; mild autolysis	change; mild autolysis	cytoplasm is slightly granular; presence of mast cells.	cytoplasm is slightly granular; presence of mast cells.
E1	**Liver**: Larger than DMSO, colour uneven, local capsule enlargement. **Kidneys**: Normal size, lighter than in E2 and DMSO. **Spleen**: normal size and colour **Lungs**: normal size and colour **Heart**: normal size and colour **Pancreas**: smaller than in DMSO **Muscle**: normal colour	No sign of chronic congestion, fibrosis, or hemosiderin accumulation; well developed white and red pulp, no sign of presence of foreign material	No sign of steatosis, fibrosis, or ischemia; no sign of pathologic Kupffer cell proliferation; mild autolysis	No sign of fibrosis or any other pathologic change; mild autolysis	No sign of fibrosis or chronic inflammation. Cells are basophilic, cytoplasm is slightly granular; presence of mast cells.	No sign of fibrosis or chronic inflammation. Cells are basophilic, cytoplasm is slightly granular; presence of mast cells.
E2	**Liver**: same as in E1, colour normal. Dark stripe on one lobe **Kidneys**: Normal size and colour, accumulation of adipose tissue around the capsule. **Spleen**: Normal size and colour, accumulation of adipose tissue around the capsule. **Lungs**: normal size and colour **Heart**: normal size and colour **Pancreas**: normal colour, smaller than DMSO **Muscle**: normal colour	No sign of chronic congestion, fibrosis, or hemosiderin accumulation; well developed white and red pulp, no sign of presence of foreign material	No sign of steatosis, fibrosis, or ischemia; no sign of pathologic Kupffer cell proliferation; mild autolysis	No sign of fibrosis or any other pathologic change; mild autolysis	No sign of fibrosis or chronic inflammation. Cells are basophilic, cytoplasm is slightly granular; presence of mast cells.	No sign of fibrosis or chronic inflammation. Cells are basophilic, cytoplasm is slightly granular; presence of mast cells.
I1	**Liver**: Smaller and lighter than in DMSO. Light stripe on one lobe. **Kidney**: larger than in I2 or DMSO, normal colour. **Spleen**: normal size and colour, accumulation of adipose tissue around the capsule. **Lungs**: normal size and colour **Heart**: normal size and colour **Pancreas**: normal size and colour **Muscle**: normal colour	No sign of chronic congestion, fibrosis, or hemosiderin accumulation; well developed white and red pulp, no sign of presence of foreign material	No sign of steatosis, fibrosis, or ischemia; no sign of pathologic Kupffer cell proliferation; mild autolysis	No sign of fibrosis or any other pathologic change; mild autolysis	No sign of fibrosis or chronic inflammation. Cells are basophilic, cytoplasm is slightly granular; presence of mast cells.	No sign of fibrosis or chronic inflammation. Cells are basophilic, cytoplasm is slightly granular; presence of mast cells.
	Liver: smaller than in I1 and DMSO, normal colour.					

I2	**Kidneys**: Larger than in DMSO, normal colour; large haemorrhage in capsule. **Spleen**: normal size and colour; adipose tissue accumulation around the capsule. **Lungs**: normal size and colour **Heart**: normal size and colour **Pancreas**: normal size and colour **Muscle**: normal colour	No sign of chronic congestion, fibrosis, or hemosiderin accumulation; well developed white and red pulp, no sign of presence of foreign material	No sign of steatosis, fibrosis, or ischemia; no sign of pathologic Kupffer cell proliferation; mild autolysis	No sign of fibrosis or any other pathologic change; mild autolysis	No sign of fibrosis or chronic inflammation. Cells are basophilic, cytoplasm is slightly granular; presence of mast cells.	No sign of fibrosis or chronic inflammation. Cells are basophilic, cytoplasm is slightly granular; presence of mast cells.
Saline	**Liver**: Normal size and colour **Kidney**: Normal colour, larger size than in DMSO. **Spleen**: Larger than in DMSO. **Lungs**: two small haemorrhages. **Heart**: Normal size, lighter than in Cy7 or DMSO **Pankreas**: smaller than in DMSO. **Muscle**: normal colour	No sign of chronic congestion, fibrosis, or hemosiderin accumulation; well developed white and red pulp, no sign of presence of foreign material	No sign of steatosis, fibrosis, or ischemia; no sign of pathologic Kupffer cell proliferation; mild autolysis	No sign of fibrosis or any other pathologic change; mild autolysis	No sign of fibrosis or chronic inflammation. Cells are basophilic, cytoplasm is slightly granular; presence of mast cells.	No sign of fibrosis or chronic inflammation. Cells are basophilic, cytoplasm is slightly granular; presence of mast cells.
Cy7	**Liver**: normal size, lighter than in DMSO **Kidney**: normal size and colour **Spleen**: larger than in DMSO, less fat. **Lungs**: small haemorrhage. Small fibrotic granule **Heart**: normal size and colour **Pancreas**: normal size and colour **Muscle**: normal colour	No sign of chronic congestion, fibrosis, or hemosiderin accumulation; well developed white and red pulp, no sign of presence of foreign material	No sign of steatosis, fibrosis, or ischemia; no sign of pathologic Kupffer cell proliferation; mild autolysis	No sign of fibrosis or any other pathologic change; mild autolysis	No sign of fibrosis or chronic inflammation. Cells are basophilic, cytoplasm is slightly granular; presence of mast cells.	No sign of fibrosis or chronic inflammation. Cells are basophilic, cytoplasm is slightly granular; presence of mast cells.
DMSO	**Liver**: used as reference for the rest of the samples **Kidney**: used as reference for the rest of the samples **Spleen**: used as reference for the rest of the samples **Lungs**: used as reference for the rest of the samples **Heart**: used as reference for the rest of the samples **Pancreas**: used as reference for the rest of the samples **Muscles**: used as reference for the rest of the samples	No sign of chronic congestion, fibrosis, or hemosiderin accumulation; well developed white and red pulp, no sign of presence of foreign material	No sign of steatosis, fibrosis, or ischemia; no sign of pathologic Kupffer cell proliferation; mild autolysis	No sign of fibrosis or any other pathologic change; mild autolysis	No sign of fibrosis or chronic inflammation. Cells are basophilic, cytoplasm is slightly granular; presence of mast cells.	No sign of fibrosis or chronic inflammation. Cells are basophilic, cytoplasm is slightly granular; presence of mast cells.

*Colour changes of liver, kidney, spleen, and heart were probably caused by anaesthesia and autopsy (redistribution of blood in organs). Haemorrhages were probably *post-mortem* changes. The signs of mild autolysis of the specimen; autolysis of liver was probably caused during processing.

S17. Observations of mice behaviour after the polymer administration

One hour after the administration, most mice exhibited at least some level of agitation, discomfort to pain in the left hind leg after the administration. By the day 2, the mice exhibited no agitation or fear of researchers, but 36 % (13/36) exhibited at least some decrease of strength in the administered leg and/or pain; 31 % (4/13) of them exhibited a complete paralysis and limping, possibly caused by the nerve injury during the administration.* By the day 8, the 25 % (9/36) of all mice exhibited some level of hind leg/foot weakness; the paralysed mice exhibited a significant recovery process, all mice were able to use both their hind legs and more rather well. By the day 11, 3 % (1/36) exhibited any limping and inability to grab by their hind feet. By the day 16, this mouse began to use their hind leg normally (**Figure 16**).

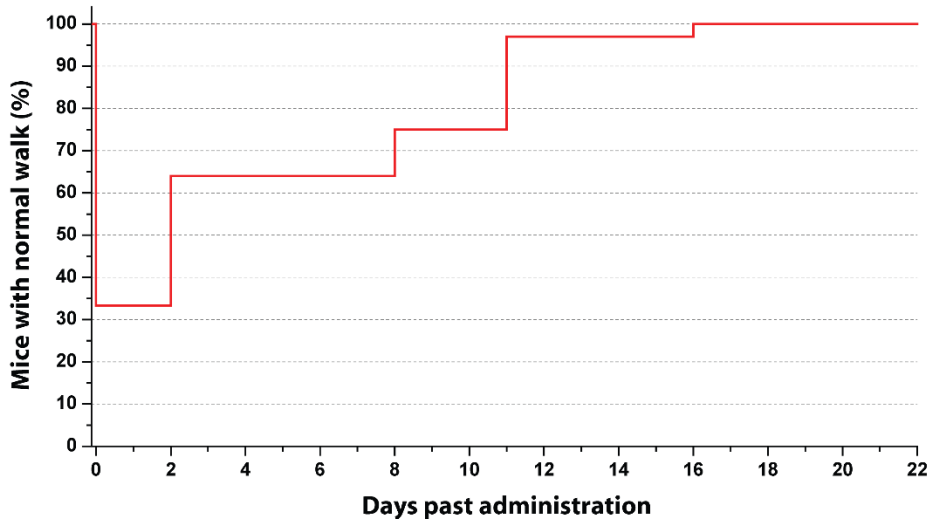

Figure S88. Percentage of mice with normal walk as a function of time.

*Nerve injury during intramuscular administration cannot be avoided even when using smallest possible needles. Despite popular belief, aspiration during the intramuscular administration does not improve the safety of the intramuscular administration, therefore, we avoided it.[S11]

S18. Co-authors contributions

Babuka, David (D.B.) - Investigation, Methodology, Data curation, Software
Beneš, Hynek (H.B.) - Investigation, Methodology, Data curation
Černoch, Peter (P.Č.) - Investigation
Dalecká, Linda (L.D.) - Investigation, Methodology
Groborz, Ondřej (O.G.) - Conceptualization, Supervision, Methodology, Data curation, Investigation, Formal analysis, Visualization, Project administration, Writing – original draft, Writing – review & editing, Funding acquisition, Resources, Software
Hoogenboom, Richard (R.H.) - Validation, Methodology, Writing – review & editing, Resources, Funding acquisition, Supervision
Hovořáková, Mária (M.Ho.) - Investigation, Methodology, Data curation
Hrubý, Martin (M.Hr.) - Resources, Validation, Funding acquisition, Writing – review & editing, Supervision
Kadlec, Jan (J.K.) - Methodology, Data curation, Investigation, Formal analysis, Visualization, Software
Keša, Peter (P.K.) - Investigation, Methodology, Data curation, Validation, Formal analysis, Writing – review & editing
Kolouchová, Kristýna (K.K.) - Investigation, Methodology, Data curation, Writing – original draft, Writing – review & editing, Visualization, Project administration
Krunclová, Tereza (T.Kr.) - Investigation, Methodology, Data curation, Validation, Visualization, Formal analysis, Writing – review & editing
Kučera, Tomáš (T.Ku.) - Resources, Funding acquisition
Lobaz, Volodymyr (V.L.) - Investigation, Methodology, Validation, Formal analysis, Writing – original draft, Data curation
Loukotová, Lenka (LL) - Validation, Writing – review & editing
Pankrác, Jan (J.P.) - Investigation, Methodology, Data curation, Validation, Formal analysis, Writing – review & editing
Pierzynová, Aneta (A.P.) - Investigation, Methodology, Data curation, Writing – review & editing
Rosa, Victor R. de la (V.R.R.) - Investigation, Methodology, Writing – review & editing
Šefc, Luděk (L.Š.) - Resources, Funding acquisition
Šrámek, Jaromír (J.Š.) - Investigation, Methodology, Data curation
Štěpánek, Petr (P.Št.) - Validation, Methodology, Writing – review & editing
Švec, Pavel (P.Šv.) - Validation, Data curation, Methodology, Writing – review & editing

O.G. conceived the presented ideas, K.K. synthesized the monomers, K.K., O.G. synthesized, modified, purified, and characterized the polymers (SEC, NMR). K.K. and V.R.R. measured and evaluated T_{CP} as a function of polymer temperature. V.L., and H.B. measured and evaluated calorimetry data. D.B. collected and evaluated DLS. J.P. and P.K. performed the *in vivo* biological experiments, injected the polymer into mice, performed the long-term photoacoustic imaging and evaluated corresponding data. J.K. derived the pharmacological models and the data curation. T.Kr. assessed and evaluated *in vitro* cytotoxicity on cell lines. P.Č. measured study polymers' d*n*/d*c*. A.P., J.Š., M.Ho., L.D., and T.Ku have assessed and evaluated the histological examinations. K.K., O.G., V.L., R.H., P.Št., M.Hr., D.B., H.B., and P.Šv. were involved in methodology design. K.K., O.G., V.L., R.H., P.Št., M.H., D.B., H.B., and P.Šv evaluated the measured data; O.G., K.K., and R.H. have proposed the study strategies, validated data, and formulated the conclusions of the study. M.Hr., R.H., O.G., T.Kr., T.Ku., and P.Št. and have secured the resources for this study, M.Hr., O.G. and R.H. have secured its funding. O.G. supervised the project, K.K. and O.G. controlled the project management and administration. O.G. and K.K wrote major parts of the manuscript, R.H., V.R.R., P.Šv, M.Hr., J.P., P.K., P.Št., and L.L. wrote and/ or reviewed parts of the manuscript.

S19. Additional references

(S1) Wiseman, T.; Williston, S.; Brandts, J. F.; Lin, L.-N. Rapid Measurement of Binding Constants and Heats of Binding Using a New Titration Calorimeter. *Anal. Biochem.* **1989**, *179* (1), 131–137. https://doi.org/10.1016/0003-2697(89)90213-3.

(S2) Zhao, C.; Ma, Z.; Zhu, X. X. Rational Design of Thermoresponsive Polymers in Aqueous Solutions: A Thermodynamics Map. *Prog. Polym. Sci.* **2019**, *90*, 269–291. https://doi.org/10.1016/j.progpolymsci.2019.01.001.

(S3) Bloksma, M. M.; Bakker, D. J.; Weber, C.; Hoogenboom, R.; Schubert, U. S. The Effect of Hofmeister Salts on the LCST Transition of Poly(2-Oxazoline)s with Varying Hydrophilicity. *Macromol. Rapid Commun.* **2010**, *31* (8), 724–728. https://doi.org/10.1002/marc.200900843.

S(4) Zafrani, Y.; Yeffet, D.; Sod-Moriah, G.; Berliner, A.; Amir, D.; Marciano, D.; Gershonov, E.; Saphier, S. Difluoromethyl Bioisostere: Examining the "Lipophilic Hydrogen Bond Donor" Concept. *J. Med. Chem.* **2017**, *60* (2), 797–804. https://doi.org/10.1021/acs.jmedchem.6b01691.

(S5) Horvath, A. L. *Halogenated Hydrocarbons: Solubility-Miscibility with Water*; CRC Press, 1982.

(S6) Yalkowsky, S. H. *Handbook of Aqueous Solubility Data*, 2nd ed.; CRC Press, 2003.

(S7) Izunobi, J. U.; Higginbotham, C. L. Polymer Molecular Weight Analysis by ^{1}H NMR Spectroscopy. *J. Chem. Educ.* **2011**, *88* (8), 1098–1104. https://doi.org/10.1021/ed100461v.

(S8) Qiu, X.-P.; Winnik, F. M. Facile and Efficient One-Pot Transformation of RAFT Polymer End Groups via a Mild Aminolysis/Michael Addition Sequence. *Macromol. Rapid Commun.* **2006**, *27* (19), 1648–1653. https://doi.org/10.1002/marc.200600436.

(S9) Zhou, C.; Hillmyer, M. A.; Lodge, T. P. Micellization and Micellar Aggregation of Poly(Ethylene-*Alt*-Propylene)-*b*-Poly(Ethylene Oxide)-*b*-Poly(*N*-Isopropylacrylamide) Triblock Terpolymers in Water. *Macromolecules* **2011**, *44* (6), 1635–1641. https://doi.org/10.1021/ma102786q.

(S10) Gottlieb, H. E.; Kotlyar, V.; Nudelman, A. NMR Chemical Shifts of Common Laboratory Solvents as Trace Impurities. *J. Org. Chem.* **1997**, *62* (21), 7512–7515. https://doi.org/10.1021/jo971176v.

(S11) Sisson, H. Aspirating during the Intramuscular Injection Procedure: A Systematic Literature Review. *J. Clin. Nurs.* **2015**, *24* (17–18), 2368–2375. https://doi.org/10.1111/jocn.12824.